Vegetation and climate history during the last glacial-interglacial cycle at Lake Van, eastern Anatolia

Dissertation

zur

Erlangung des Doktorgrades (Dr. rer. nat.)

der

Mathematisch-Naturwissenschaftlichen Fakultät

der

Rheinischen Friedrich-Wilhelms-Universität Bonn

vorgelegt von

Nadine Pickarski

aus

Leipzig

Bonn, Dezember 2013

Angefertigt mit Genehmigung der Mathematisch-Naturwissenschaftlichen Fakultät
der Rheinischen Friedrich-Wilhelms-Universität Bonn

1. Gutachter: Prof. Dr. Thomas Litt
2. Gutachter: Prof. Dr. Martin Langer

Tag der Promotion: 28. März 2014

Erscheinungsjahr: 2014

Table of Contents

1 Introduction

Discussions of the climate variability in the past have attracted considerable research interest. A collection of paleoenvironmental information contributed to an improved understanding of the complexity of past, present and future paleoclimate variability. In this regard, the last interglacial, equivalent to the northern European 'Eemian', is often considered as a possible scenario of climate and vegetational changes for the current interglacial (Kukla et al., 2002), without influences of human activity. In recent years, the last glacial-interglacial cycle has been intensively studied in northern and southern Europe (e.g. Aalbersberg and Litt, 1998; Allen and Huntley, 2009; Brauer et al., 2007; Djamali et al., 2008; Milner et al., 2013; Müller et al., 2003, 2011; Sánchez Goñi et al., 1999, 2005; Tzedakis, 2000; Tzedakis et al., 2006), providing insights into global climate variability. Special research interests are uncertainties regarding to the length of interglacial terrestrial conditions, the timing and nature of vegetation as well as environmental variability towards the end of the interglacial (e.g. Brauer et al., 2007; Kukla et al., 1997; Shackleton et al., 2003; Tzedakis et al., 2002a; Tzedakis, 2003; Tzedakis et al., 2004b). Available evidences suggest that in southern Europe forest usually extends into the interval of ice growth (Tzedakis, 2005).

To date, it is generally accepted that the ultimate trigger of the past major climate cycles is the change in orbital parameters (Imbrie et al., 1992, 1993). The insolation data, based on Berger (1978), provide the idea of seasonality changes and surface temperature variation. This aspect is commonly considered as a main factor for the oscillations between globally cold, glacial stages and globally warm, interglacial stages. But the understanding of the mechanisms and their consequences for climate changes is far from complete (Harrison and Sánchez Goñi, 2010). Recently, sedimentary records have been successfully correlated to Marine Isotope Stages (MIS) and orbital parameters (Tzedakis et al., 1997; Tzedakis, 2005; Tzedakis et al., 2006). A further fundamental achievement was the direct land-sea correlation of the Iberian margin record (MD95-2042; 37°48'N, 10°10'W) of the terrestrial pollen signal with deep-sea isotope data from the North Atlantic. It creates the critical link to compare marine with terrestrial records (Sánchez Goñi et al., 1999).

In general, the climate of the last interglacial has been described as a relatively stable uninterrupted warm period (Aalbersberg and Litt, 1998; Kühl and Litt, 2007; Kukla et al., 2002; NGRIP, 2004). However, less-pronounced short-term climate instability towards the middle part of the Eemian is detected in a variety of paleoarchives (e.g. Bond et al., 2001; Brauer et al., 2007; Milner et al., 2013; Müller et al., 2005; Tzedakis et al., 2003a). Throughout the last glacial, repeated and abrupt

millennial-scale climate oscillations occurred and were clearly proved by ice-, marine- and continental climate records around the Northern Hemisphere (Blockley et al., 2012; Harrison and Sánchez Goñi, 2010; Müller et al., 2011; NGRIP, 2004; Sánchez Goñi et al., 2005; Svensson et al., 2008; Tzedakis, 2005; Wolff et al., 2010). The most drastic high-frequency variability was represented by the Dansgaard-Oeschger (D-O) events, discovered in Greenland ice core records (Dansgaard et al., 1993; Grootes et al., 1993; Wolff et al., 2010). These events are becoming more important for paleoclimate research scientists throughout the last 30 years, especially to improve the understanding of the interaction between oceanic and atmospheric circulations of the North Atlantic Ocean as well as its environmental and vegetational responses. D-O events are associated with the formation of diagnostic ice-rafted deposits (IRD; McManus et al., 1994) in the marine environments.

New insights on the impact of global paleoclimate changes on regional scales are provided by studies on high-resolution paleoarchives from different regions. One of the key regions is the Mediterranean area, which has been intensively studied during the last decade. Publications of marine and terrestrial records demonstrate the close link of Mediterranean climate to the North Atlantic ocean-atmosphere system and land-sea correlations in the eastern Mediterranean, respectively (Brauer et al., 2007; Sánchez Goñi et al., 1999, 2000, 2005; Shackleton et al., 2003; Tzedakis et al., 2002a). Unlike northern Europe and eastern Mediterranean, the vegetation and climate development during the last glacial-interglacial cycles in the Near East based on continental records is poorly understood (Litt et al., subm). Only few detailed long-term investigations of paleoenvironmental conditions during the last glacial-interglacial cycle exits in the Near East, e.g. Lake Urmia (Djamali et al., 2008). Hence, the vegetation and climate history in the semi-arid continental interior are still debated for this period. Instead, a number of Holocene and late-glacial paleoenvironmental studies have refined the understanding of millennial-scale paleoclimate variability (Bar-Matthews et al., 2003; Bottema, 1986, 1995a; Djamali et al., 2008; Langgut et al., 2011; Litt et al., 2009, 2012; Schiebel, 2013; Vaks et al., 2006; van Zeist and Bottema, 1991).

Latest research provides new continuously high-resolution vegetation and environmental history based on lacustrine sediments from Lake Van, eastern Anatolia, Turkey, covering the last 130 ka BP. The aim of this study is to establish the vegetation succession and thus, the climatic evolution of the eastern Anatolia region. In particular, palynological studies in lakes are well-established as proxy data for the reconstruction of vegetation variability, the environment and natural climate evolution.

Finally, this study presents a comparison of the Lake Van pollen record with

the well-known long continental sequences from the Near East and the eastern Mediterranean region. A transect from west to east including the records from Lago Grande di Monticchio (Italy), Ioannina (NW-Greece), Tenaghi Philippon (NE-Greece) and Lake Urmia (Iran) permits a discussion of the different climatic behaviour relating to their geographical location. This aspect provides valuable information that contributes to the understanding of the vegetational succession and climate history for the last 130 ka in the Near East and the eastern Mediterranean region.

2 Current state of research

2.1 Paleovegetation and -climate investigations of the last glacial-interglacial cycle in Europe and in the Near East region

The reconstruction of vegetation and climate history within the last glacial-interglacial cycle has a long-standing tradition and is well-studied in numerous deposits in NW Europe. The first concept of vegetation for the northern Europe was proposed by Iversen (1958) and developed by Andersen (1966) and Turner and West (1968). Further palynological investigations demonstrated a uniform succession of vegetation sequences from a wide distribution of sites, which were summarized in e.g. Aalbersberg and Litt (1998); Brewer et al. (2008); Caspers et al. (2002); Sirocko et al. (2007). The subsequent environmental and vegetational investigations in northern Europe resulted in a first chronology of the last interglacial period. Therefore, previous quantitative palynological studies of the last interglacial have confirmed a duration of a widespread forest expansion of about 11,000 years (between 126-115 ka) in the northern European region (Cappers and Bottema, 2002; Holzkämper et al., 2004; Kukla et al., 2002; Müller, 1974; Sánchez Goñi, 2007).

In recent years, the emergence of new long continental and high-resolution records in southern Europe improved the understanding of climate variability during the last glacial-interglacial cycle, especially due to the well-dated investigations at Lago Grande di Monticchio (Italy) with an independent varve chronology (Allen et al., 1999; Allen and Huntley, 2000; Allen et al., 2000, 2002; Allen and Huntley, 2009; Brauer et al., 2007; Huntley et al., 1999; Watts et al., 1996, 2000), at the Ioannina basin (NW-Greece; Lawson et al., 2004; Roucoux et al., 2011; Tzedakis, 1994; Tzedakis et al., 2002a, 2003a) and due to the Tenaghi Philippon record (NE-Greece; Frogley et al., 1999; Milner et al., 2013; Peyron et al., 2011; Pross et al., 2007; Tzedakis et al., 2003b, 2006; van der Wiel and Wijmstra, 1987a,b). Regardless of a recurrent northern European pattern of the vegetational succession, these studies documented a specific development of warm-temperate forest composition, which indicated a considerable variability in geographical and in climatic conditions. Furthermore, they presented new estimates of global variability.

An important step in the research of the last glacial-interglacial cycle was the direct combination of a pollen analysis with deep-sea isotope data of the Iberian margin (Portugal) emerging in a useful connection between marine and terrestrial sequences (Roucoux et al., 2001; Sánchez Goñi et al., 1999). The direct correlation

resulted in a re-evaluation of the timing and duration, including the assessment of relative leads and lags of the last interglacial conditions in the southern European region (Tzedakis, 2005). Thus, the last interglacial woodlands in southern Europe were estimated to have a duration of about 16,000 years (126-110 ka; Shackleton et al., 2002, 2003) and consequently lasted well into the gradual build-up of the ice volume of the early glacial period (Allen and Huntley, 2009; Brauer et al., 2007; Shackleton et al., 2002, 2003; Sánchez Goñi, 2007; Tzedakis, 2005).

The major variability in vegetation and climate reconstructions within the last glacial-interglacial cycle in Europe were associated with climatic instability which are based on changes in the North Atlantic circulations (Dansgaard et al., 1993; McManus et al., 1994, 1999; Müller and Kukla, 2004). Such instabilities were intensively discussed in several publications, especially during the last glacial period by Cacho et al. (2000); Fletcher et al. (2010); Harrison and Sánchez Goñi (2010); Landais et al. (2004); Sánchez Goñi et al. (2002); Sánchez Goñi and Harrison (2010); Tzedakis et al. (2004a); Watts et al. (1996); Wolff et al. (2010).

Conversely to the well-studied European region, the last glacial-interglacial cycle in the Near East is fragmented due to the lack of detailed pollen records on vegetation and environmental history. Recently, the publications of Shumilovskikh et al. (2012, 2013) has complemented the last interglacial in Northern Anatolia (Black Sea). Furthermore, the low-resolution sequence of Lake Urmia (Iran) is available for this relevant time period (Bottema, 1986; Djamali et al., 2008; Stevens et al., 2012; van Zeist and Bottema, 1977). However, most paleoenvironmental studies on sediments from the Near East region have been focused on reconstructions of Holocene environments, for example in SW and Central Turkey by Deckers and Pessin (2010); Eastwood et al. (1998, 1999, 2007); England et al. (2008); Kaniewski et al. (2007, 2008, 2012); Roberts et al. (2001); Roberts and Wright (1993); van Zeist et al. (1975), in eastern Anatolia by Bottema (1995a, 1997); Litt et al. (2009); Wick et al. (2003); van Zeist and Woldring (1978a) as well as in Iran (El-Moslimany, 1986, 1987; Stevens et al., 2001; van Zeist and Wright, 1963).

Concluding, high resolution studies of vegetational and environmental variability of the last glacial-interglacial cycle in eastern Anatolia are not yet available and are an essential subject for ongoing research in the Near East region.

2.2 Palynological research at Lake Van

The palynological research in lake sediments is by far the most common method for detailed reconstructions of past environments. Systematic work on paleoethnobotany and vegetation history at Lake Van started rather late. The first palynological analyses were carried out on nine lacustrine sediment cores from various depth of the lake in summer 1974. Paleoenvironmental investigation at Lake Van, containing nearly the complete Holocene, was established by van Zeist and Woldring (1978a). Furthermore, Kempe and Degens (1978) developed a preliminary varve chronology of the Lake Van (varve-dated up to 9,800 BP). All results were published comprehensive in a special issue edited by Degens and Kurtman (1978).

In 1990, geochemical, geological and paleoecological investigations were continued on annually sediments of the Ahlat Ridge (Lemcke, 1996; Landmann et al., 1996a,b). During this period, pollen investigations, encompassing the last ~13 ka, documented the climate changes of the late-glacial interstadial and Holocene as well as human activity and the history of deforestation at Lake Van (Wick et al., 2003).

Based on the results of the seismic site survey, an international team of scientists started to drill a continental sequence in the frame of the International Continental Scientific Drilling Program (ICDP) in 2004 (Litt et al., 2009). The drilling campaign at the Ahlat Ridge site was able to contain 10 short sediments sequences at different locations. The multidisciplinary work on the sediment cores, including magnetic susceptibility, stable oxygen isotope and pollen analyses, showed that the retrieved record extends back to the last glacial maximum (c. 20,000 cal. BP). In addition, palynological investigations of the Northern Basin have been examined by Kaplan and Heumann (2010) and Kaplan and Örçen (2011). The efforts of volcanic eruptions on ecological succession at Lake Van were studied by Riedel (2011). Finally, the investigation in 2004 demonstrated that sedimentary evolution of Lake Van provides an excellent potential for obtaining the longest continuous and high-resolution paleoclimatic archive in the Near East.

In summer 2010, the follow up project started in the framework of the ICDP project PALEOVAN. The drilling campaign could extract almost undisturbed sequences of lacustrine sediments from the Northern Basin (~140 m) and the Ahlat Ridge (~220 m; Litt et al., 2012). The constructed composite record of the Ahlat Ridge (AR) site provides the basis for well-dated paleoenvironmental and palynological reconstructions, encompassing the last c. 600 ka (Litt et al., subm; Stockhecke et al., subm).

3 Lake Van and the eastern Anatolia region

3.1 Environmental setting

Lake Van (38.5°N, 43.0°E) is located on the Anatolian-Iranian high plateau in eastern Anatolia, Turkey, close to the border to Iran, Iraq and Syria (Figure 3.1). This lake, with an altitude of about 1,649 m above sea level (a.s.l.), is situated in the eastern continuation of the active Muş graben. The Muş basin is stretching over a distance of 250 km from east to west. Several volcanic eruptions of Nemrut (2,948 m a.s.l.) separated the Lake Van from the Muş depression (Cukur et al., 2012; Deniz and Yildiz, 2007; Sumita and Schmincke, 2013b). With a surface area of 3,574 km^2 and a volume of 607 km^3, Lake Van is the fourth largest terminal lake in the world. Furthermore, it is surrounded by a large catchment area of ~12,500 km^2, which is flanked to the north and west by the Euphrates basin, to the south by the Tigris basin and to the east by the Arax basin (Huguet et al., 2012; Kuzucuoğlu et al., 2010; Landmann et al., 1992). The maximum extension of Lake Van between Tatvan and the mouth of the Bendimahi river is at about 130 km in ENE-WSW direction (Degens et al., 1984; Litt et al., 2012).

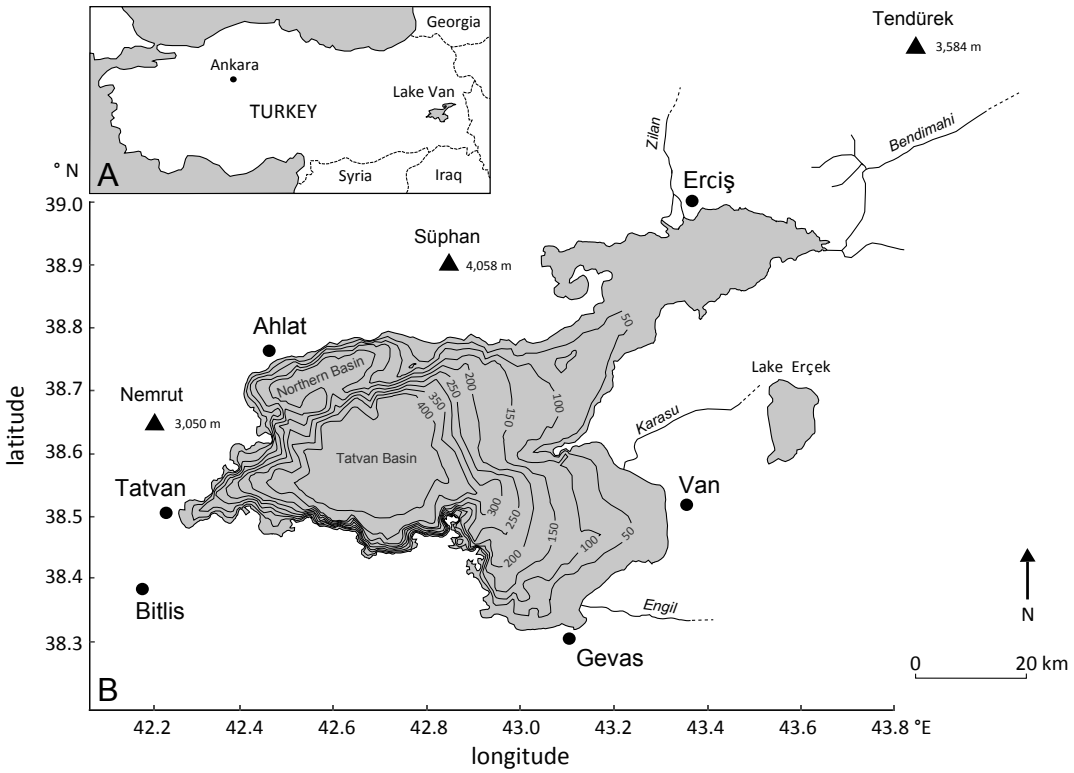

Figure 3.1: (A) Regional setting of Lake Van; (B) Bathymetric map of the Lake Van modified after Kaden et al. (2010), showing the most relevant semi-active volcanoes Nemrut, Süphan and Tendürek (▲) and major cities (•) in this region.

The Lake has two main basins, the Tatvan and the Northern Basin, which are separated by basement rises or sedimentary ridges (Ahlat Ridge), reaching depths of up to ~110 m (Kaden et al., 2010; Litt et al., 2012). The maximum water depth of the lake is about 460 m. Without any significant outflow, Lake Van get its water mainly from precipitation and snow melt inflow from several perennial rivers into the main basin (Degens et al., 1984; Huguet et al., 2011), which is shown in Figure 3.1. Furthermore, Lake Van is the largest soda lake in the world. High carbonate concentrations, volcanism and subaquatic hydrothermal exhalations are responsible for the high alkalinity (pH 9.8, salinity 21.4 ‰) of the water (Kadioğlu et al., 1997; Landmann and Kempe, 2002; Litt et al., 2012). Hence, Lake Van is characterized by a very poor amount of animal and plant species (Gessner, 1957; van Zeist and Bottema, 1991).

The climate of eastern Anatolia has a continental character with cold, wet winters and hot, dry summers resulting from the seasonal alternation of maritime subpolar and subtropical air masses (Cullen and deMenocal, 2000). Precipitation shows a strong gradient from the south-west with 600–800 mm (at high altitudes in the Bitlis mountain up to 1000 mm) to only 300–400 mm annual precipitation to the north and east of the lake (van Zeist and Woldring, 1978b). According to the distribution of precipitation, Lake Van is located in the transitional zone between two vegetation types. First, the vegetation in the south and south-west of the lake belongs to the Kurdo-Zagrosian oak steppe-forest belt, which extends from east-central Turkey to south-west Iran. Second, the steppe and desert steppe vegetation in the north and north-eastern areas is dominated by *Artemisia fragrans* with sub-Euxinian oak-forest remnants (Litt et al., 2009; Wick et al., 2003; van Zeist and Bottema, 1991; van Zeist and Woldring, 1978b; Zohary, 1973a).

3.2 Geology

3.2.1 Geology of eastern Anatolia

The eastern Anatolia region is located in a zone of complex tectonic movements, associated with the interaction of three major lithospheric plates, Arabian, African and Eurasia (Figure 3.2). Therefore, eastern Anatolia is one of several regions where an active continent-continent collision is currently taking place (Keskin, 2005; Reilinger et al., 2006).

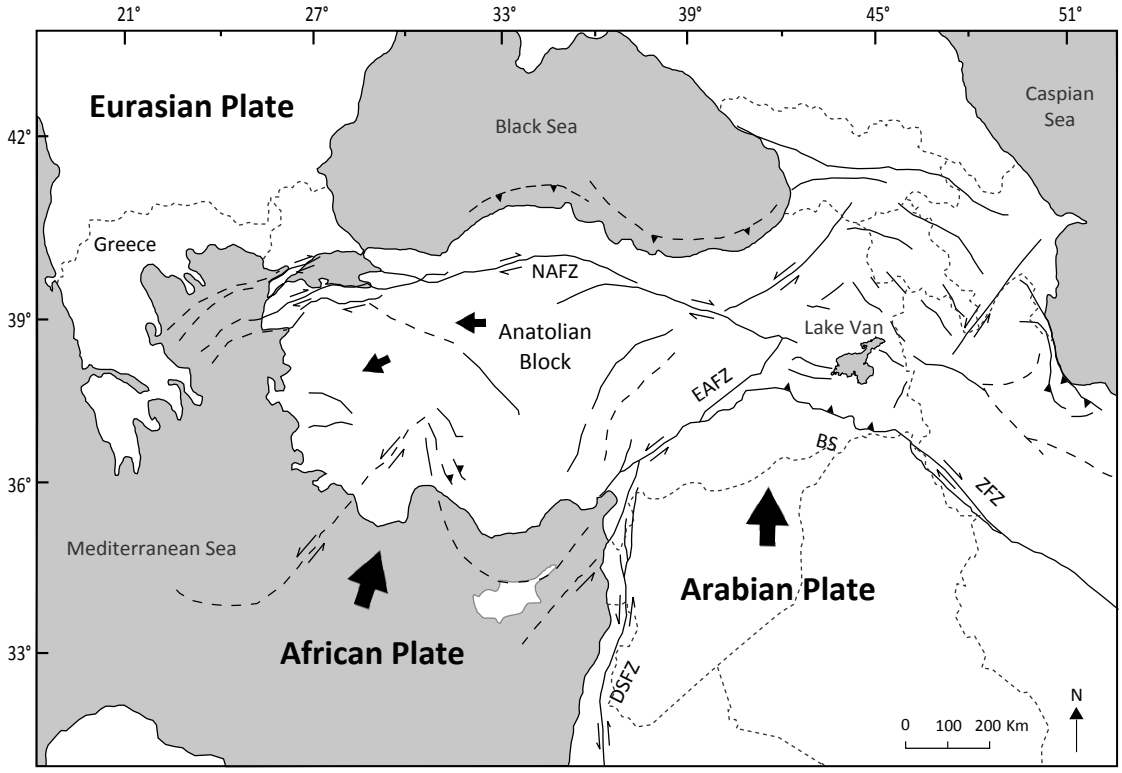

Figure 3.2: Tectonic map of Turkey showing major tectonic structures and provinces (modified from Karaoğlu et al., 2005). NAFZ: North Anatolian Fault Zone; EAFZ: East Anatolian Fault Zone; BS: Bitlis Suture; ZFZ: Zagros Fault Zone; DSFZ: Dead Sea Fault Zone.

Şengör and Yilmaz (1981) pointed out, that the convergence of the Arabian and the Eurasian plate began in the Late Cretaceous. In this connection, the Arabian plate moves in northern direction and consumed the oceanic crust of the Neo-Tethys. The process forced the Arabian plate under thrusting of the Eurasian continental margin along the Bitlis Suture and Zagros Fault Zone (BS, ZFZ), respectively (Keskin, 2005). The subduction is combined with volcanic activity, induced by the formation of Bitlis-Porturge-arc, the modern Bitlis Massif (3,500 m a.s.l.). The Bitlis trust fault is located south of Lake Van basin (Figure 3.2; Barka and Reilinger, 1997; Doğan

and Karakaş, 2013; Şengör and Yilmaz, 1981). A consequence of the closure of the Tethyan oceanic basin during the Late Eocene and the Early Oligocene was the initial contact of the Pontide arc with the Eastern Anatolia Accretionary Complex (EAAC) and Bitlis-Porturge-arc system (Figure 3.3). Another result of the closure was a crustal thickening (~25 Ma), and an abrupt uplift of the Anatolian-Iranian Plateau as a block since the Serravallian (~13-11 Ma; Keskin, 2005, 2007; Pearce et al., 1990; Şengör et al., 2003). It resulted in the highest plateaus of the Alpine-Himalaya mountain belt with an average elevation of ~2 km a.s.l. (Keskin, 2007). The uplift was followed by an extensive young volcanic activity (Keskin, 2003, 2007; Şengör et al., 2003; Yilmaz, 1990). Almost two thirds of the Anatolian-Iranian Plateau is covered by young volcanic units of collision-related volcanism (Keskin, 2007; Pearce et al., 1990; Yilmaz et al., 1998). The volcanic activity intensified and became widespread in the Late Miocene to Pliocene and continued almost without interruption into historical times (Keskin, 2007; Yilmaz, 1990). From east to west, the active volcanic centers of Ararat (double peaked with 5,165 m a.s.l. and 3,925 m), Tendürek (3,584 m a.s.l.), Süphan (4,158 m a.s.l.) and Nemrut (2,948 m a.s.l.) were developed on this plateau during the Quaternary (Karakhanian et al., 2002; Sumita and Schmincke, 2013b). The extinct volcano Incekaya, erupted ~80,000 years ago, is partly covered by the water surface today (Sumita and Schmincke, 2013b). With its large collapse caldera, fumarole activity, and the recent eruptions at 1441 AD, 1597 AD and 1692 AD, the Nemrut stratovolcano is the most interesting volcano in the region (Karakhanian et al., 2002; Özdemir et al., 2006; Pearce et al., 1990; Yilmaz et al., 1998).

As mentioned above, the Anatolia region is intensively deformed and the convergence between the Arabian and the Anatolian plates is still in progress (Yilmaz, 1990). The Anatolian plate moves nearly 25 ± 5 mm/year westwards along the two intra continental transform faults. The dextral North Anatolian Fault Zone (NAFZ - 1,300 km long), and the sinistral East Anatolian Fault Zone (EAFZ - 500 km long) are active since the Miocene (Figure 3.2; Boës et al., 2010; Bozkurt and Mittwede, 2001; Pearce et al., 1990; Reilinger et al., 2006; Yilmaz, 1990). Besides, the two strike-slip faults come together in the Karlivoa Triple Junction in the west of Lake Van (Kempe, 1977; Litt et al., 2009; Pearce et al., 1990; Yilmaz et al., 1998). In general, the eastern Anatolian region is cut by a complex of fault systems, which are trending either SE-NW or from SW-NE to SSW-NNE. Also, some E-W trending faults have been recognized in the northern margin of the Muş depression, which continuation passes Lake Van (Pearce et al., 1990). In addition, the Lake Van area is strongly affected by seismic activities. The youngest destructive and catastrophical

earthquake on October 23, 2011 (Magnitude-M_w 7.1-7.3) took place nearly 20 km away from the north-east of Van City center (Figure 3.1; Altiner et al., 2013; Sumita and Schmincke, 2013b).

3.2.2 Catchment area of Lake Van

The basement of the Anatolian-Iranian Plateau composed of several former micro-continents. The so-called terranes were amalgamated and intensely deformed during the Alpine orogeny when the Arabian plate collided with the Eurasian plate in the Late Cretaceous to the Early Tertiary (Keskin, 2007; Okay, 2008). These micro-continents are now separated from each other by ophiolite belts and accretionary complexes (Keskin, 2007), produced by progressive consumption of Tethyan oceanic lithosphere (Yilmaz, 1990). Keskin (2005, 2007) and Şengör et al. (2003) divided these terranes and the accretionary complex into five tectonic units (Figure 3.3).

From the north to the south, these are:

The eastern Rhodope-Pontide fragment is located in the northern part of the eastern Anatolia region (Keskin, 2007). This unit is formed by a north-dipping subduction under the Eurasian continental margin from the beginning of the late Cretaceous to the end of the Eocene (Pearce et al., 1990). The complete closure of the Neo-Tethys resulted in the Izmir-Ankara-Erzincan suture (AES), and marks the boundary between the Pontide belt and the Anatolian plate (Okay, 2008). This northern terrane have a paleozoic metamorphic basement (granulite, gneisses) overlain by mesozoic sediments. Pliocene and quaternary volcanic deposits from the Nemrut and Süphan volcanoes complete the first tectonic unit of the upper part (Keskin, 2007; Pearce et al., 1990; Özdemir et al., 2006; Yilmaz et al., 1998).

The North-West Iranian fragment is characterized by volcanic units. This complex is visible in Armenia, and composed of a heterogeneous rock sequence of phyillitic, plagiogranite- and granite-migmatitic lithologies (Keskin, 2007).

The East Anatolia Accretionary Complex (EAAC) is located in the middle of the eastern Anatolia region between the Aras River in the north and the Bitlis-Poturge Massif in the south of Lake Van (Keskin, 2007). The EAAC forms a 150-180 km wide SE-NW extending belt (Keskin, 2007). It represents the remnant of a huge subduction-accretion complex, which was formed by a north-dipping subduction zone located between the Rhodope-Pontide fragment and the Bitlis-Poturge Massif (Keskin, 2007). Additionally, the EAAC consists of massive limestones (late Cretaceous) intercalated with ophiolitic mélange and flysch sequences (Paleocene to late Oligocene; Keskin, 2003, 2005). Tertiary and quaternary conglomerates, carbonates, and sandstones occur in the eastern part of the lake (Degens and

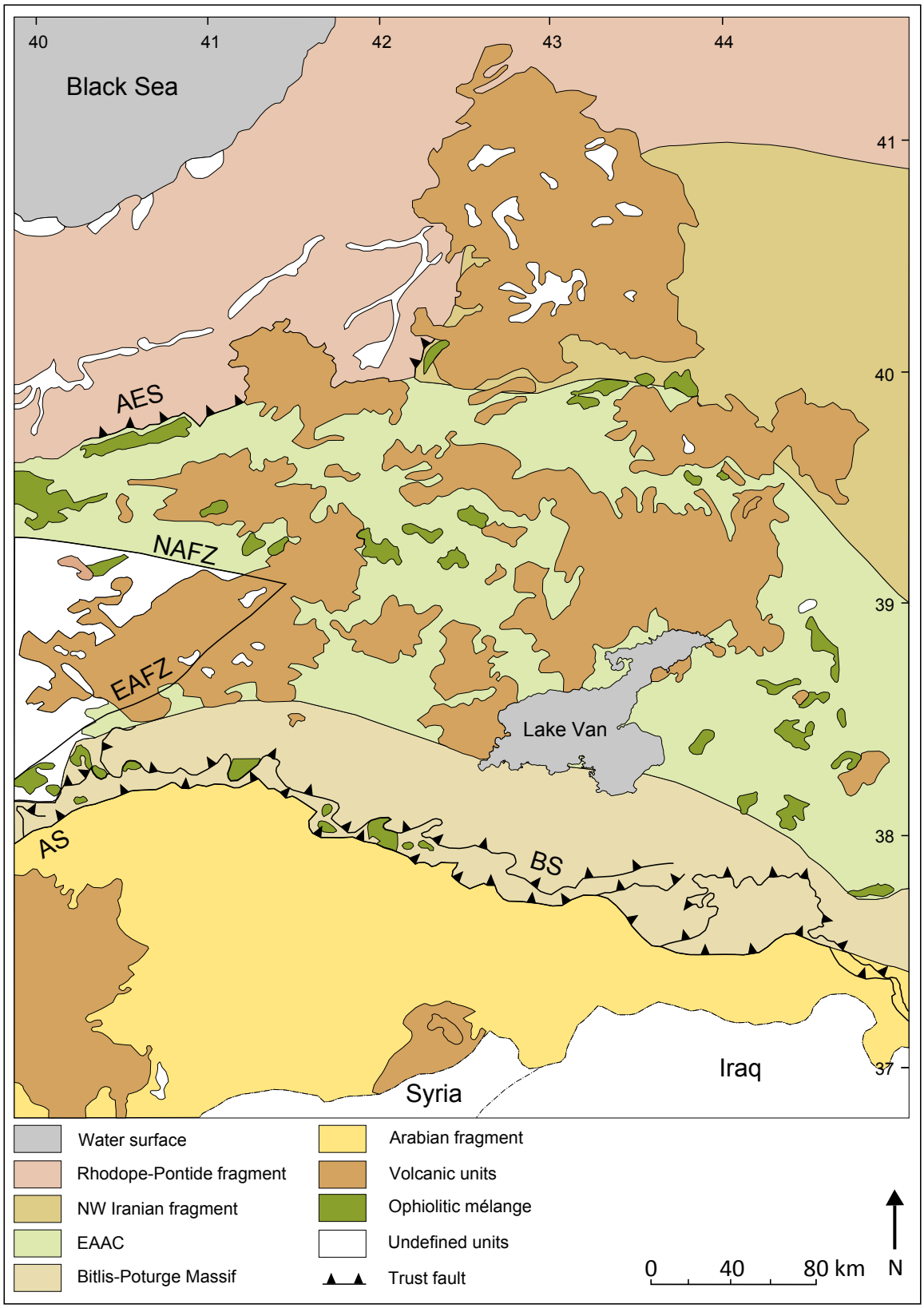

Figure 3.3: Geological map of the tectonic units in the eastern Anatolia region after Keskin (2005). Ankara-Erzincan suture (AES); Assyrian suture (AS); Bitlis suture (BS); Eastern Anatolian Accretionary Complex (EAAC); East Anatolian Fault zone (EAFZ); North Anatolian Fault Zone (NAFZ).

Kurtman, 1978; Lemcke, 1996).

The Bitlis-Poturge Massif (at ~3,000 m) in the southern part of Lake Van is presented by a SE-NW extending belt along the eastern Taurus mountain range (Kuzucuoğlu et al., 2010). This allochthonous tectonic block consists of metamorphic rocks (gneiss, mica schists) and is partly covered by paleozoic (Permo-Carboniferous) sequences and igneous units (Keskin, 2007; Lemcke, 1996; Pearce et al., 1990; Valeton, 1978).

The autochthonous unit of **the Arabian foreland** was separated from the Anatolian plate by the southern branch of the Neo-Tethys. Today the Neo-Tethys is contemporary represented by the Assyrian suture (AS; Keskin, 2007; Okay, 2008; Şengör and Yilmaz, 1981). It is characterized by a continuous stratigraphic sequence of shelf sediments of the early Palaeozoic to Miocene (Pearce et al., 1990).

3.3 Present climate conditions

The present climate condition of the eastern Anatolia region reacts sensitive to the gradient and northward displacement of the Intertropical Convergence Zone (ITCZ), which strongly influence the positions of the three main atmospheric circulations (Figure 3.4). First, by the position of the atmospheric westerly jet stream of the north and north-west. Second, by the northern branch of the subtropical high pressure systems that generally extends from the Atlantic Ocean across the Sahara. Third, by the high-latitude Siberian high pressure system, with a decreasing influence of the Mediterranean Sea as a supplier of moisture during the winter season.

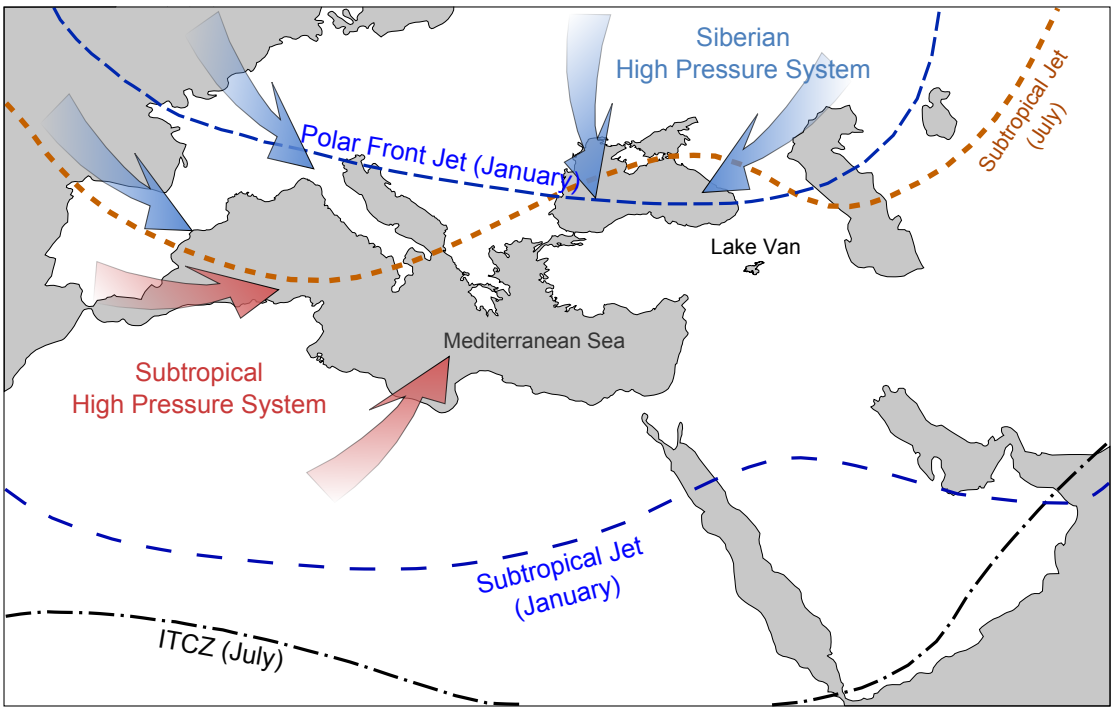

Figure 3.4: The mean position of the atmospheric circulations that influenced the climate in winter and summer in the Mediterranean region after Akçar and Schlüchter (2005); Intertropical Convergence Zone (ITCZ).

The local climate at Lake Van has a continental character with a strong seasonality, expressed in cold winters (December to February) and warm summers from July to September. The average temperature range between 22°C in July and below 0°C in January (Table 1). Due to the high salinity and the great depth of the lake, there is no possibility of ice formation on the lake surface (Huguet et al., 2011, 2012).

Table 1: Modern meteorological data at Lake Van (see Figure 3.1 for the locations). The data were provided by the Turkish State Meteorological Service. Observation period: 1975-2008.

Station	Coordinates			Mean temperature [°C]			Mean precipitation [mm]		
	Latitude °N	Longitude °E	Altitude m a.s.l.	January	July	Year	January	July	Year
Ahlat	38°48'	42°30'	1750	-3	21,9	8,9	50	6	572
Erciş	39°2'	43°22'	1750	-6	21,8	7,7	31	7	421
Van	38°27'	43°19'	1661	-4	22,2	9,0	35	4	385
Bitlis	38°24'	42°06'	1550	-2	22	9,4	161	5	1,232
Tatvan	38°30'	42°17'	1690	-3,2	21,9	8,7	95	7	816

In summer, the ITCZ is at its northern position, so that the subtropical high-pressure system controls the westerlies. During this period, the prevailing moist westerly winds shifts northward, and the sinking air masses of the subtropical high pressure system is responsible for warm and dry conditions to the entire Mediterranean region (Litt et al., 2012; Vannière et al., 2011). Therefore, the moisture-bearing winds from the Mediterranean does not reach eastern Anatolia, creating dry climatic conditions in the interior plateaus in summer (Roberts and Wright, 1993; van Zeist and Bottema, 1991). During the winter season, the southern position of the ITCZ allows storm tracks, consists of cold air masses from the polar North Atlantic and the North Sea, moving over the Mediterranean Sea (Vannière et al., 2011). As a result, the air masses become saturated with a secondary moisture and travelling eastward over land towards the eastern Anatolia region. Finally, the atmospheric precipitation falls as snow during the winter period and increases as rainfall towards spring (Akçar and Schlüchter, 2005; Roberts and Wright, 1993; Türkeş, 1996). Furthermore, the Lake Van area is affected by cold air masses from the continental Asia controlled by the Siberian high circulation during the winter (Akçar and Schlüchter, 2005).

In general, the moisture transport represents an important parameter for the distribution of regional precipitation. One significant aspect is the absence of mountain barrier south of the Alps, which allows the supplementary moisture by the Mediterranean Sea extending eastwards (Roberts and Wright, 1993). In addition, the east-west oriented mountain chains, which range along the northern (Pontic mountain) and south-western (Taurus mountain) coasts of the Anatolia Peninsula, act as an effective orographic precipitation barrier to moisture-bearing winds. For this reason, it has a great influence on the amounts of total rainfall, which decrease from the coastal belts to the interior of eastern Anatolia (Cullen and deMenocal, 2000; Stevens et al., 2012; Türkeş, 1996; van Zeist and Bottema, 1991). In addition, the mountain ranges are the principal precipitation control for the Lake Van region and determine the abundance and intensity of rainfall.

Due to the location in the rain shadow, the Lake Van region represents a strong spatial gradient from south-west to north-east. Along the Bitlis Massif, at the southern and south-western slopes of the lake, the total amounts of precipitation may receive up to 1200 mm/year, whereas the precipitation in the northern part of Lake Van region does not exceed 400 mm/year (Table 1). The diverse topography and the distribution of rainfall explain the pronounced differences in the vegetation cover at Lake Van (see section 3.4).

3.4 Recent vegetation of eastern Anatolia

Vegetation and biodiversity of eastern Anatolia has been studied by Louis (1939), Walter (1956), Zohary (1973a,b), van Zeist and Woldring (1978b), Frey and Kürschner (1989); van Zeist and Bottema (1991) and is also part of "Flora of Turkey" by Davis (1965). According to Kaya and Raynal (2001) and Zohary (1973a), the vegetation of Turkey can be divided into three important phytogeographic and ecological regions, from north to south, the Euro-Siberian-, Irano-Turanian-, as well as the Mediterranean floristic region.

In accordance with the present climate conditions (see section 3.3), each floristic region can be distinguished by their various vegetational aspects, reflecting different climate conditions (Davis, 1965; Kaya and Raynal, 2001).

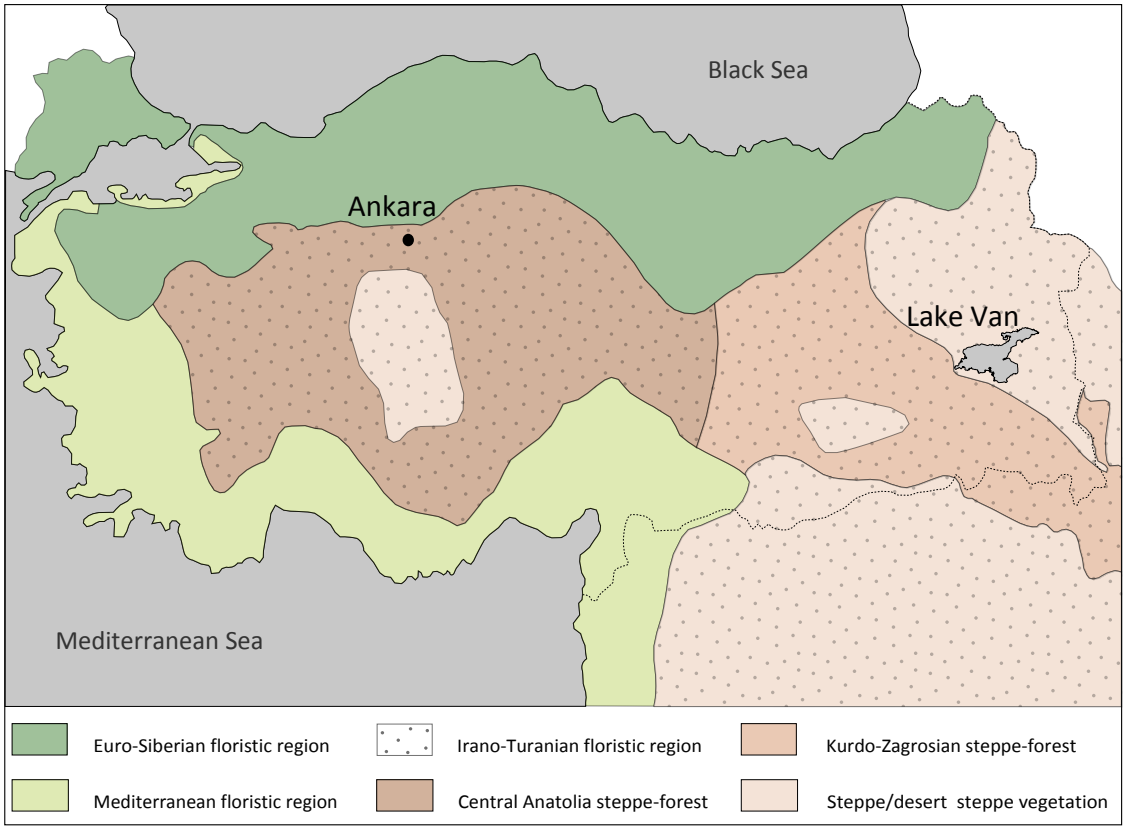

Figure 3.5: Distribution of vegetation zones in Turkey simplified after Kaya and Raynal (2001); Zohary (1973a,b). The Euro-Siberian floristic region includes the Pontic provinces and the Eu-, Sub-, and Xero-Euxinian subprovinces. The Irano-Turanian floristic region is divided into steppe and desert steppe vegetation with mosaics of Sub-Euxinian oak forest remnants. The Mediterranean floristic region is composed of the Mediterranean woodland climax and the Mediterranean subalpine forest.

The Turkish flora is the richest in endemics in the Middle East. High diversity of endemic species, cause by the clutching mountain ranges of the country, is found in the Mediterranean and the Irano-Turanian areas (Davis, 1965; Kürschner et al.,

1995; Walter, 1956). The latter consists of 70-80% of endemic species, whereas the Mediterranean region consists of about 50% of endemics. Zohary (1973a) highlighted a number of 1,800 endemic species, including the Leguminosae, Liliaceae, Euphorbiaceae, Ranunculaceae, Rosaceae and many more. Furthermore, the vegetation in eastern Anatolia is strongly influenced by human-induced degeneration of the woodland and by agricultural activity (Huguet et al., 2012; Wick et al., 2003). The human activities in the Lake Van area can be reliably dated back to 3.8 ka BP (Litt et al., 2009; Wick et al., 2003). In particular, grazing with goats, sheep, horses and camels have exercised their destructive influence on the vegetation for a long time. Moreover, the Anatolia region is characterized by the cultivation of fruits, vegetables and cereals and of former timber, pasture and farmland with secondary forest, mostly of shrubs with juniper, oak, wild fruit, elm, pine and maple (Davis, 1965; Louis, 1939).

3.4.1 Distribution of phytogeographic vegetation zones

Euro-Siberian floristic region

The Euro-Siberian region extends, together with the Pontic province (Eu-, Sub-, and Xero-Euxinian subprovinces; Davis, 1965; Kaya and Raynal, 2001; Zohary, 1973a,b), along the Black Sea coastal region and the Marmara region of Turkey (Figure 3.5). The southern boundary of the Euro-Siberian region is located at the northern slopes of the Pontic mountains (North Anatolia; Kaya and Raynal, 2001).

Due to the high average precipitation (>1,000 mm/year) along the southern coastal belt of the Black Sea, this floristic region consists predominantly of mesophytic vegetation. Deciduous forest, phanerophytes and hemicryptophytes are abundant (Davis, 1965; Kaya and Raynal, 2001). The eastern Black Sea region (up to ~800 m a.s.l.) is covered by a temperate summer-green forest of *Abies nordmanniana*, *Pinus sylvestris*, *P. nigra*, *Alnus glutinosa*, *Castanea sativa*, *Corlyus*, *Fagus orientalis*, *Picea orientalis* and *Tilia rubra* (Kaya and Raynal, 2001; Shumilovskikh et al., 2012; van Zeist and Bottema, 1991).

Irano-Turanian floristic region

The Irano-Turanian floristic region is the largest of the three phytogeographical areas in Turkey (Davis, 1965). Figure 3.5 illustrates the distribution of the Irano-Turanian zone from central Anatolia to the eastern and south-eastern Anatolia region (Kaya and Raynal, 2001). In addition, the Irano-Turanian subregions include the Syrian Desert, North Iraq, Iran, West Pakistan, and Afghanistan (Davis, 1965).

The vegetation has been described as one of the richest flora in the Near East, associated with high diversity, high endemism, and a complex specialization of several species (Djamali et al., 2012b; Zohary, 1973a,b). In general, the Irano-Turanian floristic region can be distinguished into two major vegetational zones: (i) the Kurdo-Zagrosian steppe-forest, represented by juniper, deciduous oak and pistachio, with a well-developed herbaceous ground cover in the south and south-west of the lake; and (ii) the dwarf-shrub steppe or desert steppe vegetation (treeless steppe) characterized by *Artemisia* species, especially *Artemisia fragrans* in the northern and north-eastern Lake Van region (Wick et al., 2003; van Zeist and Woldring, 1978a; van Zeist and Bottema, 1991; Zohary, 1973a,b). These differences in the vegetational cover demonstrate a strong spatial gradient in the distribution of moisture, which was described in detail in section 3.3.

The **Kurdo-Zagrosian oak steppe-forest** extends from the south-eastern Taurus mountains, including the Bitlis Massif (SW shore of Lake Van), to the southern part of the Zagros mountains (SW Iran; Kaya and Raynal, 2001; van Zeist and Woldring, 1978a; Zohary, 1973a). Frey and Kürschner (1989) describe this zone as 'mixed formation of cold-deciduous broad-leaved montane woodland and xeromorphic dwarf-shrublands´. Depending on exposure, dwarf-shrub formations (e.g. *Astragalus* and *Gypsophila* species) of the subalpine region occur above the timber line (2,500-2,700 m), which is characterized by the occurrence of *Betula verrucosa* (Frey and Kürschner, 1989; van Zeist and Bottema, 1991; Zohary, 1973a). The herbaceous vegetation of the Kurdo-Zagrosian forest consists of a dense ground cover of steppic taxa such as Gramineae, Cruciferae, Chenopodiaceae, *Ranunculus* spp., and *Rumex* sp. (Altiok and Behçet, 2005; Celenk and Bicakci, 2005; Karabacak and Behçet, 2007).

In particular, the *Quercetea brantii* forest consists mainly of: *Quercus brantii*, *Q. infectoria*, *Quercusboissieri*, *Acer monspessulanum*, *A. cinerascens*, *Pyrus syriaca*, *Pistacia atlantica*, *Juniperus oxycedrus*, as well as *Quercus ithaburensis*, *Q. libani*, *Q. robur*, *Q. petraea*, *Q. mannifera*, *Acernegundo*, *Juglans regia*, *Frangula alnus*, *Fraxinus angutifolia*, *F. rotundifolia*, *Pistacia eurycarpa*, *P. khinjuk*, *Rhamnus kurdicus*, *R. cornifolius*, *Ulmus campestris*, *Tamarix smymensis* and various Rosaceae with *Amygdalus* sp., *Crataegus* ssp., *Malus* ssp., *Prunus* ssp., *Pyrus* spp. (Altiok and Behçet, 2005; Celenk and Bicakci, 2005; Kaya and Raynal, 2001; Zohary, 1973a).

The distribution of the **Irano-Turanian steppe / desert steppe vegetation** focuses on the north and north-east region of Lake Van. After Frey and Kürschner (1989) and van Zeist and Bottema (1991), the dwarf-shrub vegetation might be originally covered a *Stipa-Bromus* steppe, which has been replaced by an *Artemisia*

steppe formation due to intensive grazing and agriculture by human activity. This treeless steppe vegetation is mainly dominated by *Artemisia fragrans* and different species of chenopods, which are associated with *Astragalus* spp., *Centaurea* spp., *Gypsophila, Cerastium, Silene, Stachys, Hypericum, Arenaria, Achillea, Rumex, Thymus, Alyssum, Thalictrum* and with some Sub-Euxinian oak forest elements (Mayer and Aksoy, 1986; van Zeist et al., 1975; Zohary, 1973a)

Mediterranean floristic region

The sub-humid to humid Mediterranean floristic region encompasses a narrow belt along the Mediterranean coast of Israel, Lebanon, Syria and Turkey, with the coastal belt of the Marmara Sea and the Aegean (Kaya and Raynal, 2001). According to Zohary (1973a,b), this landscape is characterized by a large number of thermophilous, sclerophyllous evergreen species, geophytes, phanero- and chamaephytes. Hence, the Mediterranean floristic region contains taxa such as *Quercus calliprinos*, *Q. cerris*, *Q. boissieri*, *Pistacia palaestina* and *Pyrus boissieriana*, which alternates with *Pinus brutia*. In some areas it can be overshadowed by *Genista acanthoclada*, *Cistus creticus*, *C. salviifolius*, *Daphne sericea*, *Fumana thymifolia*, and several more.

4 Material and methods

4.1 Drilling campaign

A complete succession of lacustrine sediment cores was obtained during the International Continental Scientific Drilling Program (ICDP) 'PALEOVAN' from 2^{nd} July to 23^{rd} August 2010, funded by the Deutsche Forschungsgemeinschaft (DFG), the Swiss National Science Foundation (SNF) and the Scientific and Technological Research Council of Turkey (Tübitak). DOSECC (Drilling, Observation and Sampling of the Earths Continental Crust), as the operator of the deep drilling, developed the new Deep Lake Drilling System (DLDS), which was specifically designed for coring sediments from deep lakes. Based on the previous seismic survey in 2004 (Litt et al., 2009), two sites were retrieved, Ahlat Ridge (AR) and Northern Basin (NB), at water depths of 360 m and 245 m (Figure 4.1).

The prospected and most important drill site AR (38°66'N; 42°67'E) is located on a low sedimentary ridge at the northern edge of the 440 m deep Tatvan Basin. Ahlat Ridge site was chosen for the drilling campaign in order to retrieve continuous and

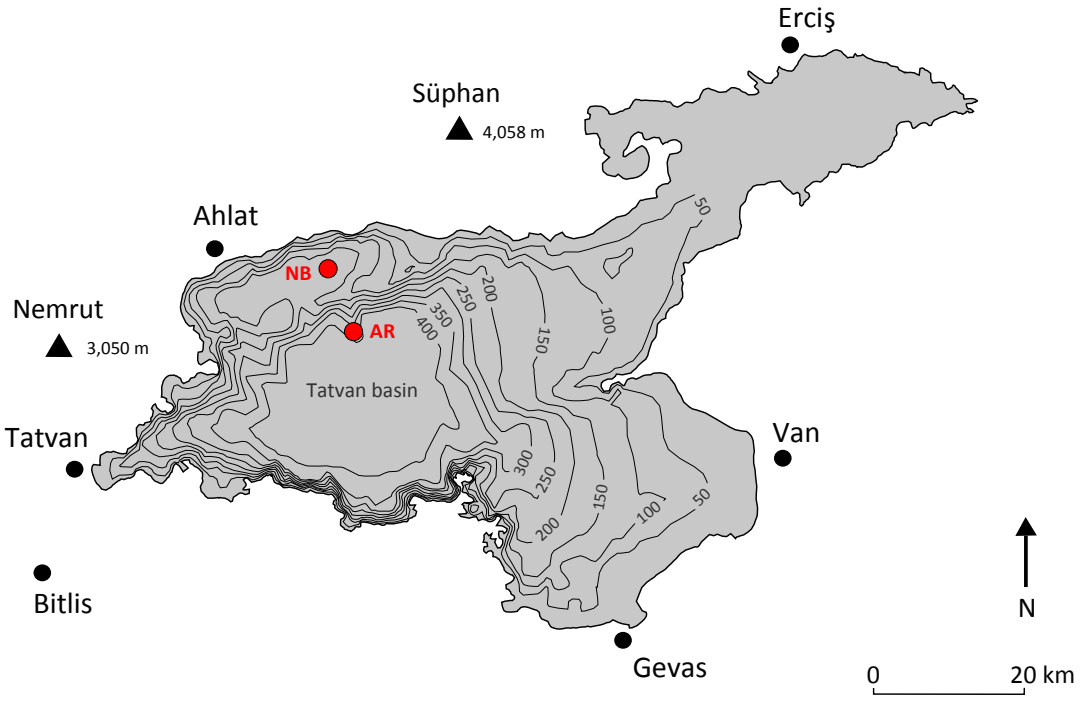

Figure 4.1: Locations of the two drill sites Northern Basin (NB) and Ahlat Ridge (AR), marked by red dots.

undisturbed sequences. The location was cored multiple times up to 219 m below lake floor (mblf) with a total of seven overlapping cores, shown in Table 2. During the drilling operation, a total of 637 m was retrieved with an average discovery of 86% (Stockhecke et al., subm). Furthermore, the sediment record reached the rock basement of the lake, which is in detail described by Litt et al. (2012). The drilling was carried out by using a variety of soft sediment sampling tools (Hydraulic Piston Core 'H', Extended Nose, non-rotating 'X', and Extended Core Bit, rotating 'A'). Furthermore, most of the drilling tools are designed to collect cores within plastic liners that have a diameter of 60 mm and a length of 3 m.

Table 2: Core recovery of the drill location Ahlat Ridge (AR), including the holes (A-Z), drilled depth in meter composite below lake floor (mcblf), drilled length in meter (m) and core recovery in percentages (%).

Site	Hole	Drilling depth [mcblf]	Drilled length [m]	Recovery [%]
AR	A	0-33	33	99
	B	33-121	88	79
	C	116-127	11	59
	D	2-118, 132-217	201	75
	E	2-102	100	87
	F	102-117,130-218	103	84
	G	108-124, 135-219	100	76
	Z	0-1	1	100

Sediment cores were opened and stored at an Integrated Ocean Drilling Program (IODP) core repository located at the University of Bremen's Center for Marine Environmental Sciences (MARUM). During the sampling campaign in spring 2011, the cores were split along the median line in two halves. After opening, one part of the section (working half) has been used for core descriptions, correlation, construction of a composite record and sampling, e.g. for physical properties, stable isotopes and palynological investigations. The other section half was used for non-destructive analyses, especially for measurements of magnetic susceptibility, XRF (X-ray fluorescence) scanning and photographing, and achieved subsequently.

4.2 Lithology

The continuous sedimentary section consists of laminated lacustrine clayey silt deposits of about 76%, reflecting the background sedimentation. In addition, the lamination was either interrupted by volcaniclastic (~17%) or fluvial deposits (~2%; turbidite), pointing to depositional events of allochthonous and reworked lacustrine material, respectively. Furthermore, environmental processes such as tectonic and volcanic activities also had influence on the annually sedimentation. In this case, six major sediment types were distinguished, separated from approximately 300 volcaniclastic deposits (V) from the neighbouring volcanos Nemrut and Süphan and from ~375 event deposits (Stockhecke et al., subm). Overall, the Ahlat Ridge sequence consists of 17% (37 m) tephra layers. The thickness varies from several meters to <1 mm (Stockhecke et al., subm; Sumita and Schmincke, 2013a,b).

The recovered laminated sedimentary record is colorful and, after oxidizing of several hours, displays a variety of shades between dark-brownish, brownish, reddish-brown, light-brownish, greenish, greyish, cream and white (Table 3). In analogy to the recent depositional conditions in Lake Van, described in Stockhecke et al. (2012), the laminae are defined as varves. The annually sedimentary depositions occur as a result of seasonal temperature changes, in particular, due to the variations in the erosion of the catchment and the biological productivity (Moore et al., 1991; Saarnisto, 1986). Especially, the onset and the end of a seasonal accumulation indicate abrupt changes in the climate conditions. Anoxic conditions at the bottom of Lake Van prevent degradation of organic matter and preserve the annually lamination from bioturbation (Kaden et al., 2010).

Table 3: Sedimentological description of the Ahlat Ridge composite record for the uppermost 60 mcblf (meter composite below lake floor), with lithological units after Stockhecke et al. (subm).

Unit	Depth [mcblf]	Color	Lithological description
I	0.00-6.60	brown, dark brown, reddish brown, beige, greenish	Laminated clayey silt (Ll)
II	6.60-12.90	grey	Transition from banded clayey silt (Lb) to faint laminated clayey silt (Lf), with intercalations of faint laminated and mottled clayey silt (LfLmo)

(continue on next page)

Table 3: continued from previous page

Unit	Depth [mcblf]	Color	Lithological description
III	12.90-14.78	grey, brown, creme	Sucession of laminated, faint laminated and mottled clayey silt (LlLfLmo) with laminated, faint laminated and banded clayey silt (LlLfLb)
	14.78-17.96		Nemrut Formation (ash layer)
	17.96-24.31	grey, brown, creme	Sucession of laminated, faint laminated and mottled clayey silt (LlLfLmo) with laminated, faint laminated and banded clayey silt (LlLfLb)
IV	24.31-27.91	brown, creme	Laminated (Ll) and banded clayey silt (Lb)
	27.91-29.11		Halepkalesi Pumice (HP-10; ash layer)
	29.11-30.00	brown, creme	Laminated (Ll) and banded clayey silt (Lb)
V	30.00-35.62	grey	Sucession of faint laminated and mottled clayey silt (LfLmo)
VI	35.62-36.96	brown, greenish, creme	Laminated clayey silt (Ll) intercalated with banded clayey silt (Lb)
	36.96-39.04		Incekaya-Dibekli (ash layer)
	39.04-39.66	brown, greenish, creme	Laminated clayey silt (Ll) intercalated with banded clayey silt (Lb)
	39.66-40.31	reddish brown, dark brown	Laminated clayey silt (Ll)
	40.31-41.91	greenish, creme	Laminated clayey silt intercalated with graded beds (LlLg)
VII	41.91-46.37		Banded clayey silt (Lb) intercalated with graded beds (Lg); calcarous nannofossils; ostracods
VIII	46.37-51.31	grey, greenish, dark brown, creme	Laminated clayey silt (Ll) intercalated with graded beds (LlLg) and massive clayey silt (Lmc)
IX	51.31-56.19	beige	Banded clayey silt (Lb); ostracods

(continue on next page)

Table 3: continued from previous page

Unit	Depth [mcblf]	Color	Lithological description
X	56.19-60.75	creme, dark brown, greenish, grey	Laminated clayey silt (Ll) with intercalations of graded beds (Lg)
XI	60.75-65.80	creme	Banded clayey silt (Lb) with rusty mottled clayey silt (Lmo)

The light carbonate clayey layer, mainly aragonite and calcite, indicates carbonate precipitation in spring and early summer controlled by Ca-rich freshwater inflow. In contrast, the dark carbonate-poor layer consists of high organic material, representing the bloom of phytoplankton from the late summer and the autumn (Lemcke, 1996; Saarnisto, 1986; Stockhecke et al., 2012). According to Litt et al. (2009) and Stockhecke et al. (subm), laminated clayey silts have been deposited during interglacial/interstadial periods, whereas the absence of any lamination and the occurrence of banded, massive and mottled clays characterize low seasonality during glacial-stadial phases. Further detailed descriptions and interpretation of the lithological units are described in Stockhecke et al. (subm).

4.3 Chronology

For the correlation of the sedimentary records, characteristic sequences such as pronounced sediment layers, slump structures, turbidities, volcaniclastic, micro-deformations were used. After the core description and correlation, a composite profile of a total length of 218.92 mcblf (meter composite below lake floor) was constructed. For the constraining of the age model (Table 7, Appendix), reworked and allochthonous deposits (volcaniclastics and events layer) were removed from the composite profile in order to obtain a 174 meter long corrected 'no-Event' depth scale in 'meters composite below lake floor-no Events' (nE-mblf; Stockhecke et al., 2013).

The age model of the event-corrected sedimentary record was based on varve counting (Landmann et al., 1996a; Lemcke, 1996), sedimentary sequences (Stockhecke et al., subm), confirmed by radiocarbon age dating, magnetostratigraphy (e.g. Laschamp and Blake excursions; details in Vigliotti et al., subm), and cosmogenic isotopes. The identification and dating, using the single crystal $^{40}Ar/^{39}Ar$ method, of six volcaniclastic layers was done to improve the chronology (Stockhecke et al., 2013). Furthermore, some proxy data were selected to establish the age model, for instance, the total organic carbon (TOC; details in Stockhecke et al., subm), the calcium/potassium-ratio measured by X-ray fluorescence (details in Kwiecien et al., subm) and the arboreal/non-arboreal pollen-ratio (details in Litt et al., subm). Therefore, the chronology was consolidated by using 'control points' derived from visual synchronization with the GICC05-based NGRIP isotopic record (NGRIP, 2004; Steffensen et al., 2008; Svensson et al., 2008; Wolff et al., 2010) for the period between 0 and 116 ka BP, the spelothem synthetic Greenland record (GLT-syn; Barker et al., 2011) for the interval 116-400 ka BP and the EDC record (European Project for Ice Coring in Antarctica Dome C ice core) for the section between 400 and 600 ka BP (EPICA, 2004; Jouzel et al., 2007). All ages for the Lake Van record are cited in thousands of years before present (ka BP; where 'present' is defined as AD 1950). Overall, the contribution of several independent methods established one robust chronology of the Lake Van record, encompassing the last 600 ka. General information about the construction of the age model of Lake Van is discussed in Stockhecke et al. (subm).

4.4 Palynological analyses

For the palynological and paleoenvironmental research of this study, encompassing the last glacial-interglacial cycle, the upper 60 mcblf of the following sediment cores: 5034/2A/1H/1 to 5034/2A/10H/1 (0.317 to 27.003 mcblf), 5034/2D/1H/2 to 5034/2D/20H/2 (3.791 to 59.697 mcblf), 5034/2E/3H/1 to 5034/2E/18A/2 (9.317 to 56.095 mcblf), and 5034/2B/1H/3 to 5034/2B/10H/2 (36.175 to 60.093 mcblf) were analysed. A total of 264 sub-samples were selected from the composite profile (0.317 to 60.093 mcblf) with an average distance between each sub-sample of 20 cm (average c. 525 years; Table 7, Appendix). For the chemical treatment, each sample had a specific sediment volume of 4 cm^3. In order to calculate the absolute pollen concentration, *Lycopodium clavatum* tablets (Batch No. 483216; 18,583 spores/tablet; Department of Quaternary; University of Lund, Sweden) were add to each sample (Stockmarr, 1971).

The standard preparation of pollen samples, followed by Faegri and Iversen (1989), includes the treatment with hot hydrochloric acid [HCL] (10 %) to remove carbonates, hot potassium hydroxide solution [KOH] (10 %), sieving with >200-µm mesh size to remove coarse sediment particles, treatment in cold hydrofluoric acid [HF] (40 %) to remove silica minerals, hydrolysis of cellulose with hot acetolysis mixture consists of nine parts of concentrated acetic anhydride [$C_4H_6O_{3\,(conc.)}$] and one part of concentrated sulphuric acid [$H_2SO_{4\,(conc.)}$], glacial acetic acid, and lastly ultrasonic sieving (10-µm mesh size) for final cleaning and to concentrate the palynomorphs. After neutralization, the remaining suspension was stored in anhydrous glycerol [$C_3H_8O_3$], stained with safranin. Pollen grains were counted by using a Zeiss Lab.A1 light microscope (AX10) at x 400 magnification.

The pollen reference collection of the Steinmann-Institute, Department of Paleobotany, was utilized for the identification of palynomorphs. In addition, the pollen and spore nomenclature of different circum-Mediterranean descriptions by Beug (2004), Moore et al. (1991), Punt (1991) and the pollen atlas of Reille (1999) were used. For each sub-sample, a minimum sum of 500 identifiable pollen grains was counted for the terrestrial pollen sum (100 %), including coniferous and broadleaved species (arboreal pollen) and herbaceous land plants (non-arboreal pollen). Pollen grains of bryophytes, pteridophytes, algae and aquatic taxa were excluded. Three samples (LV10-14, LV10-35 and LV10-39) had only total counts between 350 and 400 pollen grains due to low pollen concentrations. Moreover, they were not considered further in the pollen record, because of their poorly preserved pollen preservation. In general, corroded, concealed or unknown pollen grains, which essential morphological features cannot be assigned to known pollen types are defined as indeterminable

pollen (indet.). Determinable pollen grains were specified to the lowest possible taxonomic level.

The microcharcoal particles were identified based on diagnostic criteria, primarily by the jet black color with straight edges, and with the presence of a blue hue on edges. Finally, the pollen concentration, the charcoal particles (>20 µm) as well as pollen grains of bryophytes, pteridophytes, algae and aquatic taxa were illustrated in concentrations (grains; particles/cm^3).

The pollen diagrams shown in Figure 5.1 and 7.1 (Appendix) were constructed and plotted in TILIA software, version 1.7.14 by Eric C. Grimm (2011; Illinois State Museum, Springfield). The results of the pollen analyses are expressed as percentages values of the total pollen sum. A ten-fold exaggeration of the horizontal scale is used to show changes in low percentages of some taxa. For the sake of convenience, the pollen diagram was divided into pollen assemblage zones (PAZ) using visual inspection and examined by the constrained cluster analysis sums of squares (CONISS; Grimm, 1987). A pollen assemblage zone was assigned based on changes in the arboreal/non-arboreal (AP/NAP) composition as well as by changes in the relative frequency of individual taxa. Table 4 presents a short description of the pollen assemblage zones.

4.4.1 Principles and methods of the past flora reconstructions

The study of pollen grains and spores is by far the most common method for gaining information of past vegetation, climate conditions of the environment and human activities during the Quaternary period (Birks and Birks, 1980; Davis, 1963; Faegri and Iversen, 1989; van Zeist and Bottema, 1991). Pollen assemblages have been reconstructed from several locations with a large database from different regions of the world (Davis, 2000). A fundamental object in palynological investigations is to identify and to define the pollen source area (Sugita, 1994). Plants and thus the pollen productivity and pollen dispersal are subject to certain environmental requirements such as temperature as well as the amount of precipitation. Therefore, it is possible to reconstruct the pollen source area due to the specific interaction between environmental conditions and vegetation in geological archives, for instance, in lake sediments. However, several essential characteristics for the reconstructions of past vegetation need to be considered, including the production of pollen grains, the dispersion and deposition of pollen, and the quality of the sedimentary archive (Faegri and Iversen, 1989; Sugita, 1993). In addition, several studies of Birks and Birks (1980), Prentice (1985), Sugita (1993); Sugita et al. (1997), Tauber (1965) and others, have shown that not only the size of the sedimentary basin has an effect on

representation of past vegetation, but also turbulences of the atmosphere, wind speed and direction as well as height and strength of the pollen source area. The larger the lake is, the wider the pollen source area becomes and the mixing of pollen from various distances occurs (Moore et al., 1991; Prentice, 1985; Sugita, 1993). It can be concluded that very large lakes with several kilometers in diameter, such as Lake Van (~130 km in ENE-WSW direction), are dominated by regional pollen (Davis, 2000). Therefore, the extent and position of the vegetation changes in relation to the sedimentary archive has an important influence of the vegetational composition in the pollen record (Sugita et al., 1997; Tauber, 1965).

For the reconstruction of past vegetation, the method of pollen analysis has many advantages and disadvantages that have to be considered. In general, pollen diagrams reflect, at least indirectly, the vegetation that grew in the region at a certain time, while the sediments were deposited (Davis, 1963). But a complete species list for the past flora can never be obtained in the fossil record, because some plants produce pollen that was not preserved in the sediments (Birks and Birks, 1980). However, differences in pollen productivity and pollen dispersibility, implies that the relative abundance of a taxa may be under- or over-represented in the pollen record (Davis, 2000; Prentice, 1985; Theuerkauf et al., 2013). Wind-pollinated taxa or genera, such as *Pinus* and *Betula* are greatly overestimated or well represented in comparison with their abundance in the vegetation. Whereas insect-pollinated species, e.g. *Cistus*, Cyperaceae, Carophyllaceae and Fabaceae are generally under-represented in the pollen spectra (Birks and Birks, 1980; Birks, 1986; Bottema, 1986; Connor et al., 2004; Fall, 2012). Furthermore, it must be taken into consideration that relative proportion of under-represented pollen is not possible to estimate. For example, closed *Pistacia* woodland often produces a pollen rain with only 5% *Pistacia* pollen (van Zeist and Bottema, 1977).

Furthermore, pollen grains also differ in aerodynamic properties. As a result, the dispersal differences of pollen transport vary up to hundred kilometres, depending on their shape and structure (Birks and Birks, 1980; Davis, 2000). High dispersibility indicates more frequent presence of pollen grains in the pollen spectra, for example pine, owing to their good long-distance transport ability and particularly high resistance to degradation (Fall, 2012; Langgut et al., 2011). In terms of preservation, most pollen grains can only be identified at a genus- or family level (e.g. Gramineae, Cyperaceae). Therefore, knowledge about ecological requirements of the taxa to climatic conditions, e.g. temperature and precipitation, cannot be considered.

The traditional presentation of pollen data are pollen percentages (% of total pollen sum) for the pollen component rather than absolute pollen values. According

to Fagerlind (1952), the relationship between pollen percentages and the relative abundance of each taxon in the vegetation around the sampling site is non-linear. This phenomenon is termed the 'Fagerlind effect' (Prentice and Webb, 1986). Studies by Sugita (1993, 2007) have shown, that mathematical methods have been established to correct or to reduce the non-linearity of the pollen percentages. In addition, investigation of the interaction between the recent vegetation, and modern pollen rain are required to support the interpretation of fossil pollen data (Fall, 2012).

Similarly, regional abandonment of settlements and agriculture as a legacy of anthropogenic impact can be identified in the paleo-pollen composition. According to Behre (1990), primary and secondary anthropogenic indicators can be distinguish. Primary anthropogenic indicators are consciously cultivated plants, which directly reflect human interference with the natural vegetation. It is not evident that crop cultivation ever played a major role in the Lake Van area. The domestication of wild ancestors of cereals, for instance, is the most important evidence of agricultural activities in Europe. But *Cerealia* type has been naturally occurred in the steppe vegetation since the Late Glacial, and is therefore not necessarily diagnostic of human activity in the Near East (Behre, 1990; Wick et al., 2003). However, the cultivation of olive trees (*Olea europaea*), walnut trees (*Juglans regia*) and grapevine (*Vitis vinifera*) are a reliable indicator of Roman agriculture, which can be recognized in the pollen spectrum. Aside from this, olive trees may originate from the eastern Mediterranean and Black Sea region (Wick et al., 2003).

Secondary anthropogenic indicators are favored indirectly by different human activities. In sensitive areas a variety of farming activities, grazing in particular, trigger changes in the vegetation and landscape. Liguliflorae, *Sanguisorba minor* type, *Plantago lanceolat*a type, *Polygonum aviculare* type and *Rumex acetosella* type are often associated with human disturbances, especially for open disturbed, grazed and pasture areas (Bottema, 1975; Fall, 2012). Due to the human-induced degeneration of the primary woodland a number of shrubs and trees took advantages for instance pistachio (*Pistacia atlantica* type) and juniper (*Juniperus oxycedrus* type; Behre, 1990).

To sum up, the reconstruction of past plant communities are to be interpreted carefully in view of the prevailing wind systems, different climate conditions, pollen preservation and pollen productivity.

4.4.2 Fire activity

Charcoal particles, inferred from sedimentary records, have been widely used to reconstructed fire events, to provide insights into the complex interaction between

fire and major changes in climate, vegetation and human activity. However, there has been a limited research into long-term fire dynamics in the Near East and eastern Mediterranean region.

According to Flannigan et al. (2000), fire events are a result of direct and indirect factors. The occurrence of fire is directly controlled by climatic conditions including temperature, topography, fuel availability and precipitation (Daniau et al., 2010; Flannigan et al., 2000). Indeed, increased precipitation may also cause more vegetation growth as long as the precipitation remains low enough that it does not suppress fire (Kehrwald et al., 2013). But generally, an increase in global temperature support the global fire activity when the pollen composition shifts from an open to a forest vegetation accompanied with an expansion of woody population (Fletcher et al., 2010). Hence, changes in vegetation and productivity are the main indirect features. For example, during warm climate conditions, the increase plant productivity is responsible for a high fire activity as a result of fuel availability.

In addition, fire has an important influence on climate condition due to emitting greenhouse gases and aerosols into the atmosphere, due to the vegetation cover and to the effects on the global carbon cycle. Major fire events help to maintain vegetation diversity, productivity and a nutrient cycling (Daniau et al., 2010).

The interaction between climate, vegetation and fire regime is complex and difficult to distinguish especially under modern conditions when fire regimes are influenced by human activities (Bond et al., 2005; Turner et al., 2008). In the present interglacial, the reduction in the forest cover and the expansion of more open vegetation will lead to an increase in fire activity (Daniau et al., 2010). Therefore, it is particularly important to examine charcoal records in long-term sedimentary sequences to disentangle the response of climate and vegetation changes during interglacial periods without human activities.

5 Results

The pollen diagram in Figure 5.1 shows percentages of pollen types, which are calculated on the basis of total terrestrial pollen sums. This simplified pollen record presents a selected arboreal (AP)/non-arboreal (NAP) composition with charcoal particles. Aquatic species, algae's, ferns, mooses as well as dinoflagellates values are included in the total pollen record (Figure 7.1, Appendix). Furthermore, the record is divided into nine major pollen assemblage zones (PAZ) and several subzones. The boundaries were determined chiefly based on variations in the arboreal/non-arboreal ratio values, main vegetation groups and pollen concentration (grains/cm^3) in combination with the results of CONISS analysis (Grimm, 1987). Zone numbers and letters are designate with ascending order from bottom to top. The summary of the pollen assemblage zone description as well as criteria for defining the zone boundaries are given in Table 4. The basal limitation of the pollen diagram is determined by the end of the pollen research at 60.09 mcblf.

5.1 Pollen assemblage zones

The beginning of **PAZ I** (Chenopodiaceae - *Ephedra distachya* type) at 60.09-57.78 mcblf is characterized by high percentages of non-arboreal pollen (NAP), fluctuating over 90%. Although the Chenopodiaceae ratio decreases from 65 to 38% towards the top of this pollen zone, the steppic element dominates the herbaceous taxa. This is supported by a slight increase in *Artemisia* percentages from 14 to 26%. Only the Poaceae curve shows low variability around 10%. In comparison, the arboreal pollen ratio (AP) is fluctuating on low values, in particular *Quercus* (<5%) and *Pinus* (<1%), whereas *Ephedra distachya* type and *Betula* pollen indicate a slight expansion of forest towards the end of PAZ I

The **PAZ II** between 57.78 and 51.61 mcblf is marked by a significant resurgence of thermophilous trees with maximum values of approximately 80%. The succession of the woody taxa within this pollen zone can be distinguished into several phases. The *'Pistacia* phase' (PAZ IIa) is illustrated by a retreat of *Ephedra distachya* type (2-0%), followed by a slight increase of *Betula* (0-5%) and *Pistacia atlantica* type (~1%). A remarkable rise of *Quercus* (up to 28%) and *Ulmus minor* type (0-6%) characterized the '*Quercus* - *Ulmus* phase' between 57.20-56.61 mcblf. The subsequent short-term decline of *Quercus* (<20%) at the beginning of the subzone IIc with a simultaneous increase of *Carpinus* (up to 19%) identifies the '*Carpinus* phase' (PAZ IIc). From 55.81 mcblf the *Pinus* curve recorded a continuous increase up to 62%, which can be divided by a short-term retreat into two phases. The

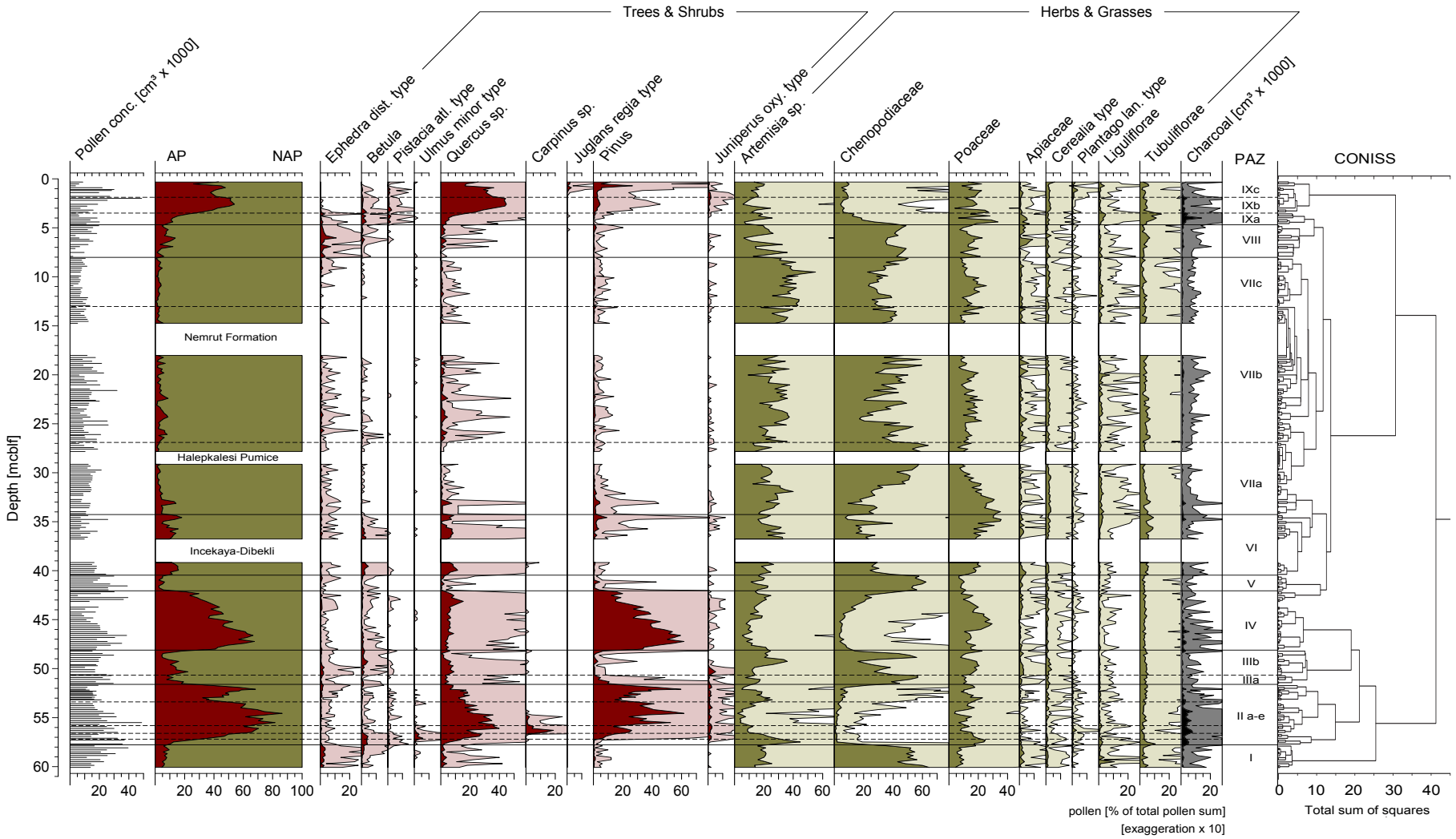

Figure 5.1: Simplified pollen diagram of Lake Van related to sediment depth. Pollen abundance is expressed as a percentage of the total pollen sum which excludes bryophytes, pteridophytes, algae and aquatic taxa. Total pollen concentration (as number of pollen grains/cm³ of sediment) is also given. A x10 exaggeration of the horizontal scale is used to demonstrate changes in low taxa percentages. Pollen assemblage zones with several subzones are documented on the right and described in Table 4. The composite profile includes the volcanic deposits Nemrut Formation (NF), Halepkalesi Pumice (HP-10) as well as the Incekaya-Dibekli (ID). AP = arboreal pollen / NAP = non-arboreal pollen.

'*Quercus* - *Pinus* phase' (PAZ IId; 55.81-53.39 mcblf) is characterized by gradual decline of *Quercus* percentages (12-37%), whereas the '*Pinus* - *Quercus* phase' (53.39-51.61 mcblf) recorded a general lower *Quercus* values (6-19%), contrary to the previous subzone. Furthermore, the rise of *Pinus* pollen, with two remarkable peaks, is accompanied by a concomitant reduction of *Artemisia* and vice versa. In detail, *Artemisia* values reflect the highest percentages of about 45% at the beginning of PAZ IIa, followed by a distinct decline to <5% at depth of 55.50 to 54.56 mcblf (PAZ IId), succeeded by a general tendency of increase (>20%) towards the top of the pollen zone II. Even the Chenopodiaceae curve shows a rapid drop at the beginning, which culminates in a minimum value of <1%, subsequently rises to approximately 22% at 51.51 mcblf (PAZ IIe) and dominates the overlying pollen zone. In contrast, Poaceae amounts fluctuate consistently between 10% and 20% throughout the PAZ II. The concentration of microscopic charcoal particles increases from c. 5000 up to 8000 particles/cm^3 towards the middle of the pollen assemblage zone II.

PAZ III (*Artemisia* - Chenopodiaceae - *Ephedra distachya* type) is dominated by high contents of non-arboreal pollen percentages (>90%). In subzone IIIa (50.66-51.61 mcblf), Chenopodiaceae reaches its maximum value (56%) at 50.71 mcblf, *Artemisia* (17%) at 51.33 mcblf, and Apiaceae (2%) at 51.11 mcblf, only Poaceae ranges consistently between 14 and 16% through the zone. Arboreal pollen percentages drop significantly at the onset of PAZ III. A distinct abrupt decline is recorded mostly by *Pinus* (22-1%) percentages, along with *Quercus* (8-3%), *Juniperus oxycedrus* type (2-1%), *Ephedra distachya* type (2-1%), and the disappearance of *Pistacia atlantica* type. The slightly increasing of *Betula* at the beginning of the subzone IIIa, retreats towards the middle part, and recovers partly at the end, but does not reach percentages above 1%.

Regarding to IIIa, the arboreal composition along with *Quercus*, *Ephedra distachya* type, *Betula*, and *Juniperus oxycedrus* type increase gradually in subzone IIIb (50.66-48.11 mcblf), whereas *Pinus* values fluctuate constantly at 1% throughout the pollen zone. Furthermore, the sporadic occurrence of *Pistacia atlantica* type and *Carpinus* sp. is another specific feature of this subzone. Species of non-arboreal pollen are still the dominant constituents, reflected by increased frequencies of *Artemisia* (12-36%) and Poaceae (8-23%), which are peaking at a depth of 49.26 mcblf and 49.69 mcblf, respectively. During the PAZ III, a decrease of charcoal particles (1548 to 349 particles/cm^3) are recorded. Finally, the abrupt reduction of the Chenopodiaceae curve with decreasing trend, showing one distinct peak at 48.86 mcblf with 56.2%, followed by a significant decline, defines the onset of PAZ IV (48.11-42.25 mcblf).

Apart from the decrease of Chenopodiaceae from 43.7% to percentages below 5%, the increasing *Pinus* ratio, exceeding 62% at a depth of 47.21 mcblf, is a further criteria for the transition to **PAZ IV** (*Pinus* - Poaceae). The expansion of forest development (up to 65%) is accompanied by a slight increase in *Quercus* (3-15%), *Juniperus oxycedrus* type (0-1%) and the sporadic occurrence of *Carpinus* sp. and *Pistacia atlantica* type. Contrary to the rising trend of thermophilous trees, the values of *Ephedra distachya* type are present constantly or receding towards the bottom of PAZ IV, e.g. *Betula* (2-1%). Moreover, the herbaceous composition shows a marked reduction of Chenopodiaceae and *Artemisia* at the beginning, followed by an increasing trend of these species at the end of pollen zone IV. The content of Poaceae varies below 20%, but reaches remarkable high frequencies of >20% between 46.01 and 44.41 mcblf. Furthermore, a distinct increase of charcoal particles, fluctuating between 1378 to 5672 particles/cm^3, characterize this zone.

The decreasing arboreal ratio defines the transition of PAZ IV to **PAZ V** (Chenopodiaceae - *Artemisia*) between 42.25 and 40.46 mcblf. The woody taxa exceeds its maximum of about 20% at a depth of 42.25 mcblf, fluctuates between 1 and 4% until 40.95 mcblf and rises again above 5% at the top of the pollen zone. However, the pollen zone is characterized by general retreat of the tree elements (30-5%), mainly by *Pinus* (20-1%), *Quercus* (7-1%), and the sporadic disappearance of *Juniperus oxycedrus* type and *Pistacia atlantica* type. Values of *Betula* and *Ephedra distachya* type demonstrate an exception, fluctuating on low-amplitude variability (~1%) throughout the PAZ V. The continuous presence of *Artemisia*, including the oscillations between 11-23%, and Poaceae percentages (7-12%) is accompanied by concomitant predominance of Chenopodiaceae amounts (44-63%). Furthermore, the charcoal particles vary on low level between 1000 and 400 particles/cm^3.

The following remarkable rapid and prolonged decline of the Chenopodiaceae ratio (58-9%) illustrates clearly the transition from pollen zone V to **PAZ VI** (40.46-34.27 mcblf). This '*Quercus* - Poaceae - *Pinus*' pollen zone reflects an episode of high contents of steppe elements (>85%). It consists of relatively high abundance of *Artemisia* pollen, averaging between 20-30%, and increased frequencies of Poaceae (7-30%), Liguliflorae (1-3%) and Tubuliflorae (4-9%) towards the top of PAZ VI. Furthermore, the arboreal pollen percentages detect a slight but pronounced rise at the beginning of the zone. However, the moderate expansion of deciduous forest is accompanied by increase of *Quercus* (up to 10%), *Pinus* (0-10%), *Betula* (~1%) and the sporadic appearance of *Juniperus oxycedrus* type and *Carpinus* sp. The only continuously occurring species is *Ephedra distachya* type (varying at 1%). Charcoal particles range constantly between 400 and 1800 particles/cm^3, but with an increasing

trend towards the top of the pollen assemblage zone (above 3300 particles/cm^3). It has to be mentioned that this pollen zone is cut by the volcaniclastic deposit 'Incekaya-Dibekli' (V-60; Sumita and Schmincke, 2013a) at 39.10-37.13 mcblf, but the general tendencies of the different taxa apparently are not affected (Figure 5.1).

During **PAZ VII** (Chenopodiaceae - *Artemisia* - Poaceae) from 34.27 to 8.01 mcblf, the non-arboreal pollen percentages increase up to 95%, demonstrated by a predominance of steppic elements, in particular by Chenopodiaceae. Especially subzone VIIa (34.27-26.90 mcblf) illustrates a rapid expansion of Chenopodiaceae (9-57%), along with fluctuations on high level of *Artemisia* (15-40%). However, the Poaceae curve shows simultaneously a significant decline from 30% to 7% at 29.51 mcblf, followed by a slightly resurgence at the top of PAZ VIIa. Arboreal taxa values, including *Quercus* (9-1%) and *Pinus* (4-1%), decrease gradually towards the end of this subzone. A continuous curve of *Ephedra distachya* type and sporadic occurrences of *Betula* and *Juniperus oxycedrus*type pollen are also recorded. Again, the pollen zone is separated by the c. 1.5 m thick 'Halepkalesi Pumice' (HP-10) fallout (V-51; Sumita and Schmincke, 2013a), whereas the tendencies of expansion and regression of vegetation compositions are not visible influenced.

The distinct oscillations on low level with increasing trend of *Quercus* (1-5%), *Pinus* (~1%) and *Ephedra distachya* type (1-2%) coupled with abrupt fluctuations of steppic elements, mainly Chenopodiaceae, *Artemisia*, Poaceae, Apiaceae and Liguliflorae, characterize subzone VIIb. Despite of the rapid oscillations, the non-arboreal pollen values dominate with high abundance of about 90% throughout the pollen zone. The volcaniclastic segment at the end of subzone VIIb between 14.89 and 18.02 mcblf consists of an approximately three meter thick 'Nemrut Formation' (V-18a, b; Sumita and Schmincke, 2013b).

After the volcaniclastic layer, in subzone VIIc, the woody taxa shows a marginal decline (<5%), especially *Quercus* (1-2%) and *Ephedra distachya* type pollen percentages, which is accompanied by a concomitant expansion of *Artemisia* and Poaceae. In particular, Poaceae values increase at the beginning of PAZ VIIc (10-24%), followed by an abrupt reduction, rise again to 21% at a depth of 11.53 mcblf, and retreat once more to the top of PAZ VII. A further significant feature is the remarkable increase of Chenopodiaceae (26-50%) and *Ephedra distachya* type (0-3%) from the middle towards the end of the subzone. Both taxa dominate the overlying pollen zone and define concurrently the onset of PAZ VIII at 8.01 mcblf. In general, the charcoal particles range between 1500 and 400 particles/cm^{3}within the PAZ VIII, but three small peaks can be identified at 33.14 mcblf (3257 particles/cm^3), 19.82 mcblf with 2010 particles/cm^3 and at 6.91 mcblf (2066 particles/cm^3).

The transition to **PAZ VIII** (*Ephedra distachya* type - *Betula* - Chenopodiaceae) at 8.01 until 4.68 mcblf is characterized primarily by the expansion of *Ephedra distachya* type, peaking at a depth of 6.02 mcblf with values of approximately 11%. The increased frequencies of AP (>10%) come along with the resurgence of *Betula* (~1%), *Quercus* (1-3%) and *Pinus* (1-2%) pollen. Moreover, *Pistacia atlantica* type and *Juniperus oxycedrus* type occur occasionally within this pollen zone. Despite of the increasing arboreal taxa, the steppic elements dominate the pollen composition. In particular, the Chenopodiaceae percentages constitute the major part of NAP, fluctuating between 48% and 50%. In addition, Poaceae (8-15%) values as well as Apiaceae (0.5-7%) and Tubuliflorae (2-5%) amounts indicate a gradual rise throughout the pollen zone. Especially, the increasing Apiaceae curve shows one distinct peak of about 9% at a depth of 6.18 mcblf. In contrast, *Artemisia* values demonstrate a general tendency of decreased abundances together with remarkable fluctuation between 7% and 36%. During this zone, the micro-charcoal particles characterize a slight increase towards the top of about 1663 particles/cm^3.

The predominance of deciduous *Quercus* is a criteria for the beginning of **PAZ IX** (*Quercus* - *Pistacia atlantica* type) at a depth of 4.68 mcblf. This pollen zone is divided into three subzone caused by the change of frequencies of *Quercus* percentages. The onset of subzone IXa (4.68-3.49 mcblf) is characterized by the decline of *Ephedra distachya* type values (~1%), accompanied by the succession of *Betula* (above 3%), *Quercus* (5-15%) and *Pinus* (up to 5%). In addition, *Pistacia atlantica* type is constantly present throughout the pollen zone. Regarding to NAP percentages, which range from 80 to 90% in IXa, are characterized by a sharp decline of Chenopodiaceae (40-9%). A remarkable retreat of *Artemisia* pollen at the beginning of this subzone is followed by a slight rise towards the end. In addition, the increasing tendency of Poaceae (15-33%) come along with high percentages of Apiaceae (>3%), Liguliflorae (1-5%) and Tubuliflorae (2-15%).

In zone IXb (3.49-1.89 mcblf), the NAP abundances drop and several deciduous trees (esp. *Quercus*) rise significantly. The *Quercus* species dominates the entire subzone, with a maximum of 45% at a depth of 2.59 mcblf. The expansion of arboreal pollen is accompanied by an increase in *Pinus* (1-3%) and *Juniperus oxycedrus* type (0-2%) taxa. *Pistacia atlantica* type taxa are present continuously, but with low values (2%). The distinct reduction of *Ephedra distachya* type and *Betula* values is also recorded in the NAP ratio, mostly by Chenopodiaceae (13-9%), Tubuliflorae (14-3%) and Liguliflorae (5-0.5%). The *Artemisia* and Poaceae curves follow the decreasing trend towards the end of subzone IXb, showing remarkable peaks at 2.99 mcblf (25%) and at 3.39 mcblf (27%), respectively.

Table 4: Synoptic description of the pollen assemblage zones (PAZ) at Lake Van, see Figure 7 and 15 (Appendix). AP = Arboreal pollen, NAP = Non-arboreal pollen.

PAZ	Depth [mcblf]	Criteria for lower boundary	Vegetational development [minimum-maximum %]
IXc	0-1.89	*Quercus* <40%	**AP:** *Quercus* (25-45%) - *Pinus* (3-12%) - *Juglans* (0-2%) - *Juniperus* (0-2%) - *Pistacia* (0-2%) - *Betula* (0-1%) - *Carpinus* (0-1%) **NAP:** *Artemisia* (12-20%) - Poaceae (9-22%) - Chenopodiaceae (5-10%) - *Plantago* (0-2%)
IXb	1.89-3.49	*Quercus* >10%	**AP:** *Quercus* (15-45%) - *Pinus* (1-3%) - *Pistacia* (1-3%) - *Juniperus* (0-2%) - *Betula* (0-1%) - *Ephedra* (0-1%) **NAP:** *Artemisia* (12-19%) - Poaceae (12-15%) - Chenopodiaceae (9-13%) - Tubuliforae (3-14%) - Liguliflorae (1-5%)
IXa	3.49-4.68	*Quercus* >5%	**AP:** *Quercus* (5-15%) - *Pinus* (1-5%) - *Betula* (1-4%) - *Ephedra* (0-1%) - *Pistacia* (0-1%) **NAP:** Poaceae (15-33%) - *Artemisia* (9-40%) - Chenopodiaceae (9-40%) - Tubuliflorae (2-15%) - Apiaceae (1-7%) - Liguliflorae (1-5%)
VIII	4.68-8.01	*Ephedra* >3%	**AP:** *Ephedra* (1-11%) - *Quercus* (1-3%) - *Pinus* (1-2%) - *Betula* (0-2%) **NAP:** Chenopodiaceae (48-50%) - *Artemisia* (20-32%) - Poaceae (8-15%) - Tubuliforae (2-5%) - Apiaceae (0-9%)
VIIc	8.01-13.02	*Quercus* <2%; *Artemisia* >40%	**AP:** *Quercus* (1-2%) - *Ephedra* (0-3%) - *Pinus* (0-1%) **NAP:** Chenopodiaceae (26-50%) - *Artemisia* (25-55%) - Poaceae (10-21%)
VIIb	13.02-26.90	*Quercus* >2%; *Artemisia* <40%	**AP:** *Quercus* (1-5%) - *Ephedra* (1-2%) - *Pinus* (0-2%) **NAP:** Chenopodiaceae (42-57%) - Poaceae (10-15%) - *Artemisia* (9-40%)
VIIa	26.90-34.27	*Quercus* >5%	**AP:** *Quercus* (1-9%) - *Pinus* (1-4%) - *Betula* (0-1%) - *Ephedra* (0-1%) - *Juniperus* (0-1%) **NAP:** *Artemisia* (15-25%) - Poaceae (15-30%) - Chenopodiaceae (9-57%)
VI	34.27-40.46	*Quercus* >5%; Chenopodiaceae <50%	**AP:** *Quercus* (1-12%) - *Pinus* (0-10%) - *Betula* (0-5%) - *Ephedra* (0-2%) - *Carpinus* (0-1%) - *Juniperus* (0-1%) **NAP:** *Artemisia* (20-30%) - Chenopodiaceae (9-58%) - Poaceae (7-30%) - Tubuliflorae (4-9%) - Liguliflorae (1-3%)

(continue on next page)

Table 4: continued from previous page

PAZ	Depth [mcblf]	Criteria for lower boundary	Vegetational development [minimum-maximum %]
V	40.46-42.25	*Quercus* >10%	**AP:** *Pinus* (1-20%) - *Quercus* (0-7%) - *Betula* (0-1%) **NAP:** Chenopodiaceae (44-63%) - *Artemisia* (11-23%) - Poaceae (7-12%)
IV	42.25-48.11	*Pinus* >30%	**AP:** *Pinus* (15-62%) - *Quercus* (3-15%) - *Betula* (0-2%) - *Carpinus* (0-1%) - *Juniperus* (0-1%) **NAP:** Poaceae (10-30%) - *Artemisia* (5-25%) - Chenopodiaceae (4-32%)
IIIb	48.11-50.66	*Quercus* >10%	**AP:** *Quercus* (1-9%) - *Betula* (1-4%) - *Ephedra* (1-3%) - *Pinus* (0-7%) - *Juniperus* (0-5%) - *Carpinus* (0-1%) - *Pistacia* (0-1%) **NAP:** Chenopodiaceae (14-56%) - *Artemisia* (12-36%) - Poaceae (8-23%)
IIIa	50.66-51.61	*Quercus* <10%	**AP:** *Quercus* (3-8%) - *Pinus* (1-22%) - *Betula* (1-2%) - *Ephedra* (1-2%) - *Juniperus* (1-2%) **NAP:** Chenopodiaceae (44-56%) - Poaceae (14-16%) - *Artemisia* (10-17%)
IIe	51.61-53.39	*Pinus* >30%	**AP:** *Pinus* (21-60%) - *Quercus* (6-19%) - *Juniperus* (1-3%) - *Ephedra* (1-2%) - *Betula* (0-2%) **NAP:** Poaceae (9-23%) - *Artemisia* (5-24%) - Chenopodiaceae (4-22%)
IId	53.39-55.81	*Pinus* >20%	**AP:** *Pinus* (15-62%) - *Quercus* (12-37%) - *Juniperus* (1-3%) - *Carpinus* (0-3%) - *Betula* (0-1%) - *Ephedra* (0-1%) **NAP:** Poaceae (4-23%) - *Artemisia* (2-26%) - Chenopodiaceae (1-6%) - Liguliflorae (0-2%)
IIc	55.81-56.61	occurrence of *Carpinus*	**AP:** *Quercus* (18-40%) - *Pinus* (14-29%) - *Juniperus* (2-3%) - *Carpinus* (1-19%) - *Ulmus* (0-3%) - *Betula* (0-1%) - *Ephedra* (0-1%) **NAP:** *Artemisia* (8-20%) - Poaceae (8-16%) - Chenopodiaceae (1-2%) - Liguliflorae (0-2%)
IIb	56.61-57.20	occurrence of *Ulmus*	**AP:** *Quercus* (15-28%) - *Pinus* (7-24%) - *Ulmus* (2-6%) - *Betula* (1-5%) - *Juniperus* (1-2%) - *Ephedra* (0-1%) - *Pistacia* (0-1%) **NAP:** Poaceae (16-20%) - *Artemisia* (10-28%) - Chenopodiaceae (1-2%) - Liguliflorae (0-2%)

(continue on next page)

Table 4: continued from previous page

PAZ	Depth [mcblf]	Criteria for lower boundary	Vegetational development [minimum-maximum %]
IIa	57.20-57.78	*Quercus* >5%; occurrence of *Pistacia*	**AP:** *Quercus* (2-13%) - *Betula* (4%) - *Ulmus* (0-2%) - *Pinus* (0-1%) - *Ephedra* (0-1%) - *Juniperus* (0-1%) - *Pistacia* (0-1%) **NAP:** *Artemisia* (29-45%) - Poaceae (17-25%) - Tubuliflorae (3-11%) - Chenopodiaceae (2-16%) - Liguliflorae (1-3%)
I	57.78-60.09	not defined	**AP:** *Quercus* (0-4%) - *Ephedra* (0-3%) - *Betula* (0-2%) - *Pinus* (0-1%) **NAP:** Chenopodiaceae (38-65%) - *Artemisia* (14-26%) - Poaceae (4-19%)

The decline of tree values (<50%), except *Pinus*, and the increase of shrub values is the significant feature of the IXc zone (1.89-0 mcblf). *Quercus* percentages illustrate a marked reduction (45-25%), followed by an increasing trend at the top of PAZ IXc. In contrast, *Pinus* values gradual rise and reach 12% in the uppermost part. *Pistacia atlantica* type pollen fluctuates around 1%, whereas percentages of *Betula* and *Juniperus oxycedrus*-type drop below 1% towards the end of the pollen zone. Pollen of *Carpinus betulus* type occur sporadic while pollen grains of Ephedra *distachya* type disappear completely in this zone. However, crop plants such as Cerealia, *Juglans regia* type and *Olea* rise in this period, accompanied by pollen of several other herbs, for instance *Artemisia* (12-20%), *Plantago lanceolata* type (0-2%), *Rumex* (~2%) and other Asteraceae. Chenopodiaceae (~9%) and Poaceae (~12%) values range on low levels throughout PAZ IX. In addition, the remarkable rise of charcoal particles, coupled with a distinct peak at 3.99 mcblf of about 14,000 particles/cm^3, is a characteristic feature in this pollen assemblage zone.

6 Discussion

In order to reconstruct climate oscillations over the last glacial-interglacial cycle in the Near East, trans-regional palynological records were examined. The pollen composition from sediment cores of Lake Van is compared with the nearest well-studied long continental palynological sequences in the Near East and the eastern Mediterranean (Figure 6.1) as well as with the record from NorthGRIP ice cores. The selected sequences encompass the last ~130 ka of the observed period at Lake Van. Hence, they provide an east-west transect across the Mediterranean area extending from the Near East via Greece to Italy.

One of the key objectives is to examine regional differences and similarities in the response of vegetation and environment to major climatic changes during the last glacial-interglacial cycle.

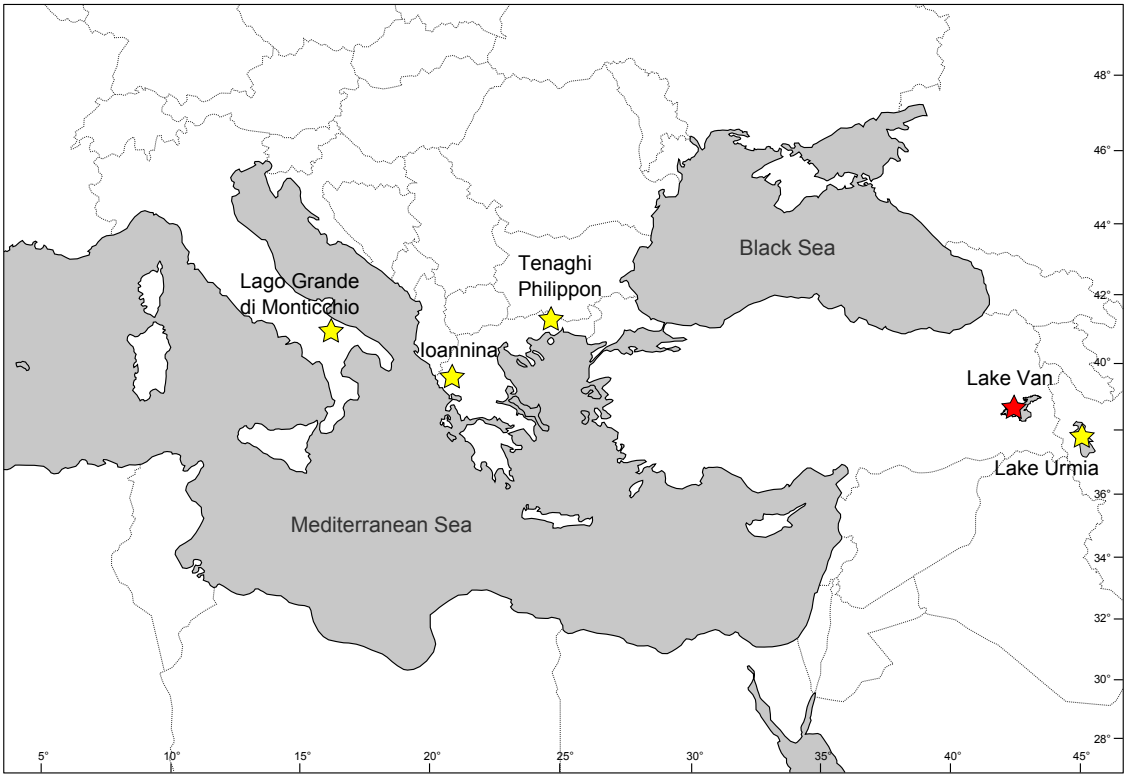

Figure 6.1: The location of Lake Van (Turkey, red star) and Lake Urmia (Iran) from the Near East region and the long continental sequences of Lago Grande di Monticchio (Italy), Ioannina basin (NW-Greece) and Tenaghi Philippon (NE-Greece) from the eastern Mediterranean region.

6.1 The late penultimate glacial

The Lake Van pollen record, presented in Figure 5.1, starts at the end of the late penultimate glacial, Marine Isotope Stage (MIS) 6. This period is additionally equivalent to the Saalian glacial of the NW European classification (Table 5), summarized by Litt et al. (2007). Although marine and terrestrial boundaries are not exactly isochronous, it has been appreciated that Marine Isotope Stages and Substages can be used for the classification of continental records (e.g. Sánchez Goñi et al., 1999; Tzedakis et al., 1997; Tzedakis, 2005 and several others).

The late penultimate glacial is represented by the pollen assemblage zone I (133.9-130.8 ka BP; 60.09-57.8 mcblf). According to Litt et al. (subm), the penultimate glacial sequence can be assumed to reflect the natural vegetation under cold and dry environmental conditions. Pollen of herbaceous and shrubby plants, such as *Artemisia*, Chenopodiaceae and *Ephedra distachya* type, characterize a dwarf-shrub steppe and desert steppe vegetation. This pollen composition is associated with an arid environment with low values of precipitation and low temperature. Furthermore, the limited pollen concentration refers to reduced plant productivity. The occurrence of *Quercus* (<5%) and *Pinus* (1%) may indicate a long-distance transport from protected areas of less strong cold conditions and more moisture availability (Figure 6.3). The absence of the frost-sensitive taxa *Pistacia* emphasizes the cold and dry climatic conditions during this period. This assumption is supported by the occurrence of cold/dry-climate lithologies at Lake Van. Furthermore, Stockhecke et al. (2013) document a period of strong bioturbation in the sediments at about 135 ka BP (Unit XI; Table 3). This indicates an increased circulation of the water body while the lake levels decreased.

The end of the penultimate glacial stage, known as Termination II (at ~132 ka BP; Shackleton et al., 2002), corresponds with the interval of most rapid reduction of continental ice volume. Consequently, the sea level rose quickly (Kukla et al., 2002). Regarding to palynological results, the transition from the late penultimate glacial into the initial warming of the last interglacial (~130.8 to 127.2 ka BP) is characterized by the occurrence of *Pistacia* as well as by the increase of *Betula*, *Quercus* and *Ulmus* at Lake Van (the criteria for defining the lower boundaries are given in Table 4).

Comparison with southern European terrestrial records

Until now, there is just a small number of detailed records that have been focused on this interval. Nevertheless, the climatic evolution of the penultimate glacial reconstructed from the Lake Van pollen record is consistent with the palynological sequences from the eastern Mediterranean and the Near East. Figure 6.2 shows the

Table 5: Proposed correlations across NW and SW European stages with marine events of the North Atlantic and NGRIP ice core records. D-O = Dansgaard-Oeschger event, C = Cooling event.

Lake Van		Terrestrial correlates, principal stages and substages			
PAZ	Age (ka BP)	NW Europe	SW Europe (Massive Central)	MIS	Marine and ice core correlates
IXa-c	11.7-present	Holocene	Holocene	1	
VII	13.1-11.7	Younger Dryas	Younger Dryas	1	
VIII	14.5-13.1	Bølling / Allerød	Bølling / Allerød	1	D-O 1
VIIc	28.1-14.5	Late Pleniglacial	Upper Pleniglacial	2	D-O 2, 3
VIIb	59.3-28.1	Middle Pleniglacial	Middle Pleniglacial	3	D-O 4-17
VIIa	74.7-59.3	Early Pleniglacial	Lower Pleniglacial	4	D-O 18, 19
VIIa	78.5-74.7		Ognon I	5	D-O 20
VI	84.6-78.5	Odderade	St Germain II	5a	D-O 21
V	88.3-84.6	Rederstall	Melisey II	5b	C21
IV	103.6-88.3	Brørup	St Germain Ib	5c	D-O 23, 22
IIIb	105.4-103.6		Montaigu event	5c	C23
IIIb	107.8-105.4	Amersfoort	St Germain Ia	5c	D-O 24
IIIa	110.9-107.8	Herning	Melisey I	5d	C24
IIe	114.5-110.9	Eemian		5e	D-O 25
IIe	115.6-114.5		Woillard event	5e	C25
IIa-d	130.8-115.6	Eemian	Ribains	5e	
I	133.9-130.8	Saalian		6	

comparison of five terrestrial records and the NorthGRIP ice core record. Compared with a relative small amplitude of arboreal percentages at Lake Van, the continental record of Lake Urmia (NW Iran), for example, documents a similar pattern during the late penultimate glacial period. According to Djamali et al. (2008, 2012a) and Stevens et al. (2012), this interval is also marked by an expansion of an *Ephedra* shrub-steppe, followed by a pronounced *Artemisia* and Chenopodiaceae steppe expansion right before the onset of the last interglacial stage. The vegetational sequence with a low forest development during the penultimate glacial suggests extremely dry and continental conditions at Lake Urmia. As observed in the lithologies of the Lake Van, the Lake Urmia sediments indicate a low lake level stand from ~145 to 130 ka until the end of the penultimate glacial (Stevens et al., 2012).

A number of pollen records show an occurrence of a Zeifen interstadial/Kattegat stadial succession similar to the late-glacial interstadial/Younger Dryas sequence during the penultimate glacial-last interglacial transition (Sánchez Goñi et al., 1999,

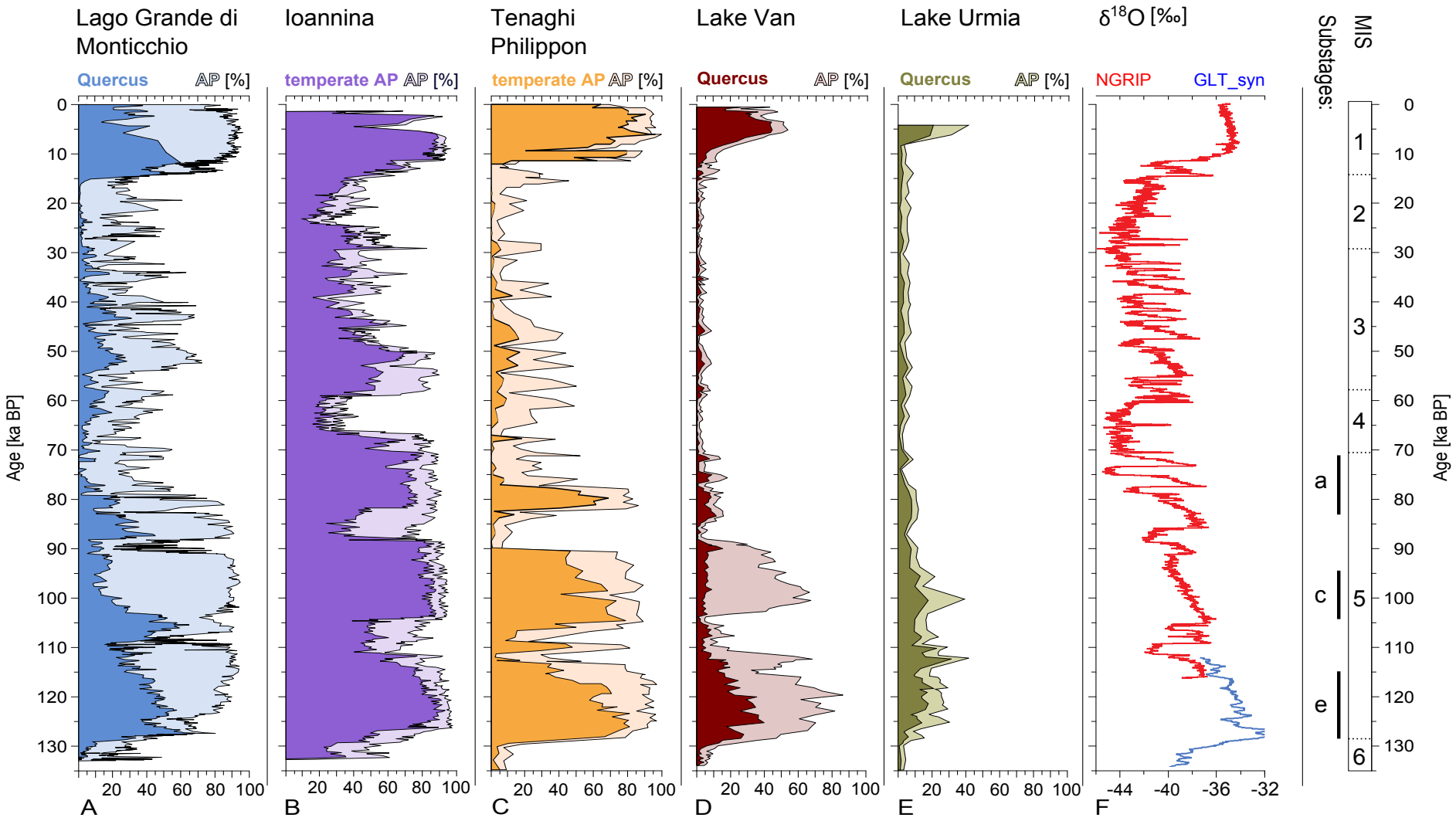

Figure 6.2: Comparison of the eastern Mediterranean and Near East pollen records with the oxygen isotope sequences of the NorthGRIP ice cores. For the terrestrial records the arboreal pollen (AP) and *Quercus* curve have been used for the correlations. Exceptions are the Ioannina basin and Tenaghi Philippon record, where only the temperate tree pollen curve, which excludes *Juniperus* and *Pinus*, were available. A - Lago Grande di Monticchio (Allen et al., 2000; Allen and Huntley, 2009; Brauer et al., 2007); B - Ioannina (Tzedakis et al., 2004a); C - Tenaghi Philippon (Tzedakis et al., 2006); D - Lake Van (this study), E - Lake Urmia (Djamali et al., 2008; Djamali, 2013, unpublished data); F - NorthGRIP (Barker et al., 2011; Stockhecke et al., 2013; Wolff et al., 2010); Boundaries of the Marine Isotope Stages (MIS) and Substages after Lisiecki and Raymo (2004).

2005; Tzedakis, 2000). At Lake Van and Tenaghi Philippon, there are no significant cooling events recorded for that time period. Regarding the terrestrial pollen records from the eastern Mediterranean area, the high resolution sequences at Ioannina basin as well as Lago Grande di Monticchio indicate unstable climate conditions during the transition zone. Tzedakis et al. (2003a) described that the late penultimate glacial contains an interstadial (~129.3-128.0 ka BP) followed by a stadial (~128.0-127.3 ka BP). Therefore, the interval from ~133 to 129.3 ka BP represents the penultimate glacial maximum at Ioannina. In contrast, at Lago Grande di Monticchio the rapid but subdued climate oscillations interrupted the transition zone, however, not as pronounced as the Younger Dryas type cooling event (Allen and Huntley, 2009; Roucoux et al., 2011; Tzedakis et al., 2003a). The record of Lake Urmia is also affected by a severe arid period within the transition zone, just before the start of the last interglacial period (Djamali et al., 2008).

In conformity with Stevens et al. (2012), most pollen records in the Mediterranean region do not show a vegetation shift until ~128 ka BP, although most sea level rises may have begun earlier. However, Roucoux et al. (2011) and Frogley et al. (1999) documented a slight increase in temperate tree concentration between ~130 and 127.5 ka BP at Ioannina, but emphasize that the landscape was still open. The occurrence of deciduous *Quercus*, *Corylus*, *Abies*, *Alnus*, *Carpinus betulus*, *Ulmus* and *Salix* suggest that small refugial woody populations were still present at Ioannina during the penultimate glacial stage (Tzedakis, 1993; Tzedakis et al., 2002a). Furthermore, Tzedakis (2003) describes a change to wetter conditions at ~127.3 ka BP at Ioannina. In the same way, the transition zone at Lago Grande di Monticchio began at ~130.55 ka BP, and lasted about 3.35 ka until ~127.2 ka BP (Allen and Huntley, 2009). The palynological composition marks a general increase of woody taxa while the abundance of steppic herbaceous taxa decreases (e.g. *Artemisia* and Chenopodiaceae). This indicates less arid environmental conditions with increasing temperature and moisture availability (Allen and Huntley, 2009; Brauer et al., 2007). The reconstructed paleovegetation at Tenaghi Philippon suggests, similar to Ioannina, that small refugial temperate tree populations were present during glacial times (Milner et al., 2013; Tzedakis, 1993; Tzedakis et al., 2002a). This is clearly reflected by the rapid increase of arboreal pollen from 10 to 90% within less than 1,000 years (Milner et al., 2013; Figure 6.2). Compared to this, the expansion of the temperate woody population during the initial warming interval at Lake Van has a delay of about 2.16 ka. An identical time lag in the spread of the deciduous tree populations (~3 ka), closely linked to dry spring and summer conditions, was already established in the Holocene sequence of Lake Van (Litt et al., 2009).

6.2 The last interglacial

Based on terrestrial deposits in NW Europe, the last interglacial can be defined as a period of climatic amelioration that is generally warm or warmer than today (Fairbridge, 1972; Harting, 1874; Jessen and Milthers, 1928). Considering the steppe-forest development as the natural interglacial vegetation in eastern Anatolia, as it was proposed by previous investigations of the recent interglacial by Litt et al. (2009) and Wick et al. (2003), the onset of the Eemian is characterized by an abrupt occurrence of *Pistacia* and the expansion in woody taxa (AP) up to 40%. The beginning of the last interglacial corresponds with the maximum of the mid-June insolation curve (Berger et al., 2007; Figure 6.3) and occurred inside the Marine Isotope Stage MIS 5e (130-115 ka; Lisiecki and Raymo, 2004) well after the melting of the continental ice volume in the Northern Hemisphere during the penultimate glacial (Sánchez Goñi et al., 2005; Shackleton et al., 2002, 2003).

In biostratigraphical terms, the initial warming at the beginning of the last interglacial stage (~130.8-127.2 ka BP; 57.78-56.61 mcblf) is assigned by the significant expansion of thermophilous trees, in particular by the increase of *Betula*, as a pioneer plant, and the sudden occurrence of *Pistacia* species (*Pistacia* phase). Especially *Pistacia atlantica*-type, which extends from western Pakistan to Turkey along the southern shores of the Mediterranean Sea, is able to withstand summer dryness and indicates mild winter temperature in eastern Anatolia (Rossignol-Strick, 1995). Moreover, the warming trend is illustrated by the rapid expansion of deciduous *Quercus* (up to 20%) and the occurrence of *Ulmus* (~129.1 ka BP; 57.2 mcblf) during the '*Quercus-Ulmus*' phase.

Contemporaneously with the spreading of woody population, the transition towards warmer climate conditions with more moisture availability is accompanied by a substantial sharp decrease in non-arboreal pollen concentrations (Figure 6.3), in particular by *Artemisia*, Chenopodiaceae and *Ephedra distachya*-type. In contrast to the general decline of steppic elements, the presence of grasses increases significantly. Hence, the shift in the relative abundance between the non-arboreal taxa implies a climate change from an arid shrub-dominated steppe to a less arid grass steppe, scattered with light-demanding species. Such vegetation change within the initial warming was already observed at the beginning of the Holocene sequence by Litt et al. (2009).

Furthermore, the early interglacial period was interrupted by intervals of colder and drier conditions within the transition zone, recorded by frequently intermittent warm/wet-climate lithologies accompanied with event deposits at Lake Van. Stockhecke et al. (2013) described a strong lake level rise in the Lake Van sediments during

this period. However, these short-term climate oscillations are not recognized in the pollen record due to a lower sampling resolution.

The climate optimum within the last interglacial period lasted from ~56.61 to 53.39 mcblf (~127.2-115.6 ka BP) and occurred right after the early warming of the last interglacial. Based on vegetation changes recorded in the Lake Van record, this interval is characterized by the appearance and rapid expansion of *Carpinus* sp. (up to 19%). However, the contemporary decline of *Quercus* indicates colder climate conditions, concerning summer temperature, but with still high moisture availability during the '*Carpinus*' phase. The characteristic temperate woody taxa such as *Acer, Alnus, Corylus, Fagus*, *Fraxinus* and *Tilia*, recognized in the northern European succession (Aalbersberg and Litt, 1998), were only present with very low abundances at Lake Van during the last interglacial (Figure 7.1, Appendix). According to the Greenland ice cores, the reconstructed temperature curve peaked after the onset of the Eemian at about 126 ka BP, which is consistent with the palynological record. At this time, the surface temperature was 5-8°C higher than present-day values and gradually decreased thereafter during the interglacial (Dahl-Jensen et al., 2013; NEEM, 2013; NGRIP, 2004).

The onset of colder climate conditions with moderate moisture availability, is evidenced by a gradual increase of *Pinus* as well as by the decline in warm-temperate species, especially by *Quercus*, *Carpinus* and *Ulmus* after ~124 ka BP (Figure 6.3). The slight climatic deterioration reflects the reduction of the mid-June insolation and the maximum mid-January insolation between ~119 and 118 ka BP. The observed cooling trend corresponds to the gradual decline of the Greenland reconstructed temperature (at ~122 ka; NEEM, 2013; NGRIP, 2004; Sirocko et al., 2005), while the ice thickness was still unchanged (Dahl-Jensen et al., 2013). Also Crucifix and Loutre (2002) point to a decrease in summer temperature of 2-3°C in the mid-latitudes of Eurasia. Within this interval of cooler temperature and low moisture availability, the Lake Van record presents a slight increase of the charcoal particles (Figure 6.3.

A special attention is paid to the gradual increase of pine (>60%) in combination with the simultaneous disappearance of *Carpinus* sp. as well as the moderate retreat in *Quercus* abundances at ~119.3 ka BP (54.48 mcblf). According to the intensive discussion in Litt et al. (subm), pine tolerates colder conditions with more moisture deficiency. In dry environments, like the area of Lake Van, changes of forest populations correspond to moisture availability, which is further coupled to both warm and cold climate conditions. However, the final period of the last interglacial stage is characterized by a higher continentality index compared to the present-day conditions in the Anatolian region. Besides, high frequencies of charcoal deposits

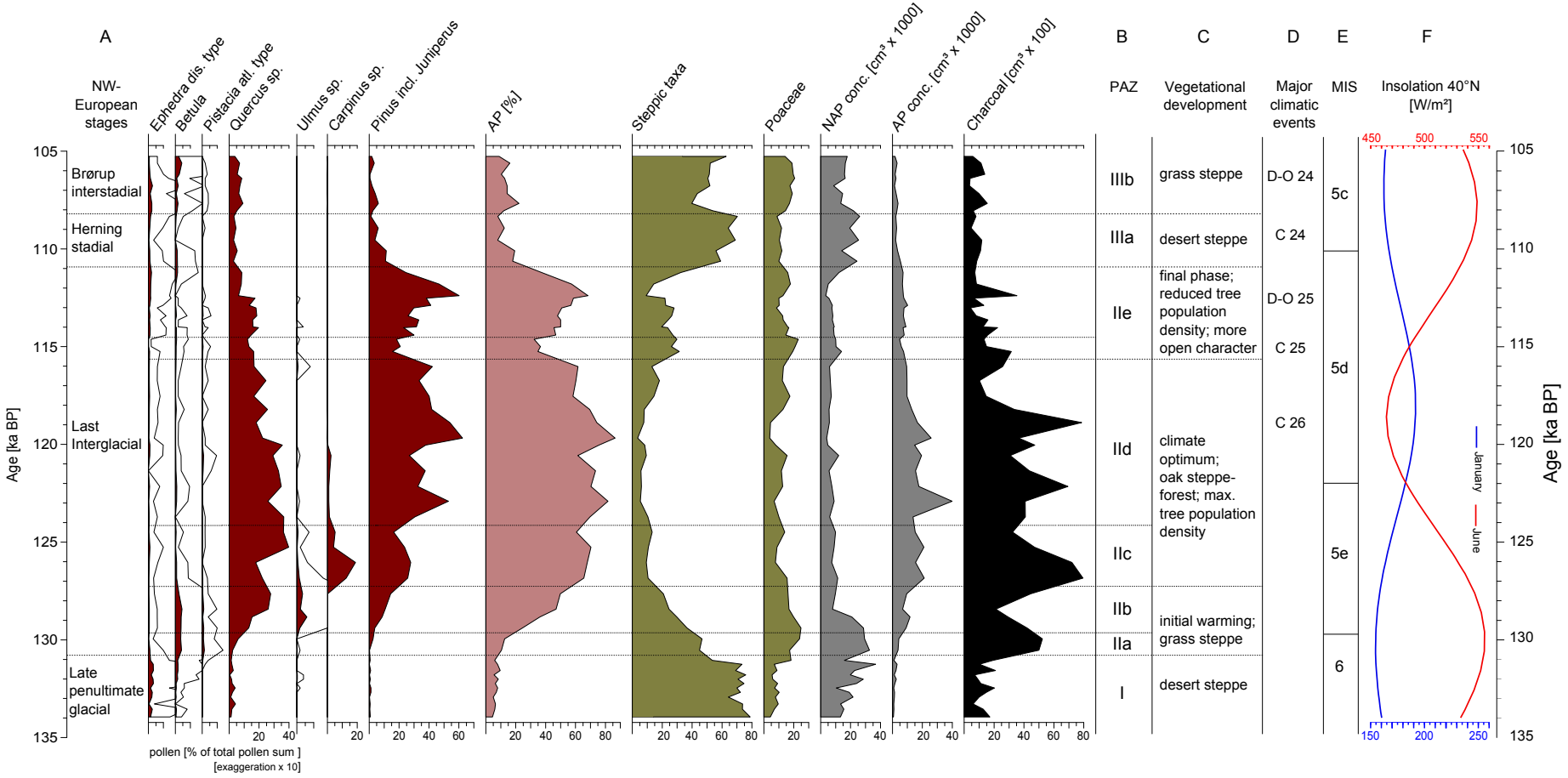

Figure 6.3: Pollen diagram of Lake Van during the last interglacial stage. The selected taxa are presented in percentages [%]. Arboreal (AP) and non-arboreal pollen (NAP) curves as well as charcoal particles are given in total concentrations [cm^3]. Steppic taxa consist of *Artemisia* and Chenopodiaceae. A - Terrestrial stages after the north-west European stratigraphy; B - Pollen assemblage zones; C - Vegetational development at Lake Van; D - Major climatic events within the marine and ice core records (McManus et al., 1994; Sirocko et al., 2005) E - Marine Isotope Stages (MIS) and Substages after Lisiecki and Raymo (2004); F - mid-June (red line) and mid-January (blue line) insolation 40°N after Berger et al. (2007).

indicate a raising fire activity and confirm the drier climatic conditions during this period. The general high pine abundance during the last interglacial period is not yet sufficiently explained. Litt et al. (subm) point out that the distribution of pine (e.g. *Pinus nigra*), which recently occurs in the central region of Anatolia (Zohary, 1973a), reached much further to the East during the last interglacial stage. In comparison Shumilovskikh et al. (2013) assumed that the expansion of the beech forest belt of the Black Sea region towards the central part of Anatolia, has led to the southward displacement of pine and oak populations during the last interglacial.

All aspects together mark the end of the climate optimum of the Eemian and may reflect the so-called marine C 26 cooling event at ~119 ka BP (also known as the Late Eemian aridity pulse in northern Germany; Sirocko et al., 2005). According to Sirocko et al. (2005) and Seelos and Sirocko (2007), cooling events within the last interglacial period were probably produced by a reduction of the North Atlantic thermohaline circulation, as a result of the southward shift of the North Atlantic Current. During these warm to cold transitions, the North Atlantic was marked by rapid decreases in sea surface temperature, indicated by an increase of ice-rafted detritus (IRD). However, the less-pronounced cooling event C 26 can hardly be explained by surging ice, because it occurs when ice sheets just started to grow (inception at ~118 ka BP; Sirocko et al., 2005; Seelos and Sirocko, 2007). Following the description of Chapman and Shackleton (1999) and Kukla et al. (2002), the C 26 event only reflects a reduction in the surface-water temperature of about 2°C during the gradual build-up of continental ice sheets. Moreover, the cold surface water condition can be assumed to have a negative effect on atmospheric cyclone activity in this region, which implies a reduction of the prevailing moist westerly jet stream intensity over Europe. Finally, no evidence of lake level fluctuations was found in the sediments of Lake Van, indicating that the reduction of moisture might be a short-term seasonal dryness, most probably in the late summer (Stockhecke et al., 2013).

After 119.29 ka BP, the forest vegetation became more open, which is documented by the continued decline of tree population density. In conformity with Tzedakis et al. (2003a), the vegetation development at Lake Van reflects the parallel increase of global ice volume, which marks the deteriorating climate towards the Weichselian glacial. The first large-scale cooling event C 25 at ~115.6 ka BP (53.39 mcblf), initiates the end of the climate optimum of the last interglacial stage (McManus et al., 1994). The widespread C 25 event occurred during the gradual build-up of continental ice sheets, accompanied with an estimated temperature drop of about 7°C (Chapman and Shackleton, 1999; Kukla et al., 2002). At Lake Van, this climate

deterioration is expressed by an opening of the forest vegetation, associated with the decrease of *Quercus* and *Pinus* frequencies and consequently with the expansion of steppic taxa (up to 30%), especially *Artemisia* and Poaceae at Lake Van. Therefore, the reduction of woody taxa at Lake Van is not only limited to the degree of summer temperature, but is further coupled to the decrease of moisture availability. Müller and Kukla (2004) describe as well that the hydrographic shift during the C 25 event was associated with a substantial cooling in northern Europe and with an interruption of moisture transfer into the Mediterranean region. This interruption of moisture supply can be recognized in eastern Anatolia and was responsible for the decline of woody taxa.

The re-expansion of the cold and drought tolerant taxa *Pinus* characterizes the final phase of the last interglacial between ~114.5 and 110.9 ka BP (52.94-51.61 mcblf). Although the woody taxa demonstrate a significant rise in abundance, the arboreal pollen concentration values display a reduced tree population density (Figure 6.3). This aspect indicates that the forest development at Lake Van becomes increasingly more open in character. Furthermore, even if the mid-June insolation curve illustrates a raise during the final phase and even though Chapman and Shackleton (1999) refer to a still operating oceanic heat transport over the North Atlantic, it seems that the moisture supply did not sufficiently extend into the area of Lake Van. As a result, the pollen composition at Lake Van shows a low emergence of deciduous *Quercus* (15-18%) and high values of *Pinus* (20-60%) at the end of the last interglacial stage. Thus, the slight forest development represents the Dansgaard-Oeschger event (D-O) 25 at ~114.5 ka BP (52.94 mcblf), which is associated with warm but drier climatic conditions in the Near East (Shackleton et al., 2002). The D-O events are millennial-scale climate variability, detected in the North Greenland ice core records during the the last glacial and, therefore, they will be discussed in more detail in section 6.3 'Last Glacial'.

The extension of *Pinus* continued until ~112 ka BP, when climate and environmental conditions drastically change to a dwarf steppe vegetation. By ~110 ka the northern European ice volume had accumulated, resulting in ice-rafting events, which interrupted the thermohaline circulation in the North Atlantic. Indeed, the first widespread cooling event C 24 (also referred to Heinrich event HE 10; Heinrich, 1988) led to a reduction of moisture availability and consequently to a regression of tree population (Chapman and Shackleton, 1999; McManus et al., 1994; Sánchez Goñi et al., 2005; Tzedakis, 2005). This distinct vegetational change to stadial conditions is marked by a decrease of arboreal pollen and introduced the end of the interglacial stage. However, the pollen record of Lake Van documents that the woody population

persisted well into the interval of ice growth until approximately 111 ka BP.

Comparison with southern European terrestrial records

The inception of the last interglacial at Lake Van is in a reasonably close agreement with previously published estimates from terrestrial records of the Near East and the Mediterranean region, although the amplitude and the succession of the tree population vary according to the geographical position and to local factors. For example, the onset of the transition to the last interglacial at Lago Grande di Monticchio, based on an independent varve chronology, occurred at ~130.55 ka BP (Allen and Huntley, 2009; Brauer et al., 2007). The long-term increase in relative abundance of temperate deciduous woody taxa including the rapid increase of sclerophyllous taxa began at ~127.2 ka BP (Allen and Huntley, 2009). Especially the increase of deciduous *Quercus* during interglacial periods is a characteristic feature in the Mediterranean pollen records (Allen and Huntley, 2009; Sánchez Goñi et al., 1999; Tzedakis et al., 2003a). This gradual forest development accompanied with a decline in herbaceous taxa is comparable to that of Lake Van with an initial warming at ~130.8 ka BP and the beginning of the climate optimum at ~127.2 ka BP.

Both astronomically calibrated records in Greece, Tenaghi Philippon and Ioannina, document a spread of deciduous woody population simultaneous with Mediterranean elements, such as *Pistacia*, *Olea* and *Phillyera.* Moreover, the onset of the last interglacial at Tenaghi Philippon (at ~129 ka BP) is characterized by an increase of arboreal pollen from ~10 to 90% within several hundreds of years (Milner et al., 2013). Furthermore, Tzedakis et al. (2002a) defined the beginning of the last interglacial at Ioannina by the presence of forest communities at 127.3 ka BP. At Lake Van, the presence of *Pistacia* occurs simultaneously with the slow expansion of *Quercus* within the initial warming period at the beginning of the last interglacial at ~130.8 ka BP.

An exception provides the sequences of Lake Urmia. Due to the large errors derived from radiocarbon dating, the chronology is based on extrapolation of similar events with distant European records. Such event stratigraphy precludes changes in climate variability and possible lags in vegetation response (Stevens et al., 2012). According to Djamali et al. (2008), the initial warming period (at ~130-127 ka; Stevens et al., 2012) of the last interglacial at Lake Urmia is defined by the appearance of juniper pollen including the increase in relative percentages of oak and pistachio.

The beginning of the last interglacial stage in the marine benthic $\delta^{18}O$ record of the Iberian margin core MD95-2042 (37°48'N, 10°10'E, water depth of 3,146 m) started much earlier at about 132 ka BP (Shackleton et al., 2002), while in the same core the last interglacial was established at ~126.1 ka BP by palynological results

(Sánchez Goñi et al., 1999). According to Shackleton et al. (2003), the early inception of the last interglacial stage in the Iberian record, based on isotope data, implies that the ice sheets had completely melted before the onset of interglacial climatic conditions started in terrestrial European pollen records. Furthermore, Sánchez Goñi et al. (2005) mentioned that the onset of the continental interglacial condition, related on palynological results, lagged the beginning of the Marine Isotope Stage MIS 5e by nearly 6,000 years.

The termination of the last interglacial stage demonstrates a similar discrepancy. At Lake Van, the end of the Eemian period is recognizable at ~110.9 ka BP, when the forest vegetation rapidly opened up and the abundances of temperate trees decrease. This corresponds well with the end of the last interglacial at ~111.8 ka BP regarding the Ioannina basin (Tzedakis et al., 2003a), at about 111 ka regarding the Tenaghi Philippon record (Milner et al., 2013) and at ~109.5 ka BP concerning the record of Lago Grande di Monticchio (Allen and Huntley, 2009). At Lake Urmia, however, the Eemian lasted until ~118-115 ka (Stevens et al., 2012) as a result of the decrease of arboreal pollen. Due to the low sampling resolution and large uncertainties in the chronology, this termination will not be considered in the following discussion.

Reconstructed by the marine benthic $\delta^{18}O$ record of the Iberian margin, the Eemian lasted until ~115 ka, whereas after the pollen-based reconstruction the last interglacial terminates at ~109.7 ka (Sánchez Goñi et al., 1999, 2005). As the onset of the last interglacial period, the pollen sequences from the deep sea core MD95-2042 as well as from the Mediterranean and Near East region lagged the accumulation of substantial ice volume of about 5,000 years (Sánchez Goñi et al., 2005). The differences in the time can be explained by the fact that the forest expansion in southern European sites were not limited by a decline in temperature, such as the northern European pollen records (Holzkämper et al., 2004; Müller, 1974; Müller and Kukla, 2004), but largely by the deficiency of moisture (Tzedakis, 2005).

During the early stage of ice growth (~115-110 ka), the oceanic heat transport continued to operate over the North Atlantic (Chapman and Shackleton, 1999; McManus et al., 2002), providing a moisture source for the woody populations in southern Europe. After sufficient ice volume accumulation (~110 ka), the ice rafting events (IRD) disrupted the thermohaline circulation and lead to a reduction in moisture supply into the Mediterranean region (Tzedakis, 2005). Consequently, this moisture deficiency is responsible for the decline of woody taxa in the Mediterranean and the Near East. Similar to Lake Van, the prolonged interglacial in the eastern Mediterranean pollen sequences extended well into the interval of global ice growth of the Marine Isotope Substage MIS 5d (Kukla et al., 1997; Martinson et al., 1987;

Müller and Kukla, 2004; Shackleton et al., 2002). Finally, the duration of the temperate forest interval in eastern Mediterranean as well as at Lake Van comprises ~16-17 ka. In northern European sites, investigations from laminated records suggest a forest interval of about 10-11 ka (Caspers et al., 2002; Müller, 1974; Seelos and Sirocko, 2007).

In most southern European records the climate optimum occurred between ~127 and 120 ka BP (Allen and Huntley, 2009; Frogley et al., 1999; Tzedakis et al., 2002a, 2003a). The main vegetational differences between the record of Lake Van and the sequences of the Mediterranean region are the higher diversity of the woody population in the Mediterranean sequences as well as the generally higher frequencies of the individual warm-temperate tree taxa. For example, the early interglacial stage at Lago Grande di Monticchio reflects a pronounced shift to temperate forests from ~30 to 80% (Allen and Huntley, 2009), while the arboreal pollen percentages in Greece rose up to ~96% in Ioannina (Frogley et al., 1999) and from ~10 to 90% in the Tenaghi Philippon sequences (Milner et al., 2013). The high frequency of deciduous *Quercus* (average ~70%) accompanied with the appearance of evergreen sclerophyllous taxa, notably *Olea*, *Phillyrea* and *Pistacia*, is a characteristic feature in all eastern Mediterranean sequences (Allen and Huntley, 2009; Frogley et al., 1999; Milner et al., 2013). Especially *Quercus ilex* type is consistently present during the climate optimum (Allen and Huntley, 2009; Milner et al., 2013). In contrast, evergreen *Quercus* was rarely found at Lake Van and Lake Urmia (Djamali et al., 2008).

Although *Ulmus* sp. and *Carpinus* sp. are recognizable at Lake Van at the beginning of the last interglacial, compared to Mediterranean records their occurrence was noticeably shortened and not continuous (Allen and Huntley, 2009; Frogley et al., 1999; Milner et al., 2013). Furthermore, the average low pine percentages (~10%) at Lago Grande di Monticchio and Ioannina basin played only a secondary role during the last interglacial (Allen and Huntley, 2009; Frogley et al., 1999). Whereas the general higher pine values (up to ~45%) at Tenaghi Philippon suggest an increasing continentality towards the East (Milner et al., 2013). Finally, within the climate optimum the vegetational composition at Tenaghi Philippon illustrates a more favorable environmental condition for warm-temperate summergreen forest development in the Mediterranean areas as compared to the Near East.

At Lago Grande di Monticchio, the stepwise decrease in temperature during the declining stage of the last interglacial period (~122 ka BP; Allen and Huntley, 2009) is indicated by the increase of woody taxa such as *Abies*, *Alnus* and *Fagus*, which were constantly absent at Lake Van and Lake Urmia (Djamali et al., 2008).

Simultaneously, the sclerophyllous vegetation (especially *Quercus ilex* type) decreased in several Mediterranean records at 122 ka BP (Allen and Huntley, 2009; Frogley et al., 1999).

Furthermore, the selected terrestrial records reveal a similar sequence of events as it is recorded at Lake Van. The North Atlantic cooling events C 26 and C 25 are conceivably visible at Ioannina basin (~118.2 ka and 114.2 ka BP), Tenaghi Philippon (~119 ka and 112 ka) and at about ~119 and 115.8 ka BP at Lago Grande di Monticchio (Brauer et al., 2007; Frogley et al., 1999; Milner et al., 2013; Tzedakis et al., 2003a) due to the changes in the individual pollen compositions. A range of warm-temperate woody taxa was continuously present, although some of them (e.g. pollen of Mediterranean taxa and *Carpinus* sp.) were less frequent than before (Allen and Huntley, 2009; Frogley et al., 1999).

At Lake Van, the cooling events can be detected by the decrease in relative abundance of deciduous oak when open vegetation expanded considerably. Moreover, the short-term effect of the C 26 event, recorded with uncertainties at Lake Van, can now be confirmed. The climatic deterioration during the C 26 was probably not strong enough to be identified at Lake Urmia (Djamali et al., 2008). Another reason may be that the event-like structure is often associated with sand layers, which are systematically avoided for pollen sampling (Sirocko et al., 2005). Nevertheless, the pronounced C 25 event implies that the first widespread change in North Atlantic circulation has an important impact on stepwise declining temperate forest cover in terrestrial records from southern Europe. Even at Lake Urmia (at ~116 ka), an effect of the cooling event C 25 is clearly recognizable due to the reduction of juniper and pistachio (Stevens et al., 2012).

The increased aridity after 114 ka BP is evidenced by high frequencies of pine (up to 45%) in the Tenaghi Philippon record (Milner et al., 2013) as well as by high fire activity at Lago Grande di Monticchio (Brauer et al., 2007). This significant change in vegetational and environmental conditions indicates the regression from an interglacial to glacial conditions in this region.

An exception provides the rapid re-expansion of deciduous oak population at Ioannina (112.3-111.8 ka BP; Tzedakis et al., 2003a), reflecting the key position of the Mediterranean area as a refugial location during cold phases. It further indicates the strong influence of the Mediterranean climate in this region.

6.3 Last glacial

The last glacial period is characterized by substantial millennial-scale vegetation and climate instability. This instability comprises rapid changes in oceanic and atmospheric circulations, which is responsible for the variability in the humidity balance of the Northern Hemisphere (van Kreveld et al., 2000; Sánchez Goñi et al., 2002). Although the climate instability in Europe has been intensively studied over the last decades, the mechanism and their consequences for environmental and vegetational response remain unclear (e.g. Allen and Huntley, 2000; Allen et al., 2000; Sánchez Goñi et al., 2002, 2005; Watts et al., 2000; Wolff et al., 2010). Especially sedimentary records are often not suitable for the investigation of rapid climate variability due to an insufficient time-resolution. However, ice core records, such as the North Greenland ice core record (NGRIP), document the temperature evolution from the last interglacial into the last glacial period (NGRIP, 2004). In contrast, the variability in marine sequences refers to changes in the ice volume (Heinrich, 1988) as well as changes in the thermohaline circulation, for example sea surface temperature changes (SST) and atmospheric circulation of the North Atlantic (Cacho et al., 2000; Chapman and Shackleton, 1999).

Within the NGRIP record, the stable oxygen isotope sequences discover a strong, reproducible pattern of millennial-scale alternation between warm Greenland Interstadials (IS) and cold Greenland Stadials (GS) since 123 ka BP (NGRIP, 2004; Sánchez Goñi and Harrison, 2010; Svensson et al., 2006). These periods of unstable environmental conditions, characterized by rapid fluctuations of warm and cold phases, are known as Dansgaard-Oeschger (D-O) cycles (Dansgaard et al., 1993; Grootes et al., 1993; Wolff et al., 2010). These events are commonly used for the stratigraphic classification of marine and terrestrial records in Europe.

Dansgaard-Oeschger interstadials are marked by rapid temperature increases, of ~8°C up to 16°C within decades, followed by gradual decreases and abrupt returns to glacial conditions lasting a few centuries to several thousand years (Genty et al., 2003; Johnsen et al., 1997; NGRIP, 2004; Sánchez Goñi and Harrison, 2010; Thomas et al., 2009; Wolff et al., 2010). 24 of such warm Dansgaard-Oeschger events have been numbered within the last glacial (NGRIP, 2004; Wolff et al., 2010), whereas the D-O 25 occurred during the last interglacial (see section 6.2).

The responsible mechanism of the millennial-scale D-O events and its environmental consequences are fairly elusive. It has been assigned to changes in the thermohaline circulation in the North Atlantic and the parallel operation of an additional atmospheric mechanism above Greenland. Especially the prominent westerly atmospheric circulation over the North Atlantic and Europe is expected to

have a significant impact on temperature and precipitation in European terrestrial ecosystems (Bond et al., 1997; Cacho et al., 1999; Tzedakis, 2005).

In general, the temperature variability in the North Atlantic was closely preceded by ice-rafted deposits (IRD) and fresh water supply into the oceanic system. A reduction of ice melting has a major effect on deep water formation including the cooling in the North Atlantic region. The cooling, in turn, reduces the melting process and re-establishes the North Atlantic circulation. The cycle closes when the temperature rises again, as a result of further fresh water input into the North Atlantic (Blunier and Brook, 2001; Bond and Lotti, 1995).

The climatic signal of abrupt temperature decreases within the Dansgaard-Oeschger stadials (Greenland Stadial), registered in the NGRIP records, corresponds with iceberg discharges and sea surface temperature (SST) variations in the marine sequences of the North Atlantic. The most pronounced cooling events (stadials) refer to Heinrich events (HE), which were defined as a period of massive iceberg melting in the North Atlantic, recorded by a strong imprint (Heinrich layers; Heinrich, 1988) in marine sediments (Bond and Lotti, 1995; Cacho et al., 1999). Throughout the last ~130 ka, six Heinrich events occurred in the North Atlantic. They display a periodicity of 7,000 to 13,000 years (Bond et al., 1993; Bond and Lotti, 1995; Broecker, 1994). During Heinrich events, a reduction of the SST lowers the evaporation and, therefore, the moisture content of low-pressure systems moving across the Mediterranean region, which intensify the aridity in southern Europe (Tzedakis, 2005).

Regarding to vegetational and environmental variability within the Lake Van record, the last glacial period can be divided into two principal parts: the early Weichselian (110.9-74.7 ka BP) and the Weichselian pleniglacial, including the last glacial maximum (74.7-14.7 ka BP).

6.3.1 Early Weichselian

The palynological results of Lake Van emphasize that this region reacted very sensitive to the rapid climate and environmental variability during the early glacial phase, as described in the North Atlantic region.

Based on the NW European classification (Table 5), the early Weichselian can be divided into four main climatic phases. In accordance with Behre and Lade (1986), the following intervals can be referred to the Herning stadial, the Brørup interstadial, the Rederstall stadial and the Odderade interstadial (Figure 6.4). The term 'interstadial' is defined as an interval of temporary improvement of climate conditions within a glacial phase, which have been either too short to permit full expansion of thermophilous trees or too cold to reach the climate optimum of an

interglacial period in the same region (Jessen and Milthers, 1928). In comparison, the term 'stadial' corresponds to cold intervals marked not by global but by local ice readvances (Lowe and Walker, 1984). In conformity with Gibbard and van Kolfschoten (2004), this definition is still valid in the climatic stratigraphy, and was established for the Lake Van region by Litt et al. (subm).

At Lake Van, the onset of the early Weichselian (at ~110.9 ka BP) is characterized by a remarkable change of climatic and environmental conditions. This variability towards climatic deterioration corresponds to the Herning stadial (~110.9-107.8 ka BP; 51.61-50.46 mcblf). Due to the continuously increasing global ice accumulation in the northern high latitudes a widespread continental aridity and a sharp decline of temperature occurred during this period (Kukla et al., 2002; Seelos and Sirocko, 2007). Consequently, the declining deciduous oak steppe-forest of the last interglacial stage was replaced by a dwarf-shrub steppe and desert steppe vegetation at Lake Van. During the following ~3,000 years, the landscape at Lake Van was dominated by herbaceous elements (80-90%), e.g. chenopods and *Artemisia*.

Within the Herning stadial, the pronounced cooling event C 24 (at ~107.55 ka BP; Shackleton et al., 2002), recorded in the marine records of the North Atlantic, refers to the collapse of the continental land ice volume (glacier) and the ice sheets in the Northern Hemisphere (Chapman and Shackleton, 1999; McManus et al., 1994; Shackleton et al., 2002). As a result, the cooling event is related with iceberg discharges (Sánchez Goñi et al., 2005), which are in turn associated with an increase of ice-rafting events (IRD) in the Atlantic Ocean (Chapman and Shackleton, 1999; McManus et al., 1994). At Lake Van, this event is recognizable between ~109.8 and 108.2 ka BP (51.23-50.66 mcblf) due to a rapid expansion of Chenopodiaceae (Figure 6.4).

The transition from steppic vegetation to a subsequent steppe-forest period corresponds with the beginning of the northern European Brørup interstadial, including the Amersfoort interstadial and the Brørup interstadial (Aalbersberg and Litt, 1998; Table 5). In biostratigraphical terms, the pollen assemblage zone (PAZ) IIIb from 50.66 to 42.06 mcblf (~107.8 to 88.33 ka BP) is characterized by an alternation between the re-expansion of pioneer and temperate woody taxa (e.g. *Quercus*) and the resurgence of desert steppe vegetation. Based on the results of the palynological data, the Brørup interstadial can be divided into three subzones (Figure 6.4). A first re-establishment of warmer climate condition characterizes the beginning of the interstadial stage (Amersfoort interstadial; D-O 24) with increased values of *Ephedra*, *Betula*, *Juniperus* and *Quercus* (10-20% AP), followed by a short-term terrestrial cooling event (C 23) with low values of woody taxa (5-10% AP) and the

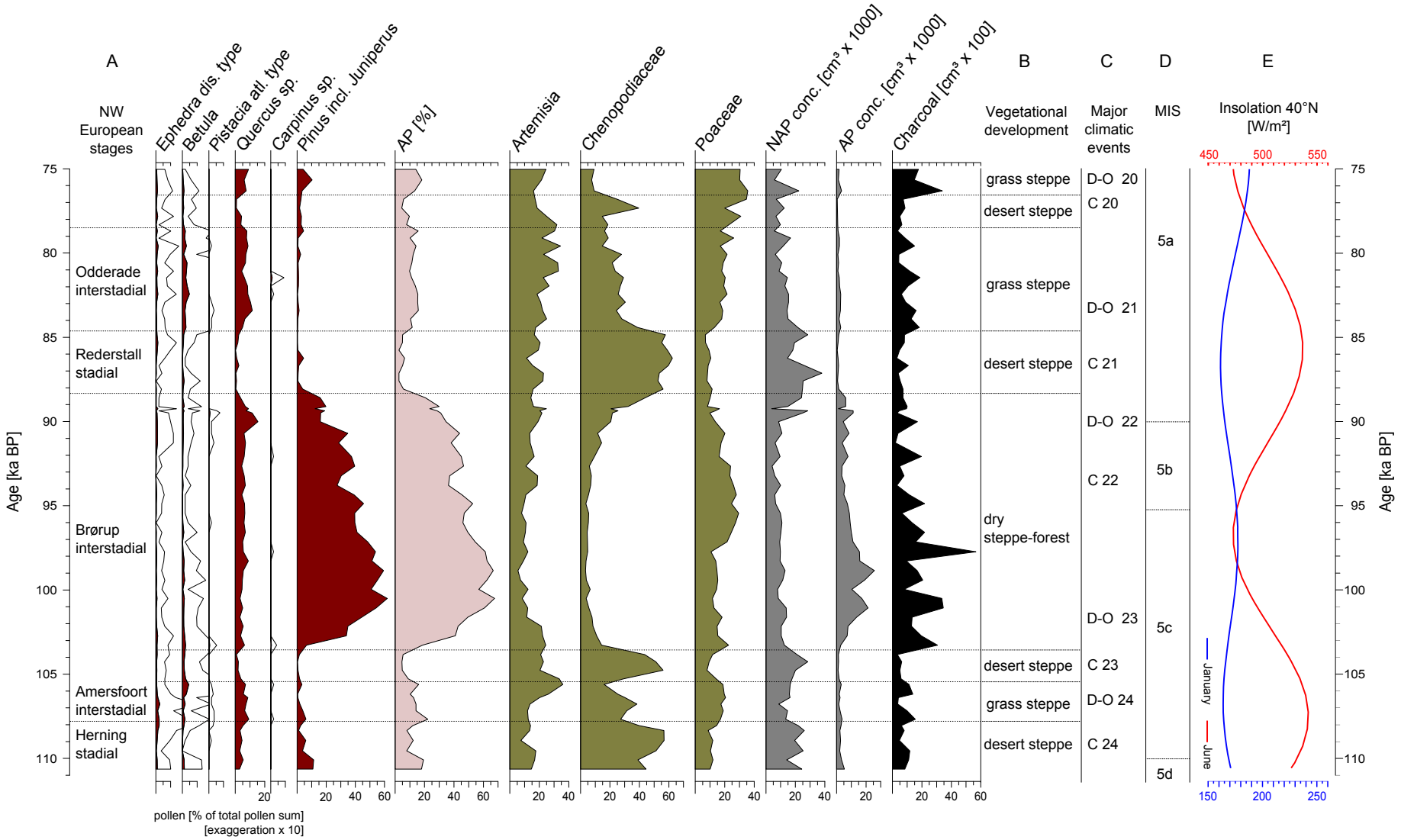

Figure 6.4: Simplified pollen diagram of the early Weichselian at Lake Van. A - Terrestrial stages after the northern European stratigraphy; B - Vegetational development at Lake Van; C - Major climatic events; D - Marine Isotope Stages (MIS) and Substages after Lisiecki and Raymo (2004); E - mid-June (red line) and mid-January (blue line) insolation 40°N after Berger et al. (2007).

subsequently development of a steppe-forest (30-63% AP) throughout the second part of the Brørup interstadial (MIS 5c).

The short-term climatic amelioration within the D-O 24 (Amersfoort interstadial; 107.8-105.44 ka BP; 50.66-49.17 mcblf) is coupled with high mid-June insolation values. The increase in summer insolation is responsible for the melting of the ice sheets. This is evident due to a less expansion of the northern continental ice volume, compared to glacial extension (Chappell et al., 1996; Sánchez Goñi et al., 2005). The resulting warming trend during the D-O 24 is associated with increase of deciduous oak and high Poaceae abundance, albeit at reduced tree population densities. The slight expansion of woody taxa (e.g. *Quercus*) indicates a shift from desert steppe vegetation to a grass steppe, which is in turn combined with a still open landscape character.

The following terrestrial cooling event C 23, which took place between 105.44 and 103.56 ka BP (49.17-48.34 mcblf) at Lake Van, refers to a short climate deterioration from a transitional grass steppe towards a more open *Artemisia* - Chenopodiaceae desert steppe vegetation. Thus, the C 23 event corresponds to the Montaigu event in SW European pollen sequences (de Beaulieu and Reille, 1992, Table 5) and with rather low values of ice-rafting debris (IRD) in the marine sequences of the North Atlantic (McManus et al., 1994). Even astronomical forcing is not able to convincingly demonstrate such a short event. Due to the lack of the IRD signal from the deep sea cores, the C 23 event reflects only a reduction in the sea surface temperature (McManus et al., 1994). Nevertheless, during this cold event, the predominance of steppic elements at Lake Van refers to rather dry climatic environments culminating in a shift to desert steppe vegetation.

According to the sedimentary evolution of Lake Van, the unstable climate and environmental conditions at the beginning of the early Weichselian, between ~110 and 98 ka BP, can be confirmed by the frequent occurrence of 'mass-move' deposits and rapid changes in the lake level, indicating severe climate variability (Stockhecke et al., 2013).

The second part of the Brørup interstadial (D-O 23; 103.56-88.33 ka BP; 49.17-42.06 mcblf) is characterized by reduced amplitude of temperate woody taxa (e.g. deciduous oak). Nevertheless, the pronounced warm phase documents a pre-dominance of pine, but with significant lower values of oak than the previous interglacial. As a result, the pollen composition suggests that moisture availability was too low to enable an expansion of oak. The warm/dry-climate deposits in the sedimentary record support this assumption and further point to a strong seasonality at Lake Van (Stockhecke et al., 2013).

Another important aspect is the variation in the intensity of mid-June insolation, which is lower during the Brørup interstadial compared to the previous interglacial. This confirms the assumption that the environmental conditions were generally too cold for a full forest expansion, especially during the winter. Based on these considerations, this aspect can probably be explained by the predominant role of pine, which in turn allows the conclusion of a more continental climate condition during the interstadial. A further important factor to be considered is the high pollen production and the pollen dispersal of pine. This pattern leads to an over-representation in the pollen record especially in open-landscape environments (Davis, 2000; Prentice, 1985).

After a period of approximately 5,500 years the predominance of *Pinus* declined and the forest composition shifted to a more open forest character. In this case, the transition from Brørup interstadial to the following cold phase appears to occur rather steadily. In particular, a phase of slow cooling and low oscillating tree pollen is clearly recorded from ~98 ka BP, where maximum mid-January and minimum mid-June insolation values simultaneously occurred (Figure 6.4). The slight cooling trend is documented by a continuous increase in herbaceous taxa, especially by Poaceae, as well as by the continuous decrease of charcoal particles from the middle part of the interstadial period. Chapman and Shackleton (1999) and McManus et al. (1994) describe a further much less pronounced cooling event C 22 at the end of the Brørup interstadial, indicated by a very low IRD signal. This corresponds to the gradual decline of woody taxa in the Lake Van pollen record between ~94.07 and 92.93 ka BP (44.93-44.53 mcblf). The continuous cooling trend within the Brørup interstadial was interrupted by a temporary increase of oak values, accompanied by a resurgence of thermophilous steppe-forest (e.g. *Quercus*, *Betula*). This short-term climatic amelioration can be correlated with the Dansgaard-Oeschger event D-O 22 at ~90.36-89.43 ka BP (43.44-42.85 mcblf; Figure 6.4).

At ~88.3 ka BP (42.06 mcblf), the *Pinus-Quercus* steppe-forest was replaced by a dramatic increase of the desert steppe vegetation (>70%), dominated by chenopods and *Artemisia.* The very high abundance of Chenopodiaceae in the vegetation composition indicates a marked development of seasonal dryness (Allen et al., 2000). The Rederstall stadial (MIS 5b; 88.33-84.63 ka BP; 42.06-40.47 mcblf) is associated with the short-term cooling event C 21. One short period during the Rederstall stadial is characterized by a partial spreading of woody taxa, indicating an apparent instability of climate and consequently a fluctuation in the nature of the vegetational cover.

The expansion of several woody taxa between ~84.63 and 78.5 ka BP (40.47-

35.67 mcblf) marks the transition into the Odderade interstadial (MIS 5a; D-O 21). In this study, the environmental conditions of this interstadial cannot be completely resolved. The interruption of the ~2 m thick Incekaya-Dibeli tephra layer (at ~80 ka; Sumita and Schmincke, 2013b) and the fragmentary documentation of the vegetation signal complicates the reconstruction of the climate condition during the Odderade interstadial (Figure 5.1). Lithological investigations within this interval confirm the climate amelioration as a result of high lake level stand (Stockhecke et al., 2013). However, one exception occurred. Pine abundance was less prominent, while more Poaceae, *Quercus* and *Betula* are recorded during this period. Due to the lower woody taxa (~10-15%) and to the continuously higher herbaceous taxa (~85-90%), the pollen assemblage of the Odderade interstadial points to lower temperatures and higher moisture deficiency than the previous interstadial.

A brief cold interval C 20 (~78.5-76.56 ka BP; 35.67-34.88 mcblf) of about 1,900 years followed the interstadial period. It is characterized by desert steppe vegetation. This vegetational change indicates a return to cold climate conditions with less moisture availability. The subsequent short-term interstadial D-O 20 (~77.07-74.70 ka BP; 35.08-34.28 mcblf) documents a re-succession of wooded steppe populations. The resurgence of *Betula*, *Pinus* and *Quercus* is the response of climate amelioration. It illustrates that the Dansgaard-Oeschger event D-O 20 appears with relatively high moisture availability due to the strong North Atlantic drift. The warm current reached far into the north, which in turn provides warmer temperature and more precipitation for the central European continent (Sirocko et al., 2005). Finally, the termination of the early Weichselian in the Lake Van pollen record at ~34.28 mcblf is consistent with the end of the Marine Isotope Stage (MIS) 5 at ~73.9 ka (Martinson et al., 1987).

The examined observations and the reconstruction of the early Weichselian lead to the suggestion that those periods of climatic transitions, either from interstadial to glacial or vice versa, are particularly sensitive for short-term climatic and environmental fluctuations. In addition, the observed changes in atmospheric circulations during the cooling events are a result of the southward shift of the westerly winds, indicating a strong effect on the environment in the Near East.

Comparison with southern European terrestrial records

The environmental and vegetational variability that was observed at Lake Van can be compared with terrestrial pollen records from the eastern Mediterranean region. Due to large errors, missing core sections and uncertainties regarding the age model of Lake Urmia (Stevens et al., 2012), a comparison with Lake Van is not recommendable for the early Weichselian and, therefore, will not be discussed in the following section.

The inception of the early glacial is characterized by the re-establishment of the southern European steppe vegetation, indicating a prevalence of at least seasonal aridity (Allen and Huntley, 2009; Tzedakis, 1993). Besides, the eastern Mediterranean areas were not directly influenced by periglacial conditions. Such protected refugial areas of less strong cold conditions with more moisture availability allow the presence of woody populations at Ioannina basin and at Lago Grande de Monticchio during stadial conditions (Allen and Huntley, 2000; Tzedakis, 1994). At Lago Grande di Monticchio (109.5-107.6 ka BP; 86.6-84.2 ka BP), the vegetation changed to a savannah-like structure with less than 60% arboreal pollen (Allen and Huntley, 2000, 2009). In addition, the pollen composition at Ioannina basin (111.8-104.5 ka; 88-83 ka) refers to an open *Quercus-Pinus* steppe-forest (40-70% AP) with *Juniperus* abundances (Tzedakis et al., 2002b). This suggests that even extreme cooling events were not severe enough to eliminate the complete local tree population (Tzedakis, 2005). Tenaghi Philippon is generally characterized by a more continental climate. This is supported by an almost complete absence of temperate woody plants during stadial periods (Tzedakis, 1993). Nevertheless, the stadial vegetation in the eastern Mediterranean indicates that, although cold, this period had greater moisture availability than the Near East during the entire glacial periods. Furthermore, several short intervals with partial resurgence of forest cover on low amplitudes were detected in the southern European records. This illustrates the 'sensitivity' of climate variability in various archives in relation to their geographical location and to their local environmental features (Allen and Huntley, 2000; Allen et al., 2000; Tzedakis et al., 2003b; Tzedakis, 2005). Due to the lower sampling resolution at Lake Van, several short-term fluctuations were not identified in the palynological sequences.

During the interstadials the landscape of the Near East and southern Europe was, adapted to the warm climatic conditions, predominantly forested. At Ioannina basin (~104.5-88 ka; 83-68 ka; Tzedakis et al., 2002b), Tenaghi Philippon (~106-90 ka BP; 82-73 ka BP) and Lago Grande di Monticchio (~107.6-86.6 ka; 84.2-72 ka Allen et al., 1999, 2000), the temperate forest consists of 70-90% woody taxa. A brief period of *Fagus*, *Alnus* and *Abies* expansion as well as the presence of *Quercus*, *Carpinus*, *Ulmus* and *Tilia* underlines the higher diversity, which points to warm

moist summers in the eastern Mediterranean region during the interstadials (Allen and Huntley, 2000; Allen et al., 2000; Tzedakis, 1994).

At Lake Van, a dry *Pinus-Quercus* steppe-forest dominated the interstadials and refers to open woodlands rather than closed forest. Furthermore, herbaceous pollen taxa, in particular Poaceae, were constantly present along with low abundances of arboreal pollen taxa. The less pronounced cooling event (C 22), which is detected with uncertainties at Lake Van, can now be supported by the significant decline of *Quercus* in the Lago Grande di Monticchio sequence (~93.8 ka BP; Allen et al., 2000). Also the C 23 event was recorded at several European sites, for instance at Tenaghi Philippon (Wijmstra, 1969). However, the rapid re-expansion of temperate woody taxa indicates that such short-term cold periods are characterized by the presence of abundant refuges in southern Europe.

Furthermore, the investigation of the interstadial/stadial boundary (MIS 5c/5b) reveals a similar situation as discussed above for the MIS 5e/5d boundary (see section 6.2). According to Lisiecki and Raymo (2004) and Martinson et al. (1987), the marine isotope record documents that the transition to the following Rederstall stadial (C 21 cooling event) was at ~94 ka, whereas the end of the forest period at Lake Van and the eastern Mediterranean occurred between 88 and 86 ka. This roughly corresponds to a delay of the vegetation changes of about 6,000 years after the end of MIS 5c (Allen et al., 2000; Tzedakis, 2005). However, the transition from the Odderade interstadial into the early pleniglacial (MIS 5a/4) is difficult to determine as a result of significant climatic instability. It started with the decrease in air temperature and the cooling event C 20, followed by two prominent Dansgaard-Oeschger events (D-O 20 and D-O 19). Lisiecki and Raymo (2004) identified the boundary MIS 5a/4 at ~71 ka in the marine record. By comparison, the pollen sequences of Lake Van and Tenaghi Philippon as well as Lago Grande di Monticchio indicate an end of the forest period at about 75-72 ka (Allen and Huntley, 2000; Allen et al., 2000), while the landscape in Ioannina was almost covered with a dense temperate forest until ~67 ka BP, including the MIS 4.

6.3.2 Weichselian pleniglacial

Throughout the Weichselian pleniglacial (~74.7-14.5 ka BP), the Lake Van record indicates a period of significant millennial-scale environmental and vegetational variability of irregular periodicity. The millennial-scale climate variability of the Dansgaard-Oeschger (D-O) events, registered in the North Greenland ice core sequences, is considered to trigger the temporal pattern in the vegetation response to climatological processes. The following section examines how the well-studied climate signal of the D-O events affected the vegetational composition in more distant regions.

The early pleniglacial is characterized by an interval of severe aridity in the Northern Hemisphere and by a high global ice volume of the Fennoscandian ice sheet (Fletcher et al., 2010; Sánchez Goñi and Harrison, 2010). Consequently, the pollen composition at Lake Van clearly reflects a pre-dominance of herbaceous taxa throughout the last glacial. A series of interstadials, characterized by a short-term expansion of woody taxa (e.g. *Quercus*, *Pinus* and *Juniperus*), interrupted the general dominance of desert steppe vegetation (e.g. *Artemisia*, Chenopodiaceae and *Ephedra)* in eastern Anatolia. Frost-sensitive species such as *Pistacia*, frequently found during the last interglacial (MIS 5e) and the Holocene, were constantly absent throughout the last glacial. This suggests that winter frost regularly occurred during glacial times.

In conformity with Litt et al. (subm), the lack of warm summer temperature was not only the limiting factor for tree growth in eastern Anatolia. Instead, the dominance of dry steppic taxa (e.g. chenopods and *Artemisia*) indicates low moisture availability. Therefore, the deficiency of moisture hampers the spread of woody taxa at Lake Van. For instance, deciduous *Quercus*, which requires warm summer temperature and moisture availability, was constantly present but with very low values. These limited abundances support the assumption of a long-distance transport from refugial area.

Müller et al. (2011) document a forest expansion in the eastern Mediterranean region due to the short-term increase of precipitation. Furthermore, the authors assume that the westerly winds served as the main precipitation source into Europe, as a result of an increase in sea-surface temperature of the North Atlantic. The opposing cold period is associated with changes in the thermohaline circulation in the North Atlantic. The precipitation over Europe is reduced, indicating a southward displacement of the Intertropical Convergence Zone (ITCZ) and a decrease in Northern Hemisphere monsoon activity (Harrison and Sánchez Goñi, 2010). These studies support the conclusions that short-term increases of moisture availability

interrupted the general arid environment at Lake Van.

Based on the palynological results, the Lake Van sequence can be divided into three major periods in which the D-O activity appears particularly variable. According to this, the Weichselian glacial is classified into the early pleniglacial with the pronounced D-O 19 and 18 events (MIS 4), followed by the middle pleniglacial (MIS 3; 59.2-28.1 ka BP) and the late pleniglacial including the last glacial maximum (MIS 2).

The early pleniglacial

The early pleniglacial (34.27-26.90 mcblf) is represented by the PAZ VIIa (Figure 5.1). This period corresponds to the Marine Isotope Stage (MIS) 4 (73.2-58.9 ka; Martinson et al., 1987) of the North Atlantic sequences as well as to the North Greenland ice core records (73.5-59.4 ka; Sánchez Goñi and Harrison, 2010; Wolff et al., 2010).

At Lake Van, several periods can be structured by more moisture availability. It reveals that the increase in woody taxa is associated with the climate signal of the Dansgaard-Oeschger events, recorded in the Greenland ice core records (Figure 6.5). Therefore, the Lake Van pollen record indicates the occurrence of a mild and humid climate during the D-O interstadials whereas dry and cold conditions were dominant during the D-O stadials.

The D-O 19 at 72.1-70.8 ka BP (33.26-32.53 mcblf) is characterized by a significant spread of woody taxa (~14%), and therefore it is the most recognizable interstadial during the early pleniglacial. In contrast, the Dansgaard-Oeschger events 18 (64.2-63.7 ka BP; 30.05-29.84 mcblf) and 18.1 (68.9-67.7 ka BP; 31.64-31.24 mcblf), as indicated in the Lake Van pollen record, are not as significant as the equivalent Greenland Interstadials (IS) detected in the NGRIP record. At Lake Van, they can only be observed by a slight increase in oak values (~4-5% AP). Lower increases in the sea-surface temperature of the North Atlantic and, thus, the lower moisture supply into the Near East are responsible for the smaller amplitude of these events.

Due to palynological results, each interstadial is marked by the development of wooded steppe vegetation and started with the increase of *Betula*, which is able to grow under harshest conditions as far as temperature is concerned (Zohary, 1973b). The initial warming period was followed by a temperate interval with moderate deciduous *Quercus* abundance accompanied with a decline of Chenopodiaceae, indicating more moisture availability. The D-O 19 event, one of few exceptions, immediately started with a moderate rise of oak values. This exception may results from the low sampling resolution of the Lake Van record. The pioneer species *Betula* occurred in the subsequent final phase, associated with an expansion of *Pinus* and *Ephedra*

frequencies, referring to continental and dry climate conditions towards the end of each interstadial period. The cold/dry period between two Dansgaard-Oeschger events (D-O stadial) indicates an interval of ice readvances, which in turn were responsible for the decline of woody taxa and the predominance of herbaceous taxa at Lake Van. Sánchez Goñi and Harrison (2010) describe that the D-O stadial at the end of the D-O 18 corresponds with the Heinrich event HE 6 at 63.2-60.1 ka.

Table 6: Age and length of each Dansgaard-Oeschger event (D-O) in the Lake Van pollen sequence (LV) in comparison to the NGRIP ice core record after Wolff et al. (2010). The ages are given for the onset of the D-O events; n.e. = no evidence.

Start of D-O	Age LV [ka BP]	Duration LV [ka]	Age NGRIP [ka BP]	Duration NGRIP [ka]
1	14.5	1.4	14.64	1.9
2	23.2	0.8	23.29	0.1
3	28.1	1.1	27.73	0.3
4	29.7	1.2	28.85	0.3
5	32.5	0.6	32.45	0.5
6	33.8	0.7	33.74	0.4
7	35.6	0.6	35.43	0.7
8	38.4	2.2	38.17	1.6
9	40.4	1.0	40.11	0.3
10	41.9	0.9	41.41	0.7
11	43.5	0.6	43.29	1.0
12	46.8	1.9	46.81	2.6
13	49.2	n.e.	49.23	n.e.
14	54.4	4.4	54.17	n.e.
15	55.7	0.6	55.75	n.e.
16	58.1	1.4	58.23	n.e.
17	59.9	1.3	59.39	n.e.
18	64.2	0.5	64.04	0.3
18.1	68.9	0.4	n.e.	n.e.
19	72.1	1.4	72.28	2.0
20	77.0	2.4	76.40	2.4

Heinrich events, as defined in the previous section 6.3 'Last Glacial', represent an abrupt global climate change towards colder glacial conditions. The pronounced cold intervals, recorded in the marine sequences in the North Atlantic (Heinrich, 1988), indicate amplification towards the driest and coldest phases throughout the glacial period. They apparently precede some of the most strongly expressed D-O interstadials (Bar-Matthews et al., 1997; Fletcher et al., 2010; Harrison and Sánchez Goñi, 2010). Heinrich events, also detectable in the western Mediterranean region (e.g. Portuguese margin; Roucoux et al., 2001; Sánchez Goñi et al., 2002), are associated with periods of a significant drop of AP values. At Lake Van, both types of events (Heinrich event and Dansgaard-Oeschger stadial) lead to a similar reduction

of tree taxa (especially of *Quercus*), and therefore cannot be distinguished from an average cooling event. Moreover, this illustrates that the climate conditions during the Heinrich event HE 6 has no considerable influence on the climate variability in the Near East.

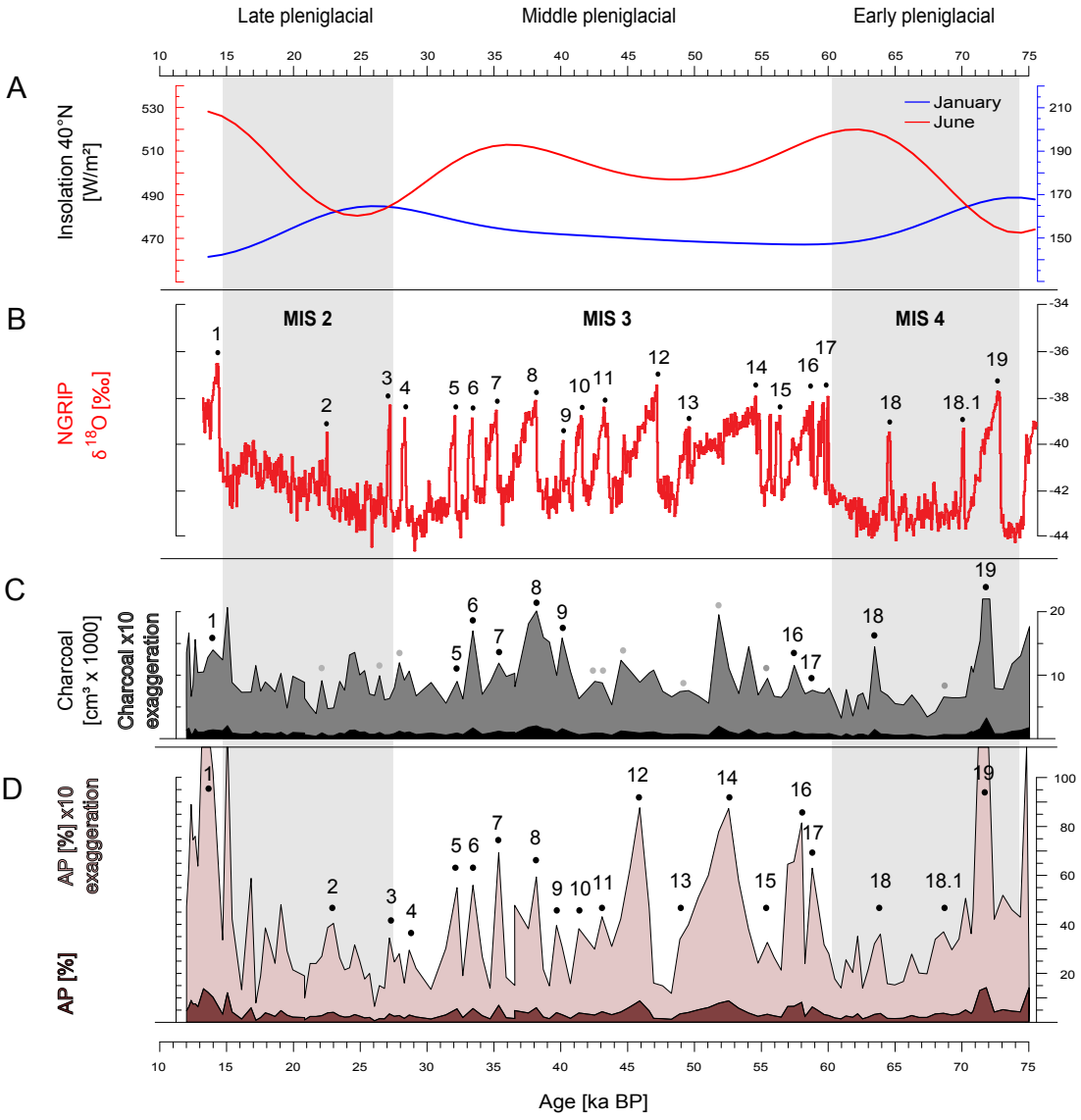

Figure 6.5: Dansgaard-Oeschger events in the Lake Van pollen record. A - mid-June (red line) and mid-January (blue line) insolation 40°N after Berger et al. (2007); B - Stable oxygen isotope data of the NGRIP record (Wolff et al., 2010); C - Charcoal concentration [particles/cm³] in black with a ten-fold exaggeration plotted in dark grey, black (•) mark the D-O events in the charcoal record, whereas the grey dots reflect the potential position of the interstadials; D - Arboreal Pollen (AP; brown) with x10 exaggeration of the woody taxa (light brown).

The determined length of each interstadial detected in the Lake Van pollen record is given in Table 5. The table should be used as a guide, because it is difficult to determine exactly the point of the beginning and the end of each interstadial due to the lower sampling resolution of the Lake Van record. Nevertheless, the table indicates that the D-O 18 and D-O 18.1 lasted only ~400 to 500 years, while D-O 19 existed for more than 1,400 years, similar to the climate signal of the NGRIP sequences (Svensson et al., 2008; Wolff et al., 2010).

The charcoal record points out that fire were by far the most important disturbance of vegetation at a regional scale. Within the last glacial, the increase of charcoal particles shows that fire has an initial immediate response to climate variability (Figure 6.5). The general tendency is that fire activity increased during the Dansgaard-Oeschger events as a result of higher vegetation productivity. This is particularly evident in the D-O 19 event. In contrast, colder and drier climate conditions reduced the vegetational productivity and, thus, the availability for burning (Daniau et al., 2010). Nevertheless, the fire activity was consistently lower during the glacial period than during the last and present interglacial (Figure 5.1).

The middle pleniglacial

Figure 6.5 illustrates the detailed nature of the Lake Van pollen record throughout the middle pleniglacial. It allows the identification of millennial-scale expansion and the contraction of total tree taxa, similar to the frequency of the climate variability resolved in the Greenland ice core records (NGRIP, 2004; Wolff et al., 2010). The figure shows a sequence of 19 identified and numbered Dansgaard-Oeschger cycles, of which 14 events (D-O 4-17) can be assigned to the middle pleniglacial. This period, recognized between 26.90-13.64 mcblf in the Lake Van pollen record, corresponds with the timing of the Marine Isotope Stage (MIS) 3 (57-29 ka; Lisiecki and Raymo, 2004) as well as with the North Greenland ice core sequences (59.4-27.8 ka; Wolff et al., 2010).

In accordance with Sánchez Goñi and Harrison (2010) and Wolff et al. (2010), the Dansgaard-Oeschger events in the MIS 3 appear to be stronger than those of the previous MIS 4. Due to the continuous high mid-June insolation curve, it can be assumed that the middle pleniglacial was characterized by a less severe aridity and less ice cover (Figure 6.5).

Furthermore, the sedimentary evolution of Lake Van shows a rhythmic alternation of lake level regression and transgression. Lithologies that are characteristic for cold/dry climate conditions were intercalated by few warm/wet climate deposits. The described accumulation implies that between ~52 and 26 ka BP the lake levels

was similar or higher than the present-day lake level (Stockhecke et al., 2013).

The pattern of the vegetational change in response to millennial-scale climate variability will be illustrated by examining the most prominent Dansgaard-Oeschger events, e.g. the D-O complex 17/16, D-O 14, D-O 12 and D-O 8. Differences in the duration of each D-O event are listed in Table 5.

Figure 6.6 pictures the diversity of pollen composition within these four interstadials. As described in the previous section, the successions of D-O 14 (54.4-49.9 ka BP; 24.82-23.62 mcblf), D-O 12 (46.8-44.8 ka BP; 22.67-22.12 mcblf) and D-O 8 (38.4-36.2 ka BP; 19.93-19.15 mcblf) followed the same vegetational pattern of an increase of *Betula* during the initial warming phase, the expansion of deciduous oak as well as an increase of *Pinus* and *Ephedra* within the final phase of an interstadial. The short-term expansion of summergreen *Quercus* indicates that the climate conditions within the interstadials became more favourable for woody taxa, due to the estimated moderate temperature changes of 7-10°C in the NGRIP records (Wolff et al., 2010). Nevertheless, the relative high abundance of *Ephedra* and *Pinus* in the tree composition of Lake Van and the continued high values of steppic elements refer to still open landscape vegetation with arid climate conditions in eastern Anatolia.

The general low values of thermophilous tree pollen point to a long-distance transport from refugial areas with greater moisture availability, e.g. from the southern slope of the Bitlis Massif or from the relative humid Caucasus Mountains (Bottema, 1986; Shumilovskikh et al., 2012). In addition, Shumilovskikh et al. (2013) revealed that the northern slopes of the Pontic Mountain served as a refugial area for trees during glacial times, as a result of the increased atmospheric moisture and higher orographic precipitation.

The Dansgaard-Oeschger event 17, which occurs in the first part of the middle pleniglacial between 59.5-58.5 ka BP (26.70-26.31 mcblf), represents an exception. By comparison, the climatic improvement of D-O 17, associated with an increased humidity, is illustrated by a simultaneous appearance of *Betula* and deciduous oak. The ending phase indicates a less arid climate period, due to the lower values of *Pinus* and *Ephedra*. However, the D-O 17 is characterized by a double-peak high amplitude temperature change in the NGRIP record (Figure 6.5). Due to the sampling resolution of 20 cm, the double peak was not recognized in the Lake Van pollen record.

The sharp climatic deterioration, which took place immediately before the onset of D-O 12, indicates a collapse of the Laurentide ice sheet associated with an iceberg discharge and results in a disruption of the North Atlantic circulation. The so-called Heinrich HE 5 event (~50-47 ka BP; Sánchez Goñi and Harrison, 2010) triggered

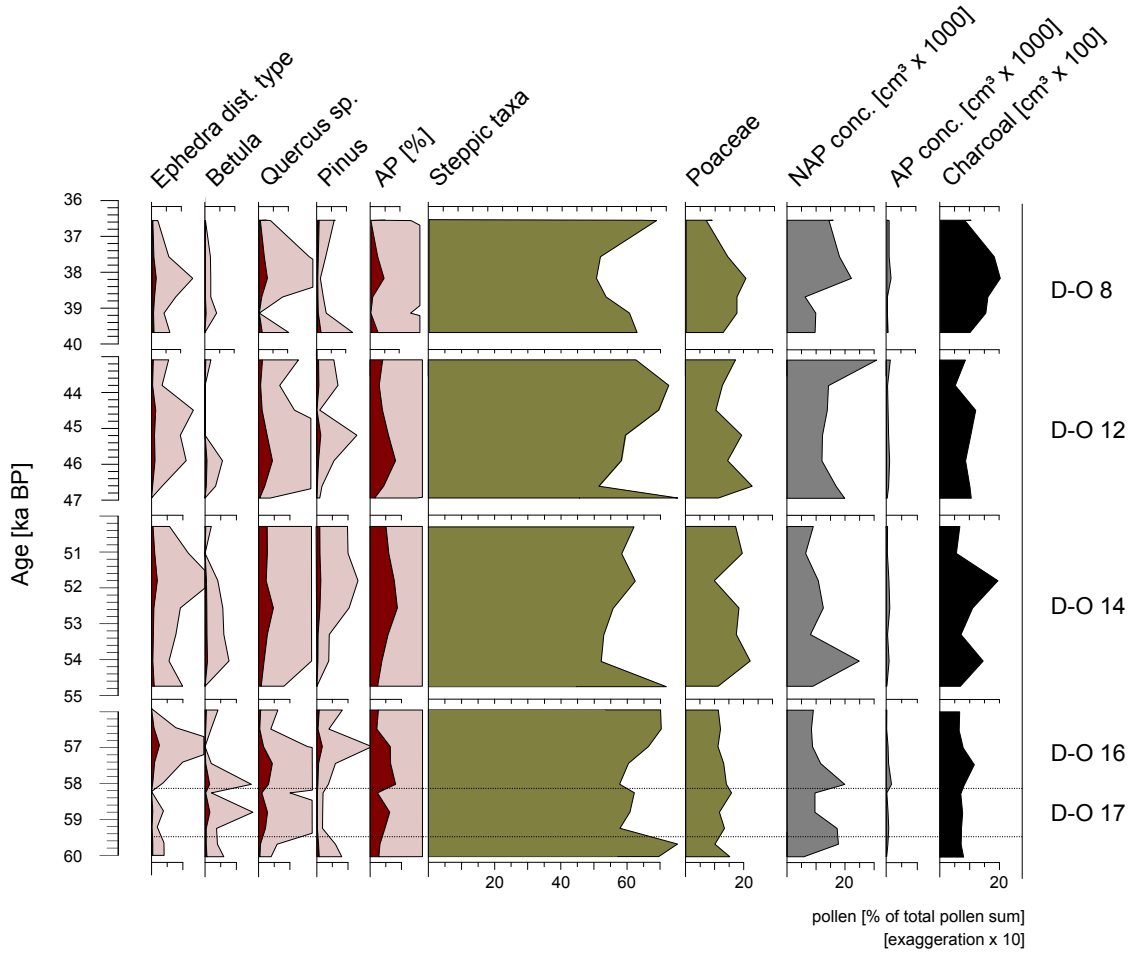

Figure 6.6: Vegetational succession of the Dansgaard-Oeschger events 17/16, D-O 14, D-O 12 and D-O 8 at Lake Van. Steppic taxa consist of *Artemisia* and Chenopodiaceae.

an extreme cold and dry climate signal in Europe (Broecker, 1994; Müller et al., 2003, 2011; Sánchez Goñi et al., 2002). The vegetation composition at Lake Van may reflect an impact of the HE 5 at 48.6-46.8 ka BP (23.23-22.67 mcblf) associated with an intensifying effect of arid climate conditions, which might be responsible for the rapid expansion of herbaceous elements. However, the palynological effects at Lake Van are too weak and, therefore, the influence of the Heinrich events in the Near East region is accompanied by great uncertainty. Obviously, the same can be assumed for the Heinrich event HE 4 (40.2-38.3 ka BP; Harrison and Sánchez Goñi, 2010), right before the Dansgaard-Oeschger event 8, and HE 3 at 32.7-31.3 ka BP (Harrison and Sánchez Goñi, 2010) in the NGRIP record. At Lake Van, the Heinrich events cannot be distinguished from conventional cooling events between two warm interstadials.

The late pleniglacial

At Lake Van, the period between 13.64 and 6.62 mcblf corresponds to the late pleniglacial including the last glacial maximum (~27-23 ka; Svensson et al., 2006, 2008). This interval correlates with the Marine Isotope Stage (MIS) 2 at 29-14 ka (Lisiecki and Raymo, 2004) and with the NGRIP sequences between 27.8 and 14.7 ka (Wolff et al., 2010).

The inception of the MIS 2 is rather problematic. Voelker (2002) defines the boundary between the middle and late pleniglacial right before the Dansgaard-Oeschger event 4. Several other authors indicate that the boundary occurs between D-O 4 and D-O 3 (Martinson et al., 1987; Shackleton et al., 2004; Wolff et al., 2010), while in turn Andersen et al. (2006) established the boundary at the end of D-O 3. In this study, the transition between middle pleniglacial and late pleniglacial is determined between D-O 4 and D-O 3 (~28-27 ka BP; 13.64-13.04 mcblf) based on the results of the pollen analysis (cluster analyse 'CONISS'; see section 5.1).

Due to the low summer insolation, the late pleniglacial is characterized by a large global ice volume, combined with a low sea level stand (Grootes and Stuiver, 1997; Sánchez Goñi and Harrison, 2010). As a result, the signal of the Dansgaard-Oeschger events, registered in the Greenland ice core records, appears to be low within the MIS 2 (Wolff et al., 2010). This pattern is also detectable in the pollen record of Lake Van (Figure 6.5) due to smaller amplitudes of woody populations (e.g. *Quercus*, *Betula*, *Pinus* and *Juniperus*) associated with an increase of moisture deficiency as well as with a temperature decrease during the last glacial maximum (Svensson et al., 2006, 2008). The arid climate conditions at Lake Van are confirmed by the predominance of semi-arid desert steppe elements such as *Artemisia*, Chenopodiaceae and Poaceae. Furthermore, the occurrence as well as the continuous increase of the shrubby plant *Ephedra* underlines the cold and dry climate conditions in eastern Anatolia.

Towards the end of MIS 2, the vegetation composition shows a series of small amplitude peaks of total arboreal tree values (especially of *Ephedra*, *Betula* and *Quercus*), which reflect short-term intervals of less-severe glacial conditions. Between 16.5 and 15.2 ka BP (7.72-7.02 mcblf) the Lake Van sequence demonstrates a cold period with less than 5% woody population. This short-term interval may be associated with the Heinrich event HE 1 (18.0-15.6 ka; Sánchez Goñi and Harrison, 2010), occurring synchronous with the rapid decay of the ice sheet in the Northern Hemisphere (Bond and Lotti, 1995).

Comparison with southern European terrestrial records

The short-term climate variabilities of the Greenland ice core sequences are also reflected in several high-resolution continental pollen records in the eastern Mediterranean region (e.g. Allen et al., 1999, 2000; Magri and Sadori, 1999; Müller et al., 2003; Tzedakis et al., 2002b; Tzedakis, 2005). Most of the terrestrial pollen records provide a temporal and environmental sensitivity to reveal the extent and the effects of these climate fluctuations throughout the last glacial. Figure 6.2 illustrates the response of vegetation to the millennial-scale climate variability in southern Europe. The glacial sequences of Lago Grande di Monticchio (~60.4-25.9 ka; Allen et al., 2000), Ioannina basin as well as of Tenaghi Philippon are characterized by high amplitude shifts of woody taxa similar to the pattern of the Dansgaard-Oeschger events in the NGRIP record (Allen et al., 2000; Müller et al., 2011; Tzedakis et al., 2002b). Although the tree population in the eastern Mediterranean records reflects the Dansgaard-Oeschger events very well, they vary in magnitude and length of the vegetational expansion depending on their geographical location. For example, the western region of Greece is marked by high precipitation as a result of the uplift of moist air from the Ionian Sea during the last glacial (Tzedakis et al., 2002b), which resulted in a moderate impact of regional aridity on woody populations at Ioannina basin. In contrast to Lake Van, the largest tree population contraction in the eastern Mediterranean sequences, at Ioannina and Lago Grande di Monticchio, are associated with the Heinrich events, while the intermediate decline of arboreal pollen corresponds to the Dansgaard-Oeschger stadials (Allen et al., 1999; Tzedakis et al., 2002b; Watts et al., 1996). The Tenaghi Philippon record provides an exception, where both, D-O stadials and Heinrich events, had an equal large impact on temperate tree populations (Müller et al., 2011). Furthermore Tzedakis (1993, 2005) and Müller et al. (2011) mentioned that the record does not show any continuous presence of warm-temperate taxa, which indicates a moisture deficiency during the glacial periods. Thus, the Tenaghi Philippon record marks the transition from high moisture availability (served by the westerly winds) of the Mediterranean region to moisture deficiency of the Near East.

The rain-shadows of major mountain ranges, as in the case of Lake Van (Bitlis Massif) and Lake Urmia (Zagros mountain), had a huge impact on moisture availability and, therefore, a strong effect on vegetation communities. In spite of the poorly dated low-resolution sequence of Lake Urmia, which does not allow a reliable identification of the vegetation and climate response, the record shows a virtual absence of Dansgaard-Oeschger events during the last glacial. However, it confirms the assumption that climate variability and moisture supply in the Near East region

were too low to release a discernible change in the vegetation.

The variation of their local climatic requirements is reflected by the different migration rate of the woody taxa between the Mediterranean and Near East records (Harrison and Sánchez Goñi, 2010). The Ioannina sequence, which is surrounded by high topographic variability, provides a range of sheltered habitats for tree population from incursions of cold polar air from the north (Lawson et al., 2004; Tzedakis et al., 2002b; Tzedakis, 2005). Such protected refugial areas of less strong cold conditions and high moisture availability allow a forest expansion or a dispersal of tree elements within less than 1,000 years. Conversely, the low development of the woody population at Lake Van points to a long-distance transport from refugial areas and therefore to a delay of the forest expansion of more than 1,000 years.

Regardless to the expansion and the amplitude of woody taxa, the high diversity of tree elements within the pollen composition is another important aspect for the climate reconstruction in southern Europe during the last glacial period. In general, most sites of the Mediterranean region show the pattern of intermediate contraction in woody populations due to cold and dry climate conditions. Moreover, the Mediterranean records reflect the similar shape of the Dansgaard-Oeschger signal throughout the pleniglacial. The picture of a low Dansgaard-Oeschger signal during the Marine Isotope Stages (MIS) 4 and MIS 2 corresponds with the low variability in temperate tree taxa. This implies that the presence of the significant ice sheet has been sufficient to suppress changes in temperate woody abundances in response to the North Atlantic variability (Tzedakis, 2005). In comparison, the climate conditions became more favourable for woodland development in southern Europe during the MIS 3. Triggered by the resumption of the North Atlantic circulation, the climate improvement was responsible for moist and mild environmental conditions over large parts of Europe (Allen et al., 1999; Fletcher et al., 2010; Müller et al., 2011; Sánchez Goñi et al., 2002).

Both records, Lago Grande di Monticchio and Tenaghi Philippon, show a period characterized by a conifer-dominated forest expansion with *Pinus* and *Juniperus* (~20-30% AP) during MIS 4 and MIS 2. The continuous abundances of *Artemisia*, Chenopodiaceae and grasses emphasize that the landscape had only sparse areas of restricted tree cover (Allen and Huntley, 2000; Huntley et al., 1999; Tzedakis et al., 2002b; Watts et al., 2000; Wijmstra, 1969). The predominant vegetation was open and steppe like, indicating at least seasonal moisture deficiency (Huntley et al., 1999). Furthermore, the Tenaghi Philippon record illustrates a higher continentality in this region due to the appearance of *Ephedra* within the forest development of deciduous oak and pine (Tzedakis et al., 2002b; Wijmstra, 1969). The subsequent warming

during the middle pleniglacial (MIS 3) resulted in open broad-leaved woodland communities, ranging from 30 up to 70%. The warm-temperate forest consists of *Betula*, *Quercus*, *Tilia*, *Ulmus*, *Carpinus*, *Pinus*, *Fraxinus* and *Abies* (Allen et al., 1999; Allen and Huntley, 2000; Watts et al., 2000). In contrast, the unique position of the Ioannina basin as a refugial area might be responsible for the enhanced expansion of several warm-temperate elements during MIS 4 and MIS 2 of about 30-40% AP, and between 50 and 80% in the MIS 3. This spread of forest includes elements such as deciduous *Quercus*, *Ulmus*, *Corylus*, *Carpinus*, *Abies* and *Fagus* (Tzedakis et al., 2002b).

The pollen compositions at Lake Van and Lake Urmia provide a complete different picture. They are characterized by small amplitude of arboreal pollen abundances as well as by lower diversity of woody elements as a result of extreme aridity and cold temperature during the pleniglacial. Furthermore, the varieties in the Dansgaard-Oeschger signal within the NGRIP record cannot be distinguished at Lake Urmia (Figure 6.2). Moreover, the last glacial maximum is not resolved in the pollen sequence due to a lack of sediments in this interval (Stevens et al., 2012). The climate conditions at Lake Urmia lead to a nearly similar vegetation community like at Lake Van: high values of arid steppic elements with a continuous appearance of *Ephedra distachya* type during stadials, and a short-term increase of moderate steppe forest expansion (e.g. *Quercus*, *Pinus*, *Juniperus* and *Betula*) during interstadials. However, the reconstructed vegetation at Lake Urmia demonstrates the occurrence of *Hippophaë rhamnoides*, which indicates low winter temperature and intense erosion due to the absence of a well-developed vegetation cover (Djamali et al., 2008). Warm-temperate woody elements such as *Carpinus*, *Ulmus*, *Fagus* and *Abies* are completely absent at Lake Urmia during the pleniglacial.

Although all five sites were affected by climatic oscillations throughout the last glacial, their ecological impact was largely determined by the extent of (i) the local moisture availability minima for survival of temperate trees and (ii) topographic variability that provided shelter from penetration of polar air. It results in different pollen records that show distinct biogeographical patterns. Arid climate conditions triggered the presence of temperate tree populations in the Near East during glacials and stadials. In contrast, Ioannina, Tenaghi Philippon and Lago Grande di Monticchio represent refugial sites, providing a huge expansion of forest during each interstadial.

6.4 Late Weichselian and Holocene

Due to the lower palynological resolution in the present study, the vegetational development during the interval of the late Weichselian and the Holocene period will be summarized very briefly. More detailed information on climate and environmental variability and its causes as well as its anthropogenic influence on the natural vegetation history at Lake Van have been discussed in the previous palynological investigations of Litt et al. (2009) and Wick et al. (2003).

6.4.1 Late-glacial interstadial and Younger Dryas

In palynological terms, the beginning of the late Weichselian at 6.62 mcblf (~14.7 ka BP) is characterized by a short-term increase of temperate woody taxa. The late-glacial interstadial complex, including the final numbered Dansgaard-Oeschger event D-O 1 (~14.7-12.7 cal. BP; Litt et al., 2003, 2009), is detected at ~6.62-5.92 mcblf in the recent palynological study of the Lake Van record. This period is generally considered to be synonymous with the Meinendorf-Bølling-Allerød interstadial complex in the terrestrial pollen records from NW Europe, summarized by Litt et al. (2003). Therefore, it forms a part of the termination I (Wolff et al., 2009).

The late-glacial interstadial complex indicates a similar characteristic vegetation succession such as previous interstadials during the last glacial (see section 6.3.2). The initial warming phase, associated with the melting of the Fennoscandian ice sheet, consists of increased *Betula* (0-2%) values, followed by a moderate expansion of deciduous *Quercus* (0-4%). Contemporaneously to the slight oak development, the late-glacial interstadial documents a spread of various herbaceous taxa, especially Poaceae (13-23%). Despite of the moderate climatic improvement towards warmer conditions and of the enhanced moisture availability within the late-glacial interstadial, the pollen composition reflects an open grass steppe, including the occurrence of several warm-temperate woody taxa such as *Acer platanoides* type and *Pistacia atlantica* type (Figure 7.1, Appendix).

The late glacial interstadial was terminated by the marked Younger Dryas (YD) cooling event at 5.92-4.49 mcblf (~12.7-11.6 ka; Litt et al., 2009) that resulted in a renewed aridity (Litt et al., 2009; Wick et al., 2003). During the late-glacial stadial, the relative abundance of woody taxa (e.g. *Quercus*, *Betula* and *Pistacia*) drops to ~5%, simultaneously to a rapid expansion of *Ephedra* (up to 11%). It indicates that the vegetation responds to the climatic deterioration due to an apparently retreat of the warm-temperate forest development. The return to a short-term arid desert steppe vegetation is accompanied with steppic herbs (>60%) such as *Artemisia* and Chenopodiaceae. It can be interpreted as a period of seasonal dryness and probably

colder climate conditions during the YD. On the contrary, Figure 6.7 illustrates that the Younger Dryas occurs within a period of maximum summer insolation. Nevertheless, the YD event might have been caused by freshwater pulses into the North Atlantic. Their effects on the oceanic and atmospheric circulation resulted in a decline of temperature and of moisture availability in Europe (Bond et al., 1997; Cacho et al., 1999; Clark et al., 2001).

6.4.2 Holocene

After the climatic deterioration during the Younger Dryas, the pronounced change in the pollen composition indicates a gradual increase in moisture availability at the onset of the recent interglacial stage, the Holocene (~11.7 ka BP; 4.49 mcblf). The replacement from relative abundance of arid steppic taxa with predominances of chenopods and *Artemisia* to a less arid grass steppe is documented by high frequencies of Poaceae percentages (up to 30%) in the early Holocene. Similar to the last interglacial stage, the Eemian, and the pollen record of Litt et al. (2009), the succession of the forest development is characterized by an initial retreat of *Ephedra distachya* type, followed by an increase of *Betula.* The spread of an oak-steppe forest (*Quercetea brantii*), defined by deciduous *Quercus, Pistacia atlantica* type and *Juniperus oxycedrus* type and is indicating the climate optimum with higher humidity after 8.2 ka (Litt et al., 2009; Wick et al., 2003). Therefore, the investigations of Wick et al. (2003) and Litt et al. (2009) identified a delay of deciduous oak forest development at about 3 ka BP, suggesting dry springs and summer weather during the early Holocene. An identical delay in the spread of the climax vegetation can be confirmed by the present palynological investigation at Lake Van.

Contrary to the last interglacial stage, the recent interglacial is characterized by low abundances of *Pinus.* Zohary (1973a,b) assumed that the moderate frequency of pine can be explained by a long-distance transport from Euxinian forests in Northern Anatolia. This presumption can be confirmed by the occurrence of *Pinus* in the Black Sea records (Shumilovskikh et al., 2012). Furthermore, the general low diversity of tree taxa during the Holocene, compared to the last interglacial, is evident by the almost complete absence of *Ulmus* and *Carpinus* taxa at Lake Van (Figure 7.1, Appendix).

According to Wick et al. (2003), the high charcoal values recorded in PAZ IXa (4.49-3.49 mcblf; Figure 5.1 and 6.7) can be assigned to the grassland dominating landscape, which provided considerably more fuel availability than the late-glacial Chenopodiaceae-*Artemisia* desert steppe vegetation. The onset of an oak steppe forest development at ~9 ka BP and the subsequent decrease in charcoal particles

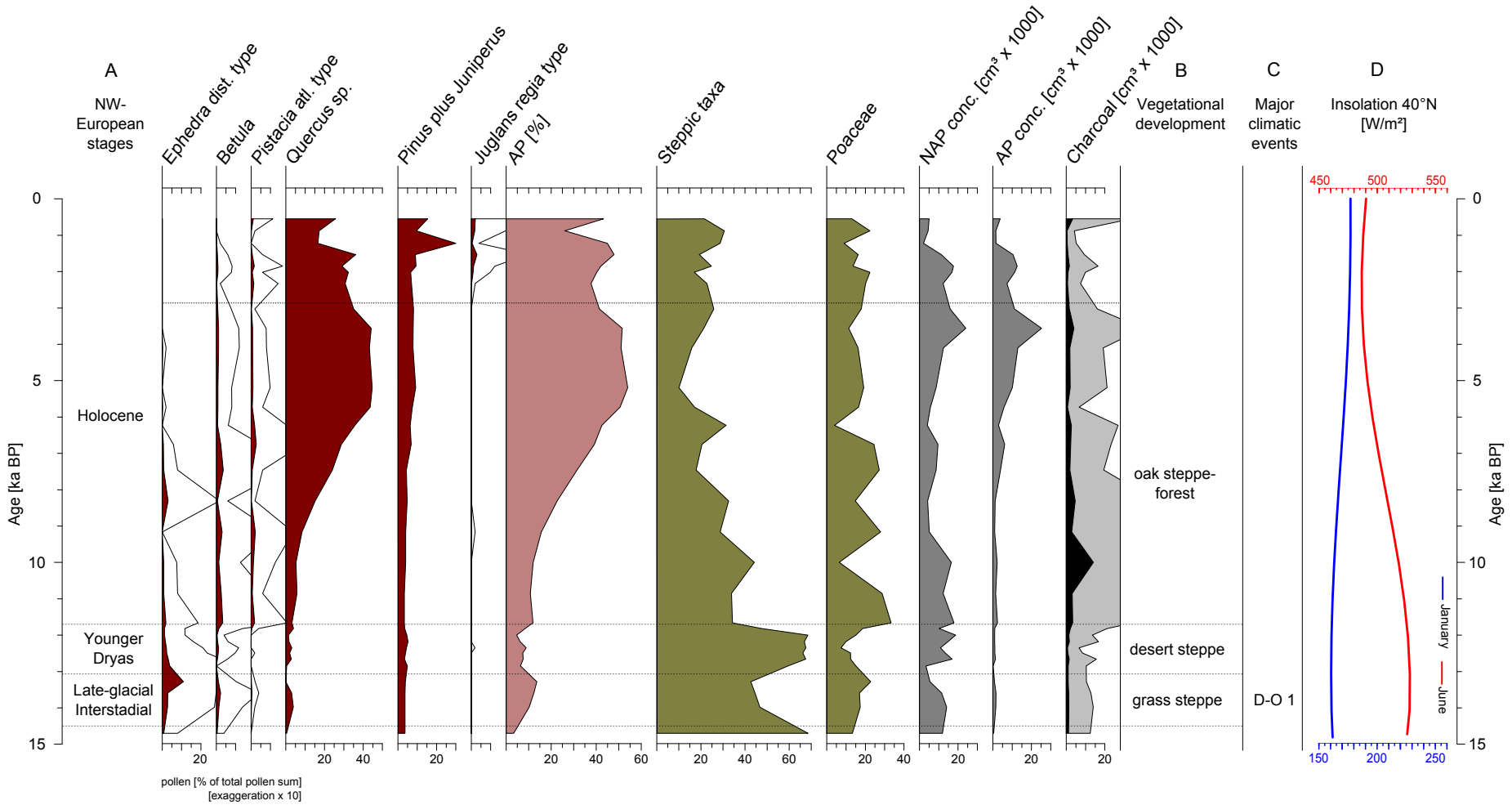

Figure 6.7: Pollen diagram of the late Weichselian and Holocene sequence at Lake Van. Steppic taxa consist of *Artemisia* and Chenopodiaceae. A - Terrestrial stages of the NW European stages; B - Vegetational development at Lake Van; C - Major climatic events; D - mid-June (red line) and mid-January (blue line) insolation 40°C curve after (Berger et al., 2007).

until ~3.8 ka BP (~2.1 mcblf), suggesting low fire frequencies due to enhanced moisture availability at Lake Van. The following slight increase of fire regimes at ~3.8 ka BP is associated with the decline of total arboreal pollen, especially of oak values. This period suggests the beginning of the anthropogenic influence due to forest clearance, agricultural activity and perhaps to subsequent burning in the Lake Van region.

Comparison with southern European terrestrial records

A comparison of the late Weichselian and Holocene period in the Near East and eastern Mediterranean sequences reveals a number of differences and similarities in the vegetational development during the climate variability.

The late-glacial interstadial in the eastern Mediterranean and Near East region, in particular in Lago Grande di Monticchio (~14.3 cal. BP; Allen et al., 2000, 2002; Huntley et al., 1999), Ioannina (~15.6 ka; Lawson et al., 2004), Tenaghi Philippon (~14.6 ka BP; Kotthoff et al., 2008) and Lake Urmia (~14 ka; Stevens et al., 2012) exhibits a spread of thermophilous, moisture-demanding woodland (mostly *Quercus*), but is also characterized by the persistence of grassland with a variety of herbaceous taxa, indicating a continuous sparsely wooded landscape. The major difference between these sites are that the eastern Mediterranean areas recorded a higher diversity and frequency of woody taxa such as *Quercus*, *Corylus*, *Fagus*, *Ulmus*, *Tilia* and *Alnus* (AP ~70%) during the late-glacial interstadial (Allen and Huntley, 2009; Huntley et al., 1999; Lawson et al., 2004). Whereas the woody composition at Lake Van and Lake Urmia, comprised of *Ephedra*, *Betula*, *Quercus* and *Pinus* taxa, reflects an increase of arboreal pollen of about 10-20% (Djamali et al., 2008).

A reversal in the process of afforestation occurred during the Younger Dryas. The resulting cooler and drier climate conditions can be identified at Lago Grande di Monticchio between ~12.8 and 11.2 cal. BP (Allen et al., 2000, 2002) and in the Tenaghi Philippon records at ~12.7 ka BP (Kotthoff et al., 2008). In those records with a sufficient temporal resolution, such as the eastern Mediterranean sequences, the Younger Dryas event is clearly recorded, often both by a shift in the composition of the woody taxa represented in the pollen record and by an overall modest decrease in the total tree pollen (AP percentages drop to ~65%). In general, woody taxa such as *Quercus*, *Corylus*, *Fagus*, *Fraxinus*, *Tilia* and *Ulmus* were continuously present in the Mediterranean records during the YD (Allen et al., 2000). However, a short-lived restricted decline of the most sensitive thermophilous woody taxa (e.g. *Fraxinus ornus* and *Ostrya*-type) were detected in southern Europe, whereas those of *Betula*, Gramineae and *Artemisia* increases (Allen and Huntley, 2000; Allen et al., 2000;

Huntley et al., 1999; Kotthoff et al., 2008; Lawson et al., 2004). At Ioannina, the arboreal pollen assemblage was more or less identical before and during the Younger Dryas, which clearly emphasizes the special position as a refugial area (Bottema, 1995b).

At Tenaghi Phillipon the late-glacial stadial suggested, as at Lake Van, a dry climate condition due to an increase of the semi-desert plant *Ephedra distachya* type (Kotthoff et al., 2008). Similar climatic and environmental conditions were observed at Lake Urmia, showing a desert steppe vegetation (*Artemisia* and chenopods), which were subsequently replaced by grass pollen.

The Holocene period in these regions is well-established and have been intensively discussed in several publications, e.g. in Allen and Huntley (2000); Allen et al. (2002); Bottema (1986, 1995a); Djamali et al. (2008); Huntley et al. (1999); Lawson et al. (2004); Litt et al. (2009); Schiebel (2013); Wick et al. (2003); van Zeist and Bottema (1991). Nevertheless, vegetational development in the recent interglacial stage, as observed at Monticchio and Tenaghi Philippon, are mostly dominated by a rapid increase of temperate mixed woodland (AP ~90%; Allen et al., 2000). In places where moisture availability was not limited, e.g. at Ioannina, the deciduous broad-leaf woodland expansion (especially *Quercus*, *Corylus*, *Fagus*, *Fraxinus*, *Tilia*, *Ulmus*) occurred near the Pleistocene/Holocene boundary at ~11.5 ka (Kotthoff et al., 2008). The increased summer aridity, marked by the progressive decrease of insolation at the high latitudes of the Northern Hemisphere (Jalut et al., 2009), led to the expansion of Mediterranean sclerophylls (e.g. *Phillyrea*, *Quercus ilex*). Subsequent to the spread of the Mediterranean taxa, *Abies* and *Alnus* increased at ~10.5 ka in Ioannina (Tzedakis, 2007) and at around 8 cal. BP in Lago Grandi di Monticchio (Allen and Huntley, 2000; Allen et al., 2000, 2002). Nevertheless, the persistent values of 10-15% for herbaceous taxa, especially for Gramineae, indicate that open areas of grassland were still present (Huntley et al., 1999).

In the Near East, the late-glacial to early Holocene transition was initiated at Lake Van at ~11.7 ka BP and at Lake Urmia at approximately 10 ka. The early Holocene in this region starts by a succession of *Ephedra*, *Betula*, *Pistacia* and finally *Juniperus* and *Quercus* (AP 20-50%; Djamali et al., 2008; Litt et al., 2009; Stevens et al., 2012; Wick et al., 2003). Low values of *Fagus*, *Ulmus*, *Corylus* and *Carpinus betulus* within the oak steppe-forest at Lake Van and Lake Urmia suggest a long-distance transport from a refugial area, e.g. from the Caucasus Mountains (Bottema, 1986). A detailed vegetational development of the recent interglacial period cannot be inferred at Lake Urmia as a consequence of low pollen resolution as well as the incompleteness of the Holocene sequence (Djamali et al., 2008; Stevens et al., 2012). Previous publications

of Bottema (1986) and van Zeist and Bottema (1977) present, similar to Lake Van, a *Pistacia-Quercus* steppe-forest expansion between 9,000 and 8,000 years BP.

However, a striking feature of both Near East records is that the development of the steppe-forest did not occur at the Pleistocene/Holocene transition at ~11.5 ka such as the Mediterranean pollen sequences. The interior areas of the Taurus and Zagros Mountains, e.g. at Lake Van and Lake Urmia, demonstrate a more retarded forest expansion until ~8 ka (Djamali et al., 2008; Litt et al., 2009; Wick et al., 2003). Furthermore, the considerable differences in vegetational conditions ranging from desert steppe vegetation towards a dense steppe-forest.

Major vegetational changes in the uppermost part of all Holocene sections imply an opening of the woodlands caused by an increasing aridity as well as by the gradual human-induced degeneration of the forest vegetation. It is represented by a substantial decrease in the tree cover. Various taxa point to an expansion of pastoralism and to an increase of agriculture. Common plants associated with cultivation in the Near East and eastern Mediterranean regions are, for example *Olea*, *Juglans*, *Plantago lanceolata* type, *Rumex* sp. and Umbelliferae (Allen et al., 2002; Lawson et al., 2004; Wick et al., 2003).

7 Summary

This study investigated the first continuous high-resolution pollen record from Lake Van, eastern Anatolia that encompasses the last glacial-interglacial cycle (~130 ka BP). The reconstructed paleovegetation documents a series of climatic and environmental events and yields information about vegetation succession in the Near East. Palynological analyses were extracted from the lacustrine sedimentary record obtained during the drilling campaign at the 'Ahlat Ridge' in 2010.

Being located in a semi-arid region, the regional environment at Lake Van is characterized by a continental climate. Therefore, the reconstruction of vegetation from the detailed palynological investigations reflects an alternation of an oak-steppe forest and a dwarf-shrub steppe/desert steppe vegetation. In general, cold and arid environmental conditions can be characterized by the dominance of *Ephedra*, *Artemisia*, chenopods and grasses, whereas increased temperature and moisture availability suggest more favorable environmental conditions for the expansion of a warm-temperate steppe-forest (e.g. *Quercus*). These climate cycles were strongly associated with changes in the oceanic and atmospheric circulation of the North Atlantic Ocean.

In eastern Anatolia the climate evolution within the last interglacial (~130-111 ka BP) can be described as a relatively stable warm period with one pronounced short-term climate setback (C 25 cooling event; ~115 ka) towards the end of the last interglacial period. Timing and length of the interglacial conditions are comparable with southern European pollen records. Furthermore, the palynological sequence at Lake Van documents a vegetation succession with several climatic phases: (i) the *Pistacia* phase and the *Quercus-Ulmus* phase during the initial warming (130.9-127.2 ka BP) indicating summer dryness and mild winter conditions; (ii) the *Carpinus* phase (127.2-124.1 ka BP) suggesting slightly colder temperatures with higher moisture availability; and (iii) the increasing *Pinus* phase at ~124 ka, which marks the onset of colder/drier climate conditions, that extended into the interval of global ice growth. In general, the diversity of woody taxa within the forest composition is significantly lower in the Near East compared to the eastern Mediterranean interglacial sequences.

The major difference between the last interglacial at Lake Van in comparison to the Holocene is the relatively high amount of *Pinus* during the Eemian, indicating a considerably higher continentality index during the climate optimum as compared to the recent interglacial.

Throughout the last glacial (~74.7-14.7 ka BP), the detailed nature of the Lake Van pollen record allows the identification of several millennial-scale vegetational

and environmental changes, which can be correlated with the stadial-interstadial patterns of the Dansgaard-Oeschger (D-O) events observed in the North Greenland ice core record (NGRIP). Relatively warm and humid climate conditions during the D-O interstadials enabled the emergence of an open steppe forest at Lake Van.

This study is a first attempt to establish a continuous charcoal record over the last glacial-interglacial cycles in the Near East, and to document an initial immediate response to millennial-scale climate and environmental variability. Fire regimes, confirmed to more warm/dry conditions, were considerably less frequent during glacial or cooling periods. Within the last glacial, the Marine Isotope Stage (MIS) 3 is characterized by a slightly higher fire activity than MIS 2 and 4.

New insights of paleovegetation and climate variability at Lake Van demonstrate the great potential of paleoenvironmental reconstruction. It allows the comparison with other long continental pollen records from the Near East and the eastern Mediterranean region, to contribute to the discussion of climate change and to improve the understanding of vegetational changes in the eastern Anatolia region.

List of Figures

List of Tables

List of Abbreviations

AD	Anno Domini
AES	Ankara-Erzincan suture
AP	Arboreal pollen
AR	Ahlat Ridge
AS	Assyrien suture
BP	Before present, 1950
BS	Bitlis suture
CONISS	Constrained incremental sums of squares cluster analysis
DFG	Deutsche Forschungsgemeinschaft
DLDS	Deep Lake Drilling System
D-O event	Dansgaard-Oeschger event
DOSECC	Drilling, Observation and Sampling of the Earths Continental Crust
EAAC	East Anatolia Accretionary Complex
EAFZ	East Anatolian Fault Zone
EDC	EPICA Dome C / European Project for Ice Coring in Antarctica
e.g.	exempli gratia, for example
GS	Greenland Stadials
HE	Heinrich events
HP	Halepkalesi Pumice
ICDP	International Continental Scientific Drilling Program
ID	Incekaya-Dibekli tephra layer
IODP	Integrated Ocean Drilling Program

IRD	Ice-rafted detritus
IS	Greenland Interstadials
ITCZ	Intertropical Convergence Zone
ka	'Kiloannum'; thousand years
LGM	Last glacial maximum
Ma	Million years
m a.s.l.	Meter above sea level
mblf-nE	Meter below lake floor - no Events
mcblf	Meter composite below lake floor
MIS	Marine isotope stage
NAFZ	North Anatolian Fault Zone
NAO	North Atlantic Oscillation
NAP	Non-arboreal pollen
NB	Northern Basin
NF	Nemrut Formation
NGRIP	North Greenland Ice-core Project
PAZ	Pollen assemblage zone
SNF	Swiss National Science Foundation
SST	Sea surface temperature
TOC	Total organic carbon
ZFZ	Zagros Fault Zone

References

Aalbersberg, G. and T. Litt, 1998. Multiproxy climate reconstructions for the eemian and early weichselian. Journal of Quaternary Science 13:367–390.

Akçar, N. and C. Schlüchter, 2005. Paleoglaciations in anatolia: A schematic review and first results. Eiszeitalter und Gegenwart 55:102–121.

Allen, J. R. M., U. Brandt, A. Brauer, H.-W. Hubberten, B. Huntley, J. Keller, M. Kraml, A. Mackensen, J. Mingram, J. F. W. Negendank, N. R. Nowaczyk, H. Oberhänsli, W. A. Watts, S. Wulf, and B. Zolitschka, 1999. Rapid environmental changes in southern europe during the last glacial period. Nature 400:740–743.

Allen, J. R. M. and B. Huntley, 2000. Weichselian palynological records from southern europe: correlation and chronology. Quaternary International 73-74:111–125.

Allen, J. R. M. and B. Huntley, 2009. Last interglacial palaeovegetation, palaeoenvironments and chronology: a new record from lago grande di monticchio, southern italy. Quaternary Science Reviews 28:1521–1538.

Allen, J. R. M., W. A. Watts, and B. Huntley, 2000. Weichselian palynostratigraphy, palaeovegetation and palaeoenvironment; the record from lago grande di monticchio, southern italy. Quaternary International 73-74:91–110.

Allen, J. R. M., W. A. Watts, E. McGee, and B. Huntley, 2002. Holocene environmental variability - the record from lage grande di monticchio, italy. Quarternary International 88:69–80.

Altiner, Y., W. Söhne, C. Güney, J. Perlt, R. Wang, and M. Muzli, 2013. A geodetic study of the 23 october 2011 van, turkey earthquake. Tectonophysics (in press).

Altiok, A. and L. Behçet, 2005. The flora of bitlis river valley. Turkish Journal of Botany 29:355–387.

Andersen, K. K., A. Svensson, S. J. Johnsen, S. O. Rasmussen, M. Bigler, R. Röthlisberger, U. Ruth, M.-L. Siggaard-Andersen, J. Peder Steffensen, D. Dahl-Jensen, B. M. Vinther, and H. B. Clausen, 2006. The greenland ice core chronology 2005, 15-42ka. part 1: constructing the time scale. Quaternary Science Reviews 25:3246–3257.

Andersen, S. T., 1966. Interglacial vegetational succession and lake development in denmark. Palaeobotanist 15:117–127.

Bar-Matthews, M., A. Ayalon, M. Gilmour, A. Matthews, and C. J. Hawkesworth, 2003. Sea-land oxygen isotopic relationships from planktonic foraminifera and speleothems in the eastern mediterranean region and their implication for paleorainfall during interglacial intervals. Geochimica et Cosmochimica Acta 67:3181–3199.

Bar-Matthews, M., A. Ayalon, and A. Kaufman, 1997. Late quaternary paleoclimate in the eastern mediterranean region from stable isotope analysis of speleothems at soreq cave, israel. Quarternary Research 47:155–168.

Barka, A. and R. Reilinger, 1997. Active tectonics of the eastern mediterranean region: deduced from gps, neotectonic and seismicity data. Annali di Geofisica 40:587–610.

Barker, S., G. Knorr, R. L. Edwards, F. Parrenin, A. E. Putnam, L. C. Skinner, E. Wolff, and M. Ziegler, 2011. 800,000 years of abrupt climate variability. Science 334:347–351.

Behre, K.-E., 1990. Some reflections on anthropogenic indicators and the record of prehistoric occupation phases in pollen diagrams from the near east. p. 219–230. *In* S. Bottema, G. Entjes-Nieborg, and W. van Zeist (ed.) Man‘s Role in the Shaping of the Eastern Mediterranean Landscape. Balkema, Rotterdam.

Behre, K. E. and U. Lade, 1986. Eine folge von eem und 4 weichsel-interstadialen in oerel / niedersachsen und ihr vegetationsablauf. Eiszeitalter und Gegenwart 36:11–36.

Berger, A., 1978. Long-term variations of daily insolation and quaternary climate changes. Journal of Atmospheric Sciences 35:2362–2367.

Berger, A., M. F. Loute, F. Kaspar, and S. J. Lorenz, 2007. Insolation during interglacial. p. 13–27. *In* F. Sirocko, M. Claussen, M. F. Sánchez Goñi, and T. Litt (ed.) The Climate of Past Interglacial. Elsevier, Amsterdam.

Beug, H.-J., 2004. Leitfaden der Pollenbestimmung für Mitteleuropa und angrenzende Gebiete. Pfeil, München.

Birks, H. J. B., 1986. Late-quaternary biotic changes in terrestrial and lacustrine environments, with particular reference to north-west europe. p. 3–65. *In* B. E. Berglund and M. Ralska-Jasiewiczowa (ed.) Handbook of Holocene Palaeoecology and Palaeohydrology. John Wiley & Sons.

Birks, H. J. B. and H. H. Birks, 1980. Quarternary Palaeoecology. Edward Arnold, London.

Blockley, S. P. E., C. S. Lane, M. Hardiman, S. O. Rasmussen, I. K. Seierstad, J. P. Steffensen, A. Svensson, A. F. Lotter, C. S. M. Turney, and C. Bronk Ramsey, 2012. Synchronisation of palaeoenvironmental records over the last 60,000 years, and an extended intimate event stratigraphy to 48,000 b2k. Quaternary Science Reviews 36:2–10.

Blunier, T. and E. J. Brook, 2001. Timing of millennial-scale climate change in antarctica and greenland during the last glacial period. Science 291:109–112.

Boës, X., S. B. Moran, J. King, M. N. Cağatay, and A. Hubert-Ferrari, 2010. Records of large earthquakes in lake sediments along the north anatolian fault, turkey. Journal of Paleolimnology 43:901–920.

Bond, G. C., W. S. Broecker, S. Johnsen, J. McManus, L. Labeyrie, J. Jouzel, and G. Bonani, 1993. Correlations between climate records from north atlantic sediments and greenland ice. Nature 365:143–147.

Bond, G. C., B. Kromer, J. Beer, R. Muscheler, M. N. Evans, W. Showers, S. Hoffmann, R. Lotti-Bond, I. Hajdas, and G. Bonani, 2001. Persistent solar influence on north atlantic climate during the holocene. Science 294:2130–2136.

Bond, G. C. and R. Lotti, 1995. Iceberg discharges into the north atlantic on millennial time scales during the last glaciation. Science 267:1005–1010.

Bond, G. C., W. Showers, M. Cheseby, R. Lotti, P. Almasi, P. deMenocal, P. Priore, H. Cullen, I. Hajdas, and G. Bonani, 1997. A pervasive millennial-scale cycle in north atlantic holocene and glacial climates. Science 278:1257–1266.

Bond, W. J., F. I. Woodward, and G. F. Midgley, 2005. The global distribution of ecosystems in a world without fire. New Phytologist 165:525–538.

Bottema, S., 1975. The interpretation of pollen spectra from prehistoric settlements (with special attention to liguliflorae). Palaeohistoria 17:17–35.

Bottema, S., 1986. A late quaternary pollen diagram from lake urmia (northwestern iran). Review of Palaeobotany and Palynology 47:241–261.

Bottema, S., 1995a. Holocene vegetation of the van area: palynological and chronological evidence from söğütlü, turkey. Vegetation History and Archaeobotany 4:187–193.

Bottema, S., 1995b. The younger dryas in the eastern mediterranean. Quaternary Science Reviews 14:883–891.

Bottema, S., 1997. Third millennium climate in the near east based upon pollen evidence. p. 489–515. *In* H. N. Dalfes, G. J. Kukla, and H. Weiss (ed.) Third Millennium BC Climate Change and Old World Collapse, volume 49. NATO ASI Series.

Bozkurt, E. and S. K. Mittwede, 2001. Introduction to the geology of turkey - a synthesis. International Geology Review 43:578–594.

Brauer, A., J. R. M. Allen, J. Mingram, P. Dulski, S. Wulf, and B. Huntley, 2007. Evidence for last interglacial chronology and environmental change from southern europe. Proceedings of the National Academy of Sciences 104:450–455.

Brewer, S., J. Guiot, M. F. Sánchez Goñi, and S. Klotz, 2008. The climate in europe during the eemian: a multi-method approach using pollen data. Quaternary Science Reviews 27:2303–2315.

Broecker, W. S., 1994. Massive iceberg discharges as triggers for global climate change. Nature 372:421–424.

Cacho, I., J. O. Grimalt, C. Pelejero, M. Canals, F. J. Sierro, J. A. Flores, and N. J. Shackleton, 1999. Dansgaard-oeschger and heinrich event imprints in alboran sea paleotemperatures. Paleoceanography 14:698–705.

Cacho, I., J. O. Grimalt, F. J. Sierro, N. J. s. Shackleton, and M. Canals, 2000. Evidence for enhanced mediterranean thermohaline circulation during rapid climatic coolings. Earth and Planetary Science Letters 183:417–429.

Cappers, R. T. J. and S. Bottema, 2002. The Dawn of Farming in the Near East. Studies in Early Near Eastern Production, Subsistence, and Environment 6, 1999.

Caspers, G., J. Merkt, H. Müller, and H. Freund, 2002. The eemian interglaciation in northwestern germany. Quaternary Research 58:49–52.

Celenk, S. and A. Bicakci, 2005. Aerobiological investigation in bitlis, turkey. Annals of Agricultural and Environmental Medicine 12:87–93.

Chapman, M. R. and N. J. Shackleton, 1999. Global ice-volume fluctuations, north atlantic ice-rafting events, and deep-ocean circulation changes between 130 and 70 ka. Geology 27:795–798.

Chappell, J., A. Omura, T. Esat, M. McCulloch, J. Pandolfi, Y. Ota, and B. Pillans, 1996. Reconciliaion of late quaternary sea levels derived from coral terraces at huon peninsula with deep sea oxygen isotope records. Earth and Planetary Science Letters 141:227–236.

Clark, P. U., S. J. Marshall, G. K. C. Clarke, S. W. Hostetler, J. M. Licciardi, and J. T. Teller, 2001. Freshwater forcing of abrupt climate change during the last glaciation. Science 293:283–287.

Connor, S. E., I. Thomas, E. V. Kvavadze, G. J. Arabuli, G. S. Avakov, and A. Sagona, 2004. A survey of modern pollen and vegetation along an altitudinal transect in southern georgia, caucasus region. Review of Palaeobotany and Palynology 129:229–250.

Crucifix, M. and M. F. Loutre, 2002. Transient simulations over the last interglacial period (126-115 kyr bp): feedback and forcing analysis. Climate Dynamics 19:417–433.

Cukur, D., S. Krastel, F. Demirel-Schlüter, E. Demirbağ, C. Imren, F. Niessen, M. Toker, and PaleoVan-WorkingGroup, 2012. Sedimentary evolution of lake van (eastern turkey) reconstructed from high - resolution seismic investigations. International Journal of Earth Sciences 531:1–15.

Cullen, H. M. and P. B. deMenocal, 2000. North atlantic influence on tigris-euphrates streamflow. International Journal of Climatology 20:853–863.

Dahl-Jensen, D., P. Gogineni, and J. W. C. White, 2013. Reconstruction of the last interglacial period from the neem ice core. PAGES 21:22–23.

Daniau, A.-L., S. P. Harrison, and P. J. Bartlein, 2010. Fire regimes during the last glacial. Quaternary Science Reviews 29:2918–2930.

Dansgaard, W., S. J. Johnsen, H. B. Clausen, D. Dahl-Jensen, N. S. Gundestrup, C. U. Hammer, C. S. Hvidberg, J. P. Steffensen, A. E. Sveinbjörnsdottir, J. Jouzel, and G. Bond, 1993. Evidence for general instability of past climate from a 250-kyr ice-core record. Nature 364:218–220.

Davis, M. B., 1963. On the theory of pollen analysis. American Journal of Science 261:897–912.

Davis, M. B., 2000. Palynology after y2k - understanding the source area of pollen in sediments. Annual Review of Earth and Planetray Sciences 28:1–18.

Davis, P. H., 1965. Flora of Turkey and the East Aegean Islands, volume 1. Edinburgh University Press.

de Beaulieu, J.-L. and M. Reille, 1992. The last climatic cycle at la grande pile (vosges, france) a new pollen profile. Quaternary Science Reviews 11:431–438.

Deckers, K. and H. Pessin, 2010. Vegetation development in the middle euphrates and upper jazirah (syria/turkey) during the bronze age. Quaternary Research 74:216–226.

Degens, E. T. and F. Kurtman, 1978. The Geology of Lake Van. The Mineral Research and Exploration Institute of Turkey, Ankara.

Degens, E. T., H. K. Wong, S. Kempe, and F. Kurtmann, 1984. A geological study of lake van, eastern turkey. Geologische Rundschau 73:701–734.

Deniz, O. and M. Yildiz, 2007. The ecological consequences of level changes in lake van. Water Resources 34/7:707–711.

Djamali, M., A. Baumel, S. Brewer, S. T. Jackson, J. W. Kadereit, S. López-Vinyallonga, I. Mehregan, E. Shabanian, and A. Simakova, 2012a. Ecological implications of cousinia cass. (asteraceae) persistence through the last two glacial-interglacial cycles in the continental middle east for the irano-turanian flora. Review of Palaeobotany and Palynology 172:10–20.

Djamali, M., S. Brewer, S. W. Breckle, and S. T. Jackson, 2012b. Climatic determinism in phytogeographic regionalization: A test from the irano-turanian region, sw and central asia. Flora - Morphology, Distribution, Functional Ecology of Plants 207:237–249.

Djamali, M., J.-L. de Beaulieu, M. Shah-Hosseini, V. Andrieu-Ponel, P. Ponel, A. Amini, H. Akhani, S. A. Leroy, L. Stevens, H. Lahijani, and S. Brewer, 2008. A late pleistocene long pollen record from lake urmia, nw iran. Quaternary Research 69:413–420.

Doğan, B. and A. Karakaş, 2013. Geometry of co-seismic surface ruptures and tectonic meaning of the 23 october 2011 mw 7.1 van earthquake (east anatolian region, turkey). Journal of Structural Geology 46:99–114.

Eastwood, W. J., M. J. Leng, N. Roberts, and B. Davis, 2007. Holocene climate change in the eastern mediterranean region: a comparison of stable isotope and pollen data from lake gölhisar, southwest turkey. Journal of Quarternary Science 22:327–341.

Eastwood, W. J., N. Roberts, and H. F. Lamb, 1998. Palaeoecological and archaeological evidence for human occupance in southwest turkey: The beyşehir occupation phase. Anatolian Studies 48:69–86.

Eastwood, W. J., N. Roberts, H. F. Lamb, and J. C. Tibby, 1999. Holocene environmental change in southwest turkey: a palaeoecological record of lake and catchment-related changes. Quarternary Science Reviews 18:671–695.

El-Moslimany, A. P., 1986. Ecology and late-quaternary history of the kurdo-zagrosian oak forest near lake zeribar, western iran. Vegetatio 68:55–63.

El-Moslimany, A. P., 1987. The late pleistocene climates of the lake zeribar region (kurdistan, western iran) deduced from the ecology and pollen production of nonarboreal vegetation. Vegetatio 72:131–139.

England, A., W. J. Eastwood, N. Roberts, R. Turner, and J. F. Haldon, 2008. Historical landscape change in cappadocia (central turkey): a palaeoecological investigation of annually laminated sediments from nar lake. The Holocene 18:1229–1245.

EPICA, 2004. Eight glacial cycles from antarctic ice core. Nature 429:623–628.

Faegri, K. and J. Iversen, 1989. Textbook of Pollen Analysis. The Blackburn Press.

Fagerlind, F., 1952. The real signification of pollen diagrams. Botaniska Notiser 105:185–224.

Fairbridge, R. W., 1972. Climatology of a glacial cycle. Quarternary Research 2:283–302.

Fall, P. L., 2012. Modern vegetation, pollen and climate relationships on the mediterranean island of cyprus. Review of Palaeobotany and Palynology 185:79–92.

Flannigan, M. D., B. J. Stocks, and B. M. Wotton, 2000. Climate change and forest fires. Science of The Total Environment 262:221–229.

Fletcher, W. J., M. F. Sánchez Goñi, J. R. M. Allen, R. Cheddadi, N. Combourieu-Nebout, B. Huntley, I. Lawson, L. Londeix, D. Magri, V. Margari, U. C. Müller, F. Naughton, E. Novenko, K. Roucoux, and P. C. Tzedakis, 2010. Millennial-scale variability during the last glacial in vegetation records from europe. Quaternary Science Reviews 29:2839–2864.

Frey, W. and H. Kürschner, 1989. Die Vegetation im Vorderer Orient. Erläuterungen zur Karte A VI 1 Vorderer Orient. Vegetation des "Tübinger Atlas des Vorderen Orients". Number 30 *In* Reihe A. Tübinger Atlas des Vorderen Orients, Wiesbaden.

Frogley, M. R., P. C. Tzedakis, and T. H. E. Heaton, 1999. Climate variability in northwest greece during the last interglacial. Science 285:1886–1889.

Genty, D., D. Blamart, R. Ouahdi, M. Gilmour, A. Baker, J. Jouzel, and S. Van-Exter, 2003. Precise dating of dansgaard-oeschger climate oscillations in western europe from stalagmite data. Nature 421:833–837.

Gessner, F., 1957. Van gölü, zur limnologie des großen soda-sees in ostanatolien. Archiv für Hydrobiologie 53:1–22.

Gibbard, P. and T. van Kolfschoten, 2004. The pleistocene and holocene epochs. p. 441–452. *In* A Geologic Time Scale. Cambridge University Press.

Grimm, E. C., 1987. Coniss: a fortran 77 program for stratigraphically constrained cluster analysis by the method of incremental sum of squares. Computers & Geosciences 13:13–35.

Grootes, P. M. and M. Stuiver, 1997. Oxygen 18/16 variability in greenland snow and ice with 10-3- to 105-year time resolution. Journal of Geophysical Research 102:26455–26470.

Grootes, P. M., M. Stuiver, J. W. C. White, S. Johnsen, and J. Jouzel, 1993. Comparison of oxygen isotope records from the gisp2 and grip greenland ice cores. Nature 366:552–554.

Harrison, S. P. and M. F. Sánchez Goñi, 2010. Global patterns of vegetation response to millennial-scale variability and rapid climate change during the last glacial period. Quaternary Science Reviews 29:2957–2980.

Harting, P., 1874. De bodem van het eemdal. Verslagen en Mededelingen van de Koninklijke Academie van Wetenschappen 2:282–290.

Heinrich, H., 1988. Origin and consequences of cyclic ice rafting in the northeast atlantic ocean during the past 130,000 years. Quaternary Research 29:142–152.

Holzkämper, S., A. Mangini, C. Spötl, and M. Mudelsee, 2004. Timing and progression of the last interglacial derived from a high alpine stalagmite. Geophysical Research Letters 31:L07201.

Huguet, C., S. Fietz, N. Moraleda, T. Litt, G. Heumann, M. Stockhecke, F. S. Anselmetti, and M. Sturm, 2012. A seasonal cycle of terrestrial inputs in lake van, turkey. Environmental Science and Pollution Research 19:3628–3635.

Huguet, C., S. Fietz, M. Stockhecke, M. Sturm, F. Anselmetti, and A. Rosell-Melé, 2011. Biomarker seasonality study in lake van, turkey. Organic Geochemistry 42:1289–1298.

Huntley, B., W. A. Watts, J. R. M. Allen, and B. Zolitschka, 1999. Palaeoclimate, chronology and vegetation history of the weichselian lateglacial: comparative analysis of data from three cores at lago grande di monticchio, southern italy. Quaternary Science Reviews 18:945–960.

Imbrie, J., A. Berger, E. A. Boyle, S. C. Clemens, A. Duffy, W. R. Howard, G. J. Kukla, J. Kutzbach, D. G. Martinson, A. McIntyre, A. C. Mix, B. Molfino, J. J. Morley, L. C. Peterson, N. G. Pisias, W. L. Prell, M. E. Raymo, N. J. Shackleton, and J. R. Toggweiler, 1993. On the structure and origin of major glaciation cycles 2. the 100,000-year cycle. Paleoceanography 8:699–735.

Imbrie, J., E. A. Boyle, S. C. Clemens, A. Duffy, W. R. Howard, G. J. Kukla, J. Kutzbach, D. G. Martinson, A. McIntyre, A. C. Mix, B. Molfino, J. J. Morley, L. C. Peterson, N. G. Pisias, W. L. Prell, M. E. Raymo, N. J. Shackleton, and J. R. Toggweiler, 1992. On the structure and origin of major glaciation cycles 1. linear responses to milankovitch forcing. Paleoceanography 7:701–738.

Iversen, J., 1958. The bearing of glacial and interglacial epochs on the formationand extinction of plant taxa. Uppsala Universitets Arsskrift 6:210–215.

Jalut, G., J. J. Dedoubat, M. Fontugne, and T. Otto, 2009. Holocene circum-mediterranean vegetation changes: Climate forcing and human impact. Quaternary International 200:4–18.

Jessen, A. and V. Milthers, 1928. Stratigraphical and paleontological studies of interglacial freshwater deposits in jutland and northwest germany. Danmarks Geologiske Undersøgelse 48:1–379.

Johnsen, S. J., H. B. Clausen, W. Dansgaard, N. S. Gundestrup, C. U. Hammer, U. Andersen, K. K. Andersen, C. S. Hvidberg, D. Dahl-Jensen, J. P. Steffensen, H. Shoji, A. E. Sveinbjörnsdóttir, J. White, J. Jouzel, and D. Fisher, 1997. The d18o record along the greenland ice core project deep ice core and the problem of possible eemian climatic instability. Journal of Geophysical Research 102:26397–26410.

Jouzel, J., V. Masson-Delmotte, O. Cattani, G. Dreyfus, S. Falourd, G. Hoffmann, B. Minster, J. Nouet, J. M. Barnola, J. Chappellaz, H. Fischer, J. C. Gallet, S. Johnsen, M. Leuenberger, L. Loulergue, D. Luethi, H. Oerter, F. Parrenin, G. Raisbeck, D. Raynaud, A. Schilt, J. Schwander, E. Selmo, R. Souchez, R. Spahni, B. Stauffer, J. P. Steffensen, B. Stenni, T. F. Stocker, J. L. Tison, M. Werner, and E. W. Wolff, 2007. Orbital and millennial antarctic climate variability over the past 800,000 years. Science 317:793–796.

Kaden, H., F. Peeters, A. Lorke, R. Kipfer, Y. Tomonaga, and M. Karabiyikolglu, 2010. Impact of lake level change on deep-water renewal and oxic conditions in deep saline lake van, turkey. Water Resources Research 46:W11508, pp.14.

Kadioğlu, M., Z. Şen, and E. Batur, 1997. The greatest soda-water lake in the world and how it is influenced by climatic change. Annales Geophysicae 15:1489–1497.

Kaniewski, D., E. Paulissen, V. De Laet, K. Dossche, and M. Waelkens, 2007. A high-resolution late holocene landscape ecological history inferred from an intramontane basin in the western taurus mountains, turkey. Quaternary Science Reviews 26:2201–2218.

Kaniewski, D., E. Paulissen, E. van Campo, M. Al-Maqdissi, J. Bretschneider, and K. van Lerberghe, 2008. Middle east coastal ecosystem response to middle-to-late holocene abrupt climate changes. PNAS 105:13941–13946.

Kaniewski, D., E. Van Campo, and H. Weiss, 2012. Drought is a recurring challenge in the middle east. Proceedings of the National Academy of Sciences 109:3862–3867.

Kaplan, G. and G. Heumann, 2010. Pollen profile of last 1000 years of lake van northern basin: Preliminarily findings. Journal of the Institute of Natural and Applied Sciences 15:115–120.

Kaplan, G. and S. Örçen, 2011. Late holocene paleoflora of lake van northern basin. Bulletin of the Earth Sciences Application and Research Centre of Hacettepe University 32:139–150.

Karabacak, O. and L. Behçet, 2007. The flora of akçadağ (van-turkey). Turkish Journal of Botany 31:495–528.

Karakhanian, A., R. Djrbashian, V. Trifonov, H. Philip, S. Arakelian, and A. Avagian, 2002. Holocene-historial volcanism and active faults as natural risk factors for armenia and adjacent countries. Journal of Volcanology and Geothermal Research 113:319–344.

Karaoğlu, O., Y. Özdemir, A. U. Trolluoğlu, M. Karabiyikoğlu, O. Köse, and J.-L. Froger, 2005. Stratigraphy of the volcanic products around nemrut caldera: Implications for reconstruction of the caldera formation. Türkish Journal of Earth Sciences 14:123–143.

Kaya, Z. and D. J. Raynal, 2001. Biodiversity and conservation of turkish forest. Biological Conserations 97:131–141.

Kehrwald, N., P. Zennaro, and C. Barbante, 2013. Increasing fire activity in a warming climate? ice core record insights from the present and the last interglacials. PAGES 21:16–17.

Kempe, S., 1977. Hydrographie, warven-chronologie und org. geochemie der sedimente des van sees, ost-türkei. Ph.D. thesis. Mitteilungen aus dem Geologisch-Paläontologischen Institut der Universität Hamburg 47:125–228.

Kempe, S. and E. T. Degens, 1978. Lake van varve record: The past 10.420 years. In: Degens, E.T. & Kurtman, F. (ed.): The Geology of Lake Van. MTA Press. Ankara 169:56–63.

Keskin, M., 2003. Magma generation by slab steepening and breakoff beneath a subduction-accretion complex: An alternative model for collision-related volcanism in eastern anatolia, turkey. Geophysical Research Letters 30:8046.

Keskin, M., 2005. Domal uplift and volcanism in a collision zone without a mantle plume: Evidence from eastern anatolia.

Keskin, M., 2007. Eastern anatolia: a hot spot in a collision zone without a mantle plume. GSA Special Papers 430:693–722.

Kotthoff, U., U. C. Müller, J. Pross, G. Schmiedl, I. T. Lawson, B. van de Schootbrugge, and H. Schulz, 2008. Lateglacial and holocene vegetation dynamics in the aegean region: an integrated view based on pollen data from marine and terrestrial archives. The Holocene 18:1019–1032.

Kühl, N. and T. Litt, 2007. Quantitative time series reconstruction of eemian temperature at three european sites using pollen data. p. 239–254. *In* The Climate of Past Interglacials. Elsevier, Amsterdam.

Kukla, G. J., M. L. Bender, J.-L. de Beaulieu, G. Bond, W. S. Broecker, P. Cleveringa, J. E. Gavin, T. D. Herbert, J. Imbrie, J. Jouzel, L. D. Keigwin, K.-L. Knudsen, J. F. McManus, J. Merkt, D. R. Muhs, H. Müller, R. Z. Poore, S. C. Porter, G. Seret, N. J. Shackleton, C. Turner, P. C. Tzedakis, and I. J. Winograd, 2002. Last interglacial climate. Quarternary Research 58:2–13.

Kukla, G. J., J. F. McManus, D.-D. Rousseau, and I. Chuine, 1997. How long and how stable was the last interglacial? Quaternary Science Reviews 16:605–612.

Kürschner, H., T. Raus, and J. Venter, 1995. Pflanzen der Türkei. Quelle & Meyer Verlag. Wiesbaden.

Kuzucuoğlu, C., A. Christol, D. Mouralis, A.-F. Dogu, E. Akköprü, M. Fort, D. Brunstein, H. Zorer, M. Fontugne, M. Karabiyikoglu, S. Scaillet, J.-L. Reyss, and H. Guillou, 2010. Formation of the upper pleistocene terraces of lake van (turkey). Journal of Quaternary Science 25:1124–1137.

Kwiecien, O., M. Stockhecke, N. Pickarski, G. Heumann, T. Litt, M. Sturm, F. S. Anselmetti, and H. Gerald, subm. Dynamics of the last four glacial terminations recorded in lake van, turkey. Quarternary Science Reviews .

Landais, A., J. M. Barnola, V. Masson-Delmotte, J. Jouzel, J. Chappellaz, N. Caillon, C. Huber, M. Leuenberger, and S. J. Johnsen, 2004. A continuous record of temperature evolution over a sequence of dansgaard-oeschger events during marine isotopic stage 4 (76 to 62 kyr bp). Geophysical Research Letters 31:L22211.

Landmann, G. and S. Kempe, 2002. Seesedimente als klimaarchiv - fallbespiele: Van see und totes meer. p. 1–15. *In* W. Rosendahl and A. Hoppe (ed.) Angewandte Geowissenschaften in Darmstadt., 15. Schriftenreihe der deutschen Geologischen Gesellschaft.

Landmann, G., A. Reimer, and S. Kempe, 1992. Sedimentologie und warvenchronologie des van sees. *In* S. Kempe (ed.) Abschlußbericht DFG Projekt Wo 395/2-1 bis 2-4. Selbstverlag, Hamburg.

Landmann, G., A. Reimer, and S. Kempe, 1996a. Climatically induced lake level changes at lake van, turkey, during the pleistocene/holocene transition. Global Biogeochemical Cycles 10:797–808.

Landmann, G., A. Reimer, G. Lemcke, and S. Kempe, 1996b. Dating late glacial abrupt climate changes in the 14, 570 yr long continuous varve record of lake van. turkey. Palaeogeography, Palaeoclimatology, Palaeoecology 122:107–118.

Langgut, D., A. Almogi-Labin, M. Bar-Matthews, and M. Weinstein-Evron, 2011. Vegetation and climate changes in the south eastern mediterranean during the last glacial-interglacial cycle (86 ka): new marine pollen record. Quaternary Science Reviews 30:3960–3972.

Lawson, I. T., M. Frogley, C. Bryant, R. Preece, and P. C. Tzedakis, 2004. The lateglacial and holocene environmental history of the ioannina basin, north-west greece. Quaternary Science Reviews 23:1599–1625.

Lemcke, G., 1996. Paläoklimarekonstruktion am Van See (Ostanatolien, Türkei). Diss. ETH Zürich.

Lisiecki, L. E. and M. E. Raymo, 2004. A plio-pleistocene stack of 57 globally distributed benthic d 18o records. Paleoceanography 20:1–16.

Litt, T., F. S. Anselmetti, H. Baumgarten, J. Beer, N. Çagatay, D. Cukur, E. Damci, C. Glombitza, G. Haug, G. Heumann, J. Kallmeyer, R. Kipfer, S. Krastel, O. Kwiecien, A. F. Meydan, S. Orcen, N. Pickarski, M.-E. Randlett, H.-U. Schmincke, C. J. Schubert, M. Sturm, M. Sumita, M. Stockhecke, Y. Tomonaga, L. Vigliotti, T. Wonik, and the PALEOVAN scientific team, 2012. 500,000 years of environmental history in eastern anatolia: The paleovan drilling project. Scientific Drilling Journal p. 18–29.

Litt, T., K.-E. Behre, K.-D. Meyer, H.-J. Stephan, and S. Wansa, 2007. Stratigraphische begriffe für das quartär des norddeutschen vereisungsgebietes. Eiszeitalter und Gegenwart (Quaternary Science Journal) 56(1/2):7–65.

Litt, T., S. Krastel, M. Sturm, R. Kipfer, S. Örcen, G. Heumann, S. O. Franz, U. B. Ülgen, and F. Niessen, 2009. 'paleovan', international continental scientific drilling program (icdp): site survey results and perspectives. Quaternary Science Reviews 28:1555–1567.

Litt, T., N. Pickarski, G. Heumann, M. Stockhecke, and P. C. Tzedakis, subm. A 600,000 year long continental pollen record from lake van, eastern anatolia (turkey). Quaternary Science Reviews .

Litt, T., H.-U. Schmincke, and B. Kromer, 2003. Environmental response to climatic and volcanic events in central europe during the weichselian lateglacial. Quaternary Science Reviews 22:7–32.

Louis, H., 1939. Das natürliche pflanzenkleid anatoliens. Geographische Abhandlungen 12:1–132.

Lowe, J. J. and M. J. C. Walker, 1984. Reconstructing Quaternary Environments. 2nd ed. Longman, Edinburgh.

Magri, D. and L. Sadori, 1999. Late pleistocene and holocene pollen stratigraphy at lago di vico, central italy. Vegetation History and Archaeobotany 8:247–260.

Martinson, D. G., N. G. Pisias, J. D. Hays, J. Imbrie, T. C. Moore Jr., and N. J. Shackleton, 1987. Age dating and the orbital theory of the ice ages: Development of a high-resolution 0 to 300,000-year chronostratigraphy. Quaternary Research 27:1–29.

Mayer, H. and H. Aksoy, 1986. Wälder der Türkei. Gustav Fischer Verlag, Stuttgart, New York.

McManus, J. F., G. C. Bond, W. S. Broecker, S. J. Johnsen, L. Labeyrie, and S. Higgins, 1994. High-resolution climate records from the north atlantic during the last interglacial. Nature 371:326–329.

McManus, J. F., D. W. Oppo, and J. L. Cullen, 1999. A 0.5-million-year record of millennial-scale climate variability in the north atlantic. Science 283:971–975.

McManus, J. F., D. W. Oppo, L. D. Keigwin, J. L. Cullen, and G. C. Bond, 2002. Thermohaline circulation and prolonged interglacial warmth in the north atlantic. Quarternary Research 58:17–21.

Milner, A. M., U. C. Müller, K. H. Roucoux, R. E. L. Collier, J. Pross, S. Kalaitzidis, K. Christanis, and P. C. Tzedakis, 2013. Environmental variability during the last interglacial: a new high-resolution pollen record from tenaghi philippon, greece. Journal of Quarternary Science 28:113–117.

Moore, P. D., J. A. Webb, and M. E. Collinson, 1991. Pollen Analysis. Blackwell Science.

Müller, H., 1974. Pollenanalytische untersuchungen und jahresschichtenzählung an der eemzeitlichen kieselgur von bispingen/luhe. Geologisches Jahrbuch A21:149–169.

Müller, U. C., S. Klotz, M. A. Geyh, J. Pross, and G. C. Bond, 2005. Cyclic climate fluctuations during the last interglacial in central europe. Geology 33:449–452.

Müller, U. C. and G. J. Kukla, 2004. North atlantic current and european environments during the declining stage of the last interglacial. Geology 32:1009–1012.

Müller, U. C., J. Pross, and E. Bibus, 2003. Vegetation response to rapid climate change in central europe during the past 140,000 yr based on evidence from the füramoos pollen record. Quaternary Research 59:235–245.

Müller, U. C., J. Pross, P. C. Tzedakis, C. Gamble, U. Kotthoff, G. Schmiedl, S. Wulf, and K. Christanis, 2011. The role of climate in the spread of modern humans into europe. Quarternary Science Reviews 30:273–279.

NEEM, 2013. Eemian interglacial reconstructed from a greenland folded ice core. Nature 493:489–494.

NGRIP, 2004. High-resolution record of northern hemisphere climate extending into the last interglacial period. Nature 431:147–151.

Okay, A. I., 2008. Geology of turkey: A synopsis. Anschnitt 21:19–42.

Özdemir, Y., O. Karaoğlu, A. Ümit Tolluoğlu, and N. Güleç, 2006. Volcanostratigraphy and petrogenesis of the nemrut stratovolcano (east anatolian high plateau): The most recent post-collisional volcanism in turkey. Chemical Geology 226:189–211.

Pearce, J. A., J. F. Bender, S. E. De Long, W. S. F. Kidd, P. J. Low, Y. Güner, F. Saroglu, Y. Yilmaz, S. Moorbathg, and J. G. Mitchell, 1990. Genesis of collision volcanism in eastern anatolia, turkey. Journal of Volcanology and Geothermal Research 44:189–229.

Peyron, O., S. Goring, I. Dormoy, U. Kotthoff, J. Pross, J.-L. de Beaulieu, R. Drescher-Schneider, B. Vannière, and M. Magny, 2011. Holocene seasonality changes in the central mediterranean region reconstructed from the pollen sequences of lake accesa (italy) and tenaghi philippon (greece). The Holocene 21:131–146.

Prentice, I. C., 1985. Pollen representation, source area and basin size: Toward a unified theory of pollen analysis. Quarternary Research 23:76–86.

Prentice, I. C. and T. Webb, 1986. Pollen percentages, tree abundances and the fagerlind effect. Journal of Quaternary Science 1:35–43.

Pross, J., P. C. Tzedakis, G. Schmiedl, K. Christanis, H. Hooghiemstra, U. C. Müller, U. Kotthoff, S. Kalaitzidis, and A. Milner, 2007. Tenaghi philippon (greece) revisited: Drilling a continuous lower-latitude terrestrial climate archive of the last 250,00 years. Scientific Drilling 5:44–46.

Punt, W., 1976-1991. The Northwest European Pollen Flora. Elsevier, Amsterdam.

Reilinger, R., S. McClusky, P. Vernant, S. Lawrence, S. Ergintav, R. Cakmak, H. Ozener, F. Kadirov, I. Guliev, R. Stepanyan, M. Nadariya, G. Hahubia, S. Mahmoud, K. Sakr, A. ArRajehi, D. Paradissis, A. Al-Aydrus, M. Prilepin, T. Guseva, E. Evren, A. Dmitrotsa, S. V. Filikov, F. Gomez, R. Al-Ghazzi, and G. Karam, 2006. Gps constraints on continental deformation in the africa-arabia-eurasia continental collision zone and implications for the dynamics of plate interactions. Journal of Geophysical Research 111:1–26.

Reille, M., 1999. Pollen et spores d'Europe et d'Afrique du nord. Laboratoire de Botanique Historique et Palynologie, Marseille.

Riedel, N., 2011. Der Einfluss von Vulkanausbrüchen auf die Vegetationsentwicklung und die agrarische Nutzung seit dem Weichselspätglazial in Ostanatolien anhand von palynologischen Untersuchungen an lakustrinen Sedimenten des Vansees (Türkei). Ph.D. diss. Rheinische Friedrich-Wilhelms-Universität Bonn.

Roberts, N., J. M. Reed, M. J. Leng, C. Kuzucuouğlu, M. Fontugne, J. Bertaux, H. Woldring, S. Bottema, S. Black, E. Hunt, and M. Karabiyikoğlu, 2001. The tempo of holocene climatic change in the eastern mediterranean region: new high-resolution crater-lake sediment data from central turkey. The Holocene 11:721–736.

Roberts, N. and H. E. J. Wright, 1993. Vegetational, lake level, and climatic history of the near east and southwest asia. p. 194–220. *In* H. E. J. Wright, J. E. Kutzbach, T. Webb III, W. F. Ruddiman, F. A. Street-Perrott, and P. J. Bartlein (ed.) Global Climates since the Last Glacial Maximum. Minnesota University Press.

Rossignol-Strick, M., 1995. Sea-land correlation of pollen records in the eastern mediterranean for the glacial-interglacial transition: Biostratigraphy versus radiometric time-scale. Quaternary Science Reviews 14:893–915.

Roucoux, K. H., N. J. Shackleton, L. de Abreu, J. Schönfeld, and P. C. Tzedakis, 2001. Combined marine proxy and pollen analyses reveal rapid iberian vegetation response to north atlantic millennial-scale climate oscillations. Quaternary Research 56:128–132.

Roucoux, K. H., P. C. Tzedakis, I. T. Lawson, and V. Margari, 2011. Vegetation history of the penultimate glacial period (marine isotope stage 6) at ioannina, north-west greece. Journal of Quaternary Science 26:616–626.

Saarnisto, M., 1986. Annually laminated lake sediments. p. 343–370. *In* B. E. Berglund and M. Ralska-Jasiewiczowa (ed.) Handbook of Holocene Palaeoecology and Palaeohydrology. John Wiley and Sons.

Sánchez Goñi, M. F., 2007. Introduction to climate and vegetation in europe during mis5. p. 197–205. *In* F. Sirocko, M. Claussen, M. F. Sánchez Goñi, and T. Litt (ed.) The Climate of Past Interglacials. Elsevier, Amsterdam.

Sánchez Goñi, M. F., I. Cacho, J. L. Turon, J. Guiot, F. J. Sierro, J.-P. Peypouquet, J. O. Grimalt, and N. J. Shackleton, 2002. Synchroneity between marine and terrestrial responses to millennial scale climatic variability during the last glacial period in the mediterranean region. Climate Dynamics 19:95–105.

Sánchez Goñi, M. F., F. Eynaud, J.-L. Turon, and N. J. Shackleton, 1999. High resolution palynological record off the iberian margin: direct land-sea correlation for the last interglacial complex. Earth and Planetary Science Letters 171:123–137.

Sánchez Goñi, M. F. and S. P. Harrison, 2010. Introduction: Millennial-scale climate variability and vegetation changes during the last glacial: Concepts and terminology. Quaternary Science Reviews 29:2823–2827.

Sánchez Goñi, M. F., M. F. Loutre, M. Crucifix, O. Peyron, L. Santos, J. Duprat, B. Malaizé, J.-L. Turon, and J.-P. Peypouquet, 2005. Increasing vegetation and climate gradient in western europe over the last glacial inception (122-110 ka): data-model comparison. Earth and Planetary Science Letters 231:111–130.

Sánchez Goñi, M. F., J.-L. Turon, F. Eynaud, and N. J. Shackleton, 2000. Direct land/sea correlation of the eemian, and its comparison with the holocene: a high-resolution palynological record off the iberian margin. Netherlands Journal of Geosciences 79:345–354.

Schiebel, V., 2013. Vegetation and climate history of the southern Levant during the last 30,000 years based on palynological investigation. Ph.D. diss. University of Bonn.

Seelos, K. and F. Sirocko, 2007. Abrupt cooling events at the very end of the last interglacial. *In* F. Sirocko, M. Claussen, M. F. Sánchez Goñi, and T. Litt (ed.) The Climate of the Past Interglacials. Elsevier, Amsterdam.

Şengör, A. M. C., S. Özeren, T. Genç, and E. Zor, 2003. East anatolian high plateau as a mantle-supported, north-south shortened domal structure. Geophysical Research Letters 30:8045.

Şengör, A. M. C. and Y. Yilmaz, 1981. Tethyan evolution of turkey: a plate approach. Tectonophysics 75:181–241.

Shackleton, N. J., M. Chapman, M. F. Sánchez Goñi, D. Pailler, and Y. Lancelot, 2002. The classic marine isotope substage 5e. Quaternary Research 58:14–16.

Shackleton, N. J., R. G. Fairbanks, T.-C. Chiu, and F. Parrenin, 2004. Absolute calibration of the greenland time scale: implications for antarctic time scales and for d14c. Quaternary Science Reviews 23:1513–1522.

Shackleton, N. J., M. F. Sánchez Goñi, D. Pailler, and Y. Lancelot, 2003. Marine isotope substage 5e and the eemian interglacial. Global and Planetary Change 36:151–155.

Shumilovskikh, L. S., H. W. Arz, A. Wegwerth, D. Fleitmann, F. Marret, N. Nowaczyk, P. Tarasov, and H. Behling, 2013. Vegetation end environmental changes in northern anatolia between 134 and 119 ka recorded in black sea sediments. Quaternary Research 80:349–360.

Shumilovskikh, L. S., P. Tarasov, H. W. Arz, D. Fleitmann, F. Marret, N. Nowaczyk, B. Plessen, F. Schlütz, and H. Behling, 2012. Vegetation and environmental dynamics in the southern black sea region since 18 kyr bp derived from the marine core 22-gc3. Palaeogeography, Palaeoclimatology, Palaeoecology 337-338:177–193.

Sirocko, F., M. Claussen, M. F. Sánchez Goñi, and T. Litt, 2007. The Climate of Past Interglacials. Elsevier, Amsterdam.

Sirocko, F., K. Seelos, K. Schaber, B. Rein, F. Dreher, M. Diehl, R. Lehne, K. Jager, M. Krbetschek, and D. Degering, 2005. A late eemian aridity pulse in central europe during the last glacial inception. Nature 436:833–836.

Steffensen, J. P., K. K. Andersen, M. Bigler, H. B. Clausen, D. Dahl-Jensen, H. Fischer, K. Goto-Azuma, M. Hansson, S. J. Johnsen, J. Jouzel, V. Masson-Delmotte, T. Popp, S. O. Rasmussen, R. Röthlisberger, U. Ruth, B. Stauffer, M.-L. Siggaard-Andersen, A. E. Sveinbjörnsdóttir, A. Svensson, and J. W. C. White, 2008. High-resolution greenland ice core data show abrupt climate change happens in few years. Science 321:680–684.

Stevens, L. R., M. Djamali, V. Andrieu-Ponel, and J.-L. de Beaulieu, 2012. Hydroclimatic varaiations over the last two glacial/interglacial cycles at lake urmia, iran. Journal of Paleolimnology 47:645–660.

Stevens, L. R., H. E. J. Wright, and E. Ito, 2001. Proposed changes in seasonality of climate during the lateglacial and holocene at lake zeribar, iran. The Holocene 11:747–755.

Stockhecke, M., F. S. Anselmetti, A. F. Meydan, D. Odermatt, and M. Sturm, 2012. The annual particle cycle in lake van (turkey). Palaeogeography, Palaeoclimatology, Palaeoecology 333-334:148–159.

Stockhecke, M., O. Kwiecien, L. Vigliotti, T. Litt, N. Pickarski, H.-U. Schmincke, and N. Çağatay, subm. Chronology of the 600 ka old long continental record of lake van: climatostratigraphic synchronization and dating. Quarternary Sciences Reviews .

Stockhecke, M., M. Sturm, I. Brunner, H.-U. Schmincke, M. Sumita, O. Kwiecien, D. Cukur, and F. Anselmetti, 2013. Sedimentary evolution and environmental history of lake van (turkey) over the past 600,000 years. Sedimentology .

Stockmarr, J., 1971. Tablets with spores used in absolute pollen analysis. Pollen et Spores 13:615–621.

Sugita, S., 1993. A model of pollen source area for an entire lake surface. Quaternary Research 39:239–244.

Sugita, S., 1994. Pollen representation of vegetation in quaternary sediments: Theory and method in patchy vegetation. Journal of Ecology 82:881–897.

Sugita, S., 2007. Theory of quantitative reconstruction of vegetation i: pollen from large sites reveals regional vegetation composition. The Holocene 17:229–241.

Sugita, S., G. M. MacDonald, and C. P. S. Larsen, 1997. Reconstruction of fire disturbance and forest succession from fossil pollen in lake sediments: Potential and limitations. p. 387–412. *In* J. S. Clark, H. Cachier, J. G. Goldammer, and B. Stocks (ed.) Sediments Records of Biomass Burning and Global Change, volume 51. NATO ASI Series I: Global Envirnmental Change.

Sumita, M. and H.-U. Schmincke, 2013a. Impact of volcanism on the evolution of lake van i: evolution of explosive volcanism of nemrut volcano (eastern anatolia) during the past ca. 0.4 ma. Bulletin of Volcanology 75:714–746.

Sumita, M. and H.-U. Schmincke, 2013b. Impact of volcanism on the evolution of lake van ii: Temporal evolution of explosive volcanism of nemrut volcano (eastern anatolia) during the past ca. 0.4 ma. Journal of Volcanology and Geothermal Research 253:15–34.

Svensson, A., K. K. Andersen, M. Bigler, H. B. Clausen, D. Dahl-Jensen, S. M. Davies, S. J. Johnsen, R. Muscheler, F. Parrenin, S. O. Rasmussen, R. Röthlisberger, I. Seierstad, J. P. Steffensen, and B. M. Vinther, 2008. A 60 000 year greenland stratigraphic ice core chronology. Climate of the Past 4:47–57.

Svensson, A., K. K. Andersen, M. Bigler, H. B. Clausen, D. Dahl-Jensen, S. M. Davies, S. J. Johnsen, R. Muscheler, S. O. Rasmussen, R. Röthlisberger, J. Peder Steffensen, and B. Vinther, 2006. The greenland ice core chronology 2005, 15-42 ka. part 2: comparison to other records. Quaternary Science Reviews 25:3258–3267.

Tauber, H., 1965. Differential pollen dispersion and the interpretation of pollen diagrams. with a contribution to the interprestion of the elm fall. Geological Survey of Denmark. II. Series p. 7–69.

Theuerkauf, M., A. Kuparinen, and H. Joosten, 2013. Pollen productivity estimates strongly depend on assumed pollen dispersal. The Holocene 23:14–24.

Thomas, E. R., E. W. Wolff, R. Mulvaney, S. J. Johnsen, J. P. Steffensen, and C. Arrowsmith, 2009. Anatomy of a dansgaard-oeschger warming transition: High-resolution analysis of the north greenland ice core project ice core. Journal of Geophysical Research 114:1–9.

Türkeş, M., 1996. Spatial and temporal analysis of annual rainfall variations in turkey. International Journal of Climatology 16:1057–1076.

Turner, C. and R. G. West, 1968. The subdivision and zonation of interglacial periods. Eiszeitalter und Gegenwart 19:93–101.

Turner, R., N. Roberts, and M. D. Jones, 2008. Climatic pacing of mediterranean fire histories from lake sedimentary microcharcoal. Global and Planetary Change 63:317–324.

Tzedakis, P. C., 1993. Long-term tree populations in northwest greece through multiple quaternary climatic cycles. Nature 364:437–440.

Tzedakis, P. C., 1994. Vegetation change through glacial-interglacial cycles: A long pollen sequence perspective. Philosophical Transactions of the Royal Society of London. Series B: Biological Sciences 345:403–432.

Tzedakis, P. C., 2000. Vegetation variability in greece during the last interglacial. Netherlands Journal of Geosciences 79:355–367.

Tzedakis, P. C., 2003. Timing and duration of last interglacial conditions in europe: a chronicle of a changing chronology. Quaternary Science Reviews 22:763–768.

Tzedakis, P. C., 2005. Towards an understanding of the response of southern european vegetation to orbital and suborbital climate variability. Quaternary Science Reviews 24:1585–1599.

Tzedakis, P. C., 2007. Seven ambiguities in the mediterranean palaeoenvironmental narrative. Quaternary Science Reviews 26:2042–2066.

Tzedakis, P. C., V. Andrieu, J.-L. de Beaulieu, S. Crowhurst, M. Follieri, H. Hooghiemstra, D. Magri, M. Reille, L. Sadori, N. J. Shackleton, and T. A. Wijmstra, 1997. Comparison of terrestrial and marine records of changing climate of the last 500,000 years. Earth and Planetary Science Letters 150:171–176.

Tzedakis, P. C., M. R. Frogley, and T. H. E. Heaton, 2002a. Duration of last interglacial conditions in northwestern greece. Quaternary Research 58:53–55.

Tzedakis, P. C., M. R. Frogley, and T. H. E. Heaton, 2003a. Last interglacial conditions in southern europe: evidence from ioannina, northwest greece. Global and Planetary Change 36:157–170.

Tzedakis, P. C., M. R. Frogley, I. T. Lawson, R. C. Preece, I. Cacho, and L. de Abreu, 2004a. Ecological thresholds and patterns of millennial-scale climate variability: The response of vegetation in greece during the last glacial period. Geological Society of America 32:109–112.

Tzedakis, P. C., H. Hooghiemstra, and H. Palike, 2006. The last 1.35 million years at tenaghi philippon: revised chronostratigraphy and long-term vegetation trends. Quaternary Science Reviews 25:3416–3430.

Tzedakis, P. C., I. T. Lawson, M. R. Frogley, G. M. Hewitt, and R. C. Preece, 2002b. Buffered tree population changes in a quaternary refugium: Evolutionary implications. Science 297:2044–2047.

Tzedakis, P. C., J. F. McManus, H. Hooghiemstra, D. W. Oppo, and T. A. Wijmstra, 2003b. Comparison of changes in vegetation in northeast greece with records of climate variability on orbital and suborbital frequencies over the last 450'000 years. Earth and Planetary Science Letters 212:197–212.

Tzedakis, P. C., K. H. Roucoux, L. de Abreu, and N. J. Shackleton, 2004b. The duration of forest stages in southern europe and interglacial climate variability. Science 306:2231–2235.

Vaks, A., M. Bar-Matthews, A. Ayalon, A. Matthews, A. Frumkin, U. Dayan, L. Halicz, A. Almogi-Labin, and B. Schilman, 2006. Paleoclimate and location of the border between mediterranean climate region and the saharo-arabian desert as revealed by speleothems from the northern negev desert, israel. Earth and Planetary Science Letters 249:384–399.

Valeton, I., 1978. A morphological and petrological study of the terraces around lake van, turkey. p. 64–80. *In* F. Degens, E. T. & Kurtman (ed.) The Geology of Lake Van., 169. The Mineral Research and Exploration Institute of Turkey, Ankara.

van der Wiel, A. M. and T. A. Wijmstra, 1987a. Palynology of the 112.8-197.8 m interval of the core tenaghi philippon iii, middle pleistocene of macedonia. Review of Palaeobotany and Palynology 52:89–117.

van der Wiel, A. M. and T. A. Wijmstra, 1987b. Palynology of the lower part (78-120 m) of the core tenaghi philippon ii, middle pleistocene of macedonia, greece. Review of Palaeobotany and Palynology 52:73–88.

van Kreveld, S., M. Sarnthein, H. Erlenkeuser, P. Grootes, S. Jung, M. J. Nadeau, U. Pflaumann, and A. Voelker, 2000. Potential links between surging ice sheets, circulation changes, and the dansgaard-oeschger cycles in the irminger sea, 60-18 kyr. Paleoceanography 15:425–442.

van Zeist, W. and S. Bottema, 1977. Palynological investigations in western iran. Palaeohistoria 19:87–95.

van Zeist, W. and S. Bottema, 1991. Late quaternary vegetation of the near east. Beihefte zum Tübinger Atlas des Vorderen Orients 18:11–156.

van Zeist, W. and H. Woldring, 1978a. A pollen profile from lake van; a preliminary report. p. 115–123. *In* E. T. Degens and F. Kurtman (ed.) The Geology of Lake Van, 169. MTA Press, Ankara.

van Zeist, W. and H. Woldring, 1978b. A postglacial diagram from lake van in east anatolia. Review of Palaeobotany and Palynology 26:249–276.

van Zeist, W., H. Woldring, and D. Stapert, 1975. Late quarternary vegetation and climate of southwestern turkey. Palaeohistoria 17:55–143.

van Zeist, W. and H. E. J. Wright, 1963. Preliminary pollen studies at lake zeribar, zagros mountains, southwestern iran. Science 140:65–67.

Vannière, B., M. J. Power, N. Roberts, W. Tinner, J. Carrión, M. Magny, P. Bartlein, D. Colombaroli, A. L. Daniau, W. Finsinger, G. Gil-Romera, P. Kaltenrieder, R. Pini, L. Sadori, R. Turner, V. Valsecchi, and E. Vescovi, 2011. Circum-mediterranean fire activity and climate changes during the mid-holocene environmental transition (8500-2500 cal. bp). The Holocene 21:53–73.

Vigliotti, L., J. E. T. Channell, and M. Stockhecke, subm. Paleomagnetism of lake van sediments: chronology and paleovironment since 350 ka. Quaternary Science Reviews .

Voelker, A. H. L., 2002. Global distribution of centennial-scale records for marine isotope stage (mis) 3: a database. Quaternary Science Reviews 21:1185–1212.

Walter, H., 1956. Das problem der zentralanatolischen steppe. Die Naturwissenschaften. 5:97–102.

Watts, W. A., J. R. M. Allen, and B. Huntley, 1996. Vegetation history and palaeoclimate of the last glacial period at lago grande di monticchio, southern italy. Quaternary Science Reviews 15:133–153.

Watts, W. A., J. R. M. Allen, and B. Huntley, 2000. Palaeoecology of three interstadial events during oxygen-isotope stages 3 and 4: a lacustrine record from lago grande di monticchio, southern italy. Palaeogeography, Palaeoclimatology, Palaeoecology 155:83–93.

Wick, L., G. Lemcke, and M. Sturm, 2003. Evidence of lateglacial and holocene climatic change and human impact in eastern anatolia: high resolution pollen, charcoal, isotopic and geochemical records from the laminated sediments of lake van. The Holocene 13:665–675.

Wijmstra, T. A., 1969. Palynology of the first 30 meters of a 120m deep section on northern greece. Acta Botanica Neerlandica 18:511–527.

Wolff, E. W., J. Chappellaz, T. Blunier, S. O. Rasmussen, and A. Svensson, 2010. Millennial-scale variability during the last glacial: The ice core record. Quaternary Science Reviews 29:2828–2838.

Wolff, E. W., H. Fischer, and R. Rothlisberger, 2009. Glacial terminations as southern warmings without northern control. Nature Geoscience 2:206–209.

Yilmaz, Y., 1990. Comparison of young volcanic associations of western and eastern anatolia formed under a compressional regime: a review. Journal of Volcanology and Geothermal Research 44:69–87.

Yilmaz, Y., Y. Güner, and F. Şaroğlu, 1998. Geology of the quaternary volcanic centres of the east anatolia. Journal of Volcanology and Geothermal Research 85:173–210.

Zohary, M., 1973a. Geobotanical Foundations of the Middle East, volume 1. Gustav Fischer Verlag, Swets & Zeitlinger. Stuttgart, Amsterdam.

Zohary, M., 1973b. Geobotanical Foundations of the Middle East, volume 2. Gustav Fischer Verlag, Swets & Zeitlinger. Stuttgart, Amsterdam.

Appendix

Table 7: List of samples anaylsed for pollen composition, including composite depth (mcblf), no-Event depth (mblf-nE) and age (ka BP). The 'Core Section' consists of the following components: Expedition/Site, Hole/Core, Core type/Section. According to Stockhecke et al. (subm.), volcaniclastic and event layers were removed from the composite profile to obtain the corrected 'no-Event' depth scale [mblf-nE]; 'n.e.' = no evidences for no-Event depth or Age data.

Core Section	Sample ID	Section Depth [cm]	Composite Depth [mcblf]	no-Event Depth [mblf-nE]	Age [ka BP]
5034/2A/1H/1	LV10-2	0-2	0.317	0.327	0.55
5034/2A/1H/2	LV10-3	0-2	0.517	0.517	0.88
5034/2A/1H/2	LV10-4	20-22	0.714	0.714	1.22
5034/2A/1H/3	LV10-5	11-13	0.904	0.894	1.53
5034/2A/1H/3	LV10-6	30-32	1.094	1.080	1.85
5034/2A/2H/1	LV10-8	0-2	1.193	1.183	2.02
5034/2A/2H/1	LV10-9	20-22	1.393	1.383	2.33
5034/2A/2H/1	LV10-11	60-62	1.793	1.695	3.03
5034/2A/2H/1	LV10-12	80-82	1.993	1.892	3.56
5034/2A/2H/1	LV10-13	100-102	2.193	2.095	4.10
5034/2A/2H/1	LV10-15	140-142	2.593	2.495	5.19
5034/2A/2H/2	LV10-16	12-14	2.790	2.692	5.73
5034/2A/2H/2	LV10-17	32-34	2.990	2.880	6.23
5034/2A/2H/2	LV10-18	52-54	3.190	3.080	6.75
5034/2A/2H/2	LV10-19	72-74	3.390	3.270	7.46
5034/2A/2H/2	LV10-20	92-94	3.590	3.470	8.31
5034/2D/1H/2	LV10-21	46-48	3.791	3.671	9.16
5034/2D/1H/2	LV10-22	66-68	3.991	3.870	10.00
5034/2D/1H/2	LV10-23	86-88	4.191	4.071	10.85
5034/2D/1H/2	LV10-24	106-108	4.391	4.271	11.66
5034/2A/3H/1	LV10-25	36-38	4.578	4.453	11.82
5034/2A/3H/1	LV10-26	56-58	4.778	4.650	12.00
5034/2A/3H/1	LV10-27	76-78	4.978	4.840	12.18
5034/2A/3H/1	LV10-28	96-98	5.178	5.029	12.35
5034/2A/3H/1	LV10-29	116-118	5.378	5.186	12.49
5034/2A/3H/1	LV10-30	136-138	5.578	5.370	12.66
5034/2A/3H/2	LV10-31	15-17	5.788	5.582	12.85
5034/2A/3H/2	LV10-32	39-41	6.028	5.777	13.28
5034/2A/3H/2	LV10-33	55-57	6.188	5.919	13.59
5034/2A/3H/2	LV10-34	73-75	6.368	6.098	13.98
5034/2D/2H/2	LV10-36	26-28	6.708	6.436	14.70
5034/2D/2H/2	LV10-37	46-48	6.908	6.638	15.06
5034/2D/2H/2	LV10-38	66-68	7.108	6.836	15.41
5034/2D/2H/2	LV10-40	106-108	7.508	7.236	16.13
5034/2A/4H/1	LV10-41	48-50	7.908	7.638	16.84
5034/2A/4H/1	LV10-42	68-70	8.108	7.836	17.19
5034/2A/4H/1	LV10-43	88-90	8.308	8.036	17.55
5034/2A/4H/1	LV10-44	108-110	8.508	8.236	17.90
5034/2A/4H/1	LV10-45	128-130	8.708	8.436	18.26
5034/2A/4H/2	LV10-46	1-3	8.910	8.638	18.63

(continue on next page)

Table 7: continued from previous page

Core Section	Sample ID	Section Depth [cm]	Composite Depth [mcblf]	no-Event Depth [mblf-nE]	Age [ka BP]
5034/2A/4H/2	LV10-47	21-23	9.110	8.838	19.07
5034/2E/3H/1	LV10-48	78-80	9.317	9.045	19.52
5034/2E/3H/1	LV10-49	98-100	9.517	9.245	19.96
5034/2E/3H/1	LV10-50	118-120	9.717	9.645	20.83
5034/2E/3H/1	LV10-51	138-140	9.917	9.648	20.84
5034/2E/3H/2	LV10-52	7-9	10.106	9.834	21.25
5034/2E/3H/2	LV10-53	27-29	10.306	10.034	21.69
5034/2E/3H/2	LV10-54	47-49	10.506	10.234	22.13
5034/2E/3H/2	LV10-55	67-69	10.706	10.434	22.56
5034/2E/3H/2	LV10-56	87-89	10.906	10.634	23.00
5034/2D/4H/1	LV10-57	37-39	11.127	10.855	23.46
5034/2D/4H/1	LV10-58	57-59	11.327	11.055	23.83
5034/2D/4H/1	LV10-59	77-79	11.527	11.255	24.20
5034/2D/4H/1	LV10-60	97-99	11.727	11.455	24.58
5034/2D/4H/1	LV10-61	117-119	11.927	11.658	24.96
5034/2D/4H/1	LV10-62	137-139	12.127	11.855	25.32
5034/2D/4H/2	LV10-63	4-6	12.324	12.052	25.69
5034/2D/4H/2	LV10-64	24-26	12.524	12.252	26.07
5034/2D/4H/2	LV10-65	44-46	12.724	12.452	26.44
5034/2D/4H/2	LV10-66	64-66	12.924	12.652	26.81
5034/2D/4H/2	LV10-67	84-86	13.124	12.852	27.19
5034/2D/4H/3	LV10-68	3-5	13.321	13.049	27.55
5034/2D/4H/3	LV10-69	23-25	13.521	13.249	27.92
5034/2A/6H/1	LV10-70	25-27	13.738	13.466	28.30
5034/2A/6H/1	LV10-71	45-47	13.938	13.668	28.66
5034/2A/6H/1	LV10-72	65-67	14.138	13.834	29.17
5034/2A/6H/1	LV10-73	85-87	14.338	14.034	30.29
5034/2A/6H/1	LV10-74	105-107	14.538	14.234	31.40
5034/2A/6H/1	LV10-75	125-127	14.738	14.384	32.24
Nemrut Formation (NF)					
5034/2E/6H/1	LV10-79	24-26	18.026	14.471	32.67
5034/2E/6H/1	LV10-80	44-46	18.226	14.642	33.42
5034/2E/6H/1	LV10-81	64-66	18.426	14.836	34.12
5034/2E/6H/1	LV10-82	84-86	18.626	15.021	34.71
5034/2E/6H/1	LV10-83	104-106	18.826	15.221	35.36
5034/2E/6H/1	LV10-84	124-126	19.026	15.405	35.91
5034/2E/6H/1	LV10-85	146-148	19.246	15.624	36.56
5034/2E/6H/2	LV10-86	13-15	19.408	15.620	36.55
5034/2E/6H/2	LV10-87	34-36	19.618	15.964	37.57
5034/2E/6H/2	LV10-88	54-56	19.818	16.164	38.17
5034/2E/6H/2	LV10-89	74-76	20.018	16.366	38.69
5034/2A/8H/1	LV10-90	39-41	20.197	16.543	39.14
5034/2A/8H/1	LV10-91	65-67	20.457	16.754	39.68
5034/2A/8H/1	LV10-92	81-83	20.617	16.914	40.09
5034/2A/8H/1	LV10-93	101-103	20.817	17.114	40.72

(continue on next page)

Table 7: continued from previous page

Core Section	Sample ID	Section Depth [cm]	Composite Depth [mcblf]	no-Event Depth [mblf-nE]	Age [ka BP]
5034/2A/8H/1	LV10-94	121-123	21.017	17.314	41.35
5034/2A/8H/2	LV10-96	11-13	21.449	17.644	42.54
5034/2A/8H/2	LV10-97	27-29	21.609	17.797	43.09
5034/2A/8H/2	LV10-98	47-49	21.809	17.997	43.80
5034/2A/8H/2	LV10-99	67-69	22.009	18.188	44.49
5034/2A/8H/2	LV10-100	87-89	22.209	18.384	45.19
5034/2A/8H/2	LV10-101	107-109	22.409	18.584	45.90
5034/2A/8H/2	LV10-102	127-129	22.609	18.781	46.61
5034/2E/7H/2	LV10-103	13-15	22.705	18.877	46.94
5034/2E/7H/2	LV10-104	33-35	22.905	19.077	47.61
5034/2E/7H/2	LV10-105	53-55	23.105	19.277	48.28
5034/2E/7H/2	LV10-106	75-77	23.325	19.467	48.91
5034/2E/7H/2	LV10-107	93-95	23.505	19.647	49.54
5034/2E/7H/2	LV10-108	113-115	23.705	19.847	50.29
5034/2E/7H/2	LV10-109	133-135	23.905	20.047	51.04
5034/2D/8H/1	LV10-110	48-50	24.112	20.252	51.80
5034/2D/8H/1	LV10-111	68-70	24.312	20.454	52.56
5034/2D/8H/1	LV10-112	88-90	24.512	20.654	53.30
5034/2D/8H/1	LV10-113	108-110	24.712	20.850	54.04
5034/2D/8H/1	LV10-114	128-130	24.912	21.050	54.74
5034/2D/8H/1	LV10-115	148-150	25.112	21.250	55.44
5034/2D/8H/2	LV10-116	15-17	25.287	21.415	55.95
5034/2D/8H/2	LV10-117	35-37	25.487	21.615	56.48
5034/2D/8H/2	LV10-118	55-57	25.687	21.800	56.97
5034/2D/8H/2	LV10-119	73-75	25.867	21.978	57.44
5034/2D/8H/2	LV10-120	95-97	26.087	22.196	58.02
5034/2A/10H/1	LV10-121	46-48	26.193	22.286	58.26
5034/2A/10H/1	LV10-122	67-69	26.403	22.438	58.80
5034/2A/10H/1	LV10-123	85-87	26.583	n.e.	n.e.
5034/2A/10H/1	LV10-124	107-109	26.803	22.733	59.69
5034/2A/10H/1	LV10-125	127-129	27.003	22.884	60.04
5034/2D/9H/2	LV10-126	20-22	27.217	23.078	60.49
5034/2D/9H/2	LV10-127	40-42	27.417	23.278	60.96
5034/2D/9H/2	LV10-128	58-60	27.597	23.438	61.33
5034/2D/9H/2	LV10-129	80-82	27.817	23.651	61.83
Halepkalesi Pumice (HP-10)					
5034/2D/9H/3	LV10-130	62-64	29.134	n.e.	n.e.
5034/2D/9H/3	LV10-131	82-84	29.334	23.968	62.57
5034/2D/9H/3	LV10-132	100-102	29.514	24.148	62.99
5034/2E/9H/2	LV10-133	65-67	29.731	24.350	63.46
5034/2E/9H/2	LV10-134	85-87	29.931	24.542	63.91
5034/2E/9H/2	LV10-135	107-109	30.151	24.723	64.42
5034/2E/9H/2	LV10-136	125-127	30.331	24.903	64.98
5034/2D/10H/2	LV10-137	45-47	30.536	25.108	65.62
5034/2D/10H/2	LV10-138	65-67	30.736	25.308	66.24

(continue on next page)

Table 7: continued from previous page

Core Section	Sample ID	Section Depth [cm]	Composite Depth [mcblf]	no-Event Depth [mblf-nE]	Age [ka BP]
5034/2D/10H/3	LV10-139	4-6	30.928	25.483	66.79
5034/2D/10H/3	LV10-140	24-26	31.128	25.673	67.38
5034/2D/10H/3	LV10-141	44-46	31.328	25.873	68.01
5034/2D/10H/3	LV10-142	64-66	31.528	26.073	68.63
5034/2D/10H/3	LV10-143	84-86	31.728	26.273	69.25
5034/2D/10H/3	LV10-144	104-106	31.928	26.458	69.78
5034/2D/10H/3	LV10-145	124-126	32.128	26.660	70.28
5034/2D/10H/3	LV10-146	142-144	32.308	26.828	70.69
5034/2E/10H/2	LV10-147	58-60	32.736	26.884	70.83
5034/2E/10H/2	LV10-148	78-80	32.936	27.084	71.33
5034/2E/10H/2	LV10-149	98-100	33.136	27.284	71.82
5034/2D/11H/1	LV10-150	31-33	33.372	27.512	72.42
5034/2D/11H/1	LV10-151	51-53	33.572	27.712	73.07
5034/2D/11H/1	LV10-152	91-93	33.972	27.917	73.73
5034/2D/11H/1	LV10-153	111-113	34.172	28.115	74.37
5034/2D/11H/1	LV10-154	131-133	34.372	28.317	75.03
5034/2D/11H/2	LV10-155	0-2	34.569	28.514	75.66
5034/2D/11H/2	LV10-156	20-22	34.769	28.714	76.31
5034/2D/11H/2	LV10-157	40-42	34.969	28.902	76.81
5034/2D/11H/2	LV10-158	60-62	35.169	29.102	77.33
5034/2E/11H/2	LV10-159	28-30	35.384	29.291	77.82
5034/2E/11H/2	LV10-160	48-50	35.584	29.491	78.32
5034/2E/11H/2	LV10-161	63-65	35.734	29.641	78.69
5034/2E/11H/2	LV10-162	88-90	35.984	29.811	79.11
5034/2B/1H/3	LV10-163	25-27	36.175	30.002	79.58
5034/2B/1H/3	LV10-164	45-47	36.375	30.202	80.08
5034/2B/1H/3	LV10-165	65-67	36.575	30.402	80.58
5034/2B/1H/3	LV10-166	85-87	36.775	30.602	81.07
Incekaya-Dibekli					
5034/2E/12H/2	LV10-177	97-99	39.162	30.757	81.46
5034/2D/13H/2	LV10-178	13-15	39.357	30.952	81.95
5034/2D/13H/2	LV10-179	33-35	39.557	31.152	82.44
5034/2D/13H/2	LV10-180	53-55	39.757	31.342	82.92
5034/2D/13H/2	LV10-181	73-75	39.957	31.542	83.41
5034/2D/13H/2	LV10-182	93-95	40.157	31.742	83.91
5034/2B/3H/2	LV10-183	45-47	40.366	31.945	84.42
5034/2B/3H/3	LV10-184	6-8	40.551	32.118	84.85
5034/2B/3H/3	LV10-185	26-28	40.751	32.300	85.32
5034/2B/3H/3	LV10-186	46-48	40.951	32.473	85.76
5034/2E/13H/3	LV10-187	27-29	41.152	32.654	86.24
5034/2E/13H/3	LV10-188	47-49	41.352	32.826	86.68
5034/2E/13H/3	LV10-189	67-69	41.552	32.997	87.13
5034/2E/13H/3	LV10-190	87-89	41.752	33.177	87.59
5034/2E/13H/3	LV10-191	107-109	41.952	33.362	88.07
5034/2E/13H/4	LV10-192	7-9	42.152	33.562	88.59

(continue on next page)

Table 7: continued from previous page

Core Section	Sample ID	Section Depth [cm]	Composite Depth [mcblf]	no-Event Depth [mblf-nE]	Age [ka BP]
5034/2E/13H/4	LV10-193	27-29	42.352	33.760	89.11
5034/2E/13H/4	LV10-194	46-48	42.542	n.e.	n.e.
5034/2E/13H/4	LV10-195	67-69	42.752	n.e.	n.e.
5034/2B/4H/1	LV10-196	55-57	42.934	33.909	89.49
5034/2B/4H/1	LV10-197	75-77	43.134	34.109	90.01
5034/2E/14H/1	LV10-198	55-57	43.721	34.349	90.70
5034/2E/14H/1	LV10-199	75-77	43.921	34.549	91.27
5034/2E/14H/2	LV10-200	13-15	44.216	34.834	92.08
5034/2E/14H/2	LV10-201	33-35	44.416	35.034	92.65
5034/2E/14H/2	LV10-202	53-55	44.616	35.234	93.22
5034/2E/14H/2	LV10-203	73-75	44.816	35.434	93.79
5034/2E/14H/2	LV10-204	93-95	45.016	35.634	94.35
5034/2E/14H/2	LV10-205	111-113	45.196	35.814	94.87
5034/2E/14H/2	LV10-206	133-135	45.416	36.014	95.44
5034/2B/5H/1	LV10-207	11-13	45.618	36.216	96.01
5034/2B/5H/1	LV10-208	31-33	45.818	36.416	96.58
5034/2B/5H/1	LV10-209	51-53	46.018	n.e.	n.e.
5034/2B/5H/1	LV10-210	71-73	46.218	36.818	97.73
5034/2D/16H/1	LV10-212	13-15	46.415	37.013	98.28
5034/2D/16H/1	LV10-213	33-35	46.615	37.213	98.85
5034/2D/16H/1	LV10-214	53-55	46.815	37.413	99.42
5034/2D/16H/1	LV10-215	73-75	47.015	n.e.	n.e.
5034/2D/16H/1	LV10-216	93-95	47.215	37.793	100.50
5034/2D/16H/1	LV10-217	113-115	47.415	37.993	101.07
5034/2D/16H/2	LV10-218	0-2	47.611	n.e.	101.63
5034/2D/16H/2	LV10-219	20-22	47.811	38.371	102.15
5034/2D/16H/2	LV10-220	40-42	48.011	38.571	102.72
5034/2D/16H/2	LV10-221	60-62	48.211	38.770	103.28
5034/2B/6H/1	LV10-223	7-9	48.462	38.962	103.83
5034/2B/6H/1	LV10-224	23-25	48.622	39.122	104.26
5034/2B/6H/1	LV10-225	47-49	48.862	39.327	104.77
5034/2B/6H/1	LV10-226	67-69	49.062	39.527	105.27
5034/2B/6H/1	LV10-227	87-89	49.262	39.662	105.61
5034/2B/6H/2	LV10-228	8-10	49.579	39.887	106.18
5034/2B/6H/2	LV10-229	20-22	49.699	39.972	106.39
5034/2B/6H/2	LV10-230	37-39	49.869	40.122	106.77
5034/2B/6H/2	LV10-231	60-62	50.099	40.282	107.17
5034/2B/6H/2	LV10-232	81-83	50.309	40.483	107.67
5034/2B/6H/2	LV10-233	110-112	50.599	40.633	108.05
5034/2E/16A/2	LV10-234	14-16	50.711	40.745	108.34
5034/2E/16A/2	LV10-235	34-36	50.911	40.945	108.93
5034/2E/16A/2	LV10-236	54-56	51.111	41.155	109.55
5034/2E/16A/2	LV10-237	76-78	51.331	n.e.	n.e.
5034/2E/16A/2	LV10-238	94-96	51.511	41.525	110.63
5034/2B/7H/1	LV10-239	28-30	51.708	41.722	111.21
5034/2B/7H/1	LV10-240	48-50	51.908	41.922	111.80

(continue on next page)

Table 7: continued from previous page

Core Section	Sample ID	Section Depth [cm]	Composite Depth [mcblf]	no-Event Depth [mblf-nE]	Age [ka BP]
5034/2B/7H/1	LV10-241	67-69	52.098	42.122	112.39
5034/2E/17A/1	LV10-247	31-33	52.177	42.166	112.52
5034/2B/7H/2	LV10-242	17-19	52.305	42.294	112.89
5034/2E/17A/1	LV10-248	48-50	52.347	42.336	113.02
5034/2B/7H/2	LV10-243	37-39	52.505	42.474	113.42
5034/2E/17A/1	LV10-249	71-73	52.577	42.546	113.63
5034/2B/7H/2	LV10-244	57-59	52.705	42.669	113.99
5034/2E/17A/1	LV10-250	85-87	52.717	42.681	114.03
5034/2B/7H/2	LV10-245	77-79	52.905	42.811	114.41
5034/2E/17A/1	LV10-251	111-113	52.977	42.883	114.62
5034/2B/7H/2	LV10-246	97-99	53.105	43.011	115.00
5034/2E/17A/2	LV10-252	0-2	53.182	43.098	115.25
5034/2E/17A/2	LV10-254	40-42	53.582	43.303	116.02
5034/2E/17A/2	LV10-255	60-62	53.782	43.483	116.74
5034/2E/17A/2	LV10-256	80-82	53.982	43.683	117.54
5034/2E/17A/2	LV10-257	99-101	54.172	n.e.	n.e.
5034/2B/8H/2	LV10-258	15-17	54.365	44.020	118.88
5034/2B/8H/2	LV10-259	35-37	54.565	44.220	119.68
5034/2B/8H/2	LV10-260	51-53	54.725	44.310	120.04
5034/2B/8H/3	LV10-261	20-22	54.909	44.444	120.57
5034/2B/8H/3	LV10-262	40-42	55.109	44.639	121.35
5034/2B/8H/3	LV10-263	60-62	55.309	44.839	122.15
5034/2E/18A/2	LV10-264	51-53	55.505	45.029	122.91
5034/2E/18A/2	LV10-265	71-73	55.705	45.229	123.71
5034/2E/18A/2	LV10-266	91-93	55.905	45.424	124.49
5034/2E/18A/2	LV10-267	110-112	56.095	n.e.	n.e.
5034/2B/9H/1	LV10-268	9-11	56.304	45.813	126.04
5034/2B/9H/1	LV10-269	29-31	56.504	46.013	126.84
5034/2B/9H/1	LV10-270	49-51	56.704	46.213	127.64
5034/2B/9H/1	LV10-271	69-71	56.904	46.413	128.43
5034/2B/9H/2	LV10-272	13-15	57.096	46.553	128.83
5034/2B/9H/2	LV10-273	32-34	57.286	46.743	129.39
5034/2B/9H/3	LV10-274	2-4	57.488	46.935	129.95
5034/2B/9H/3	LV10-275	22-24	57.688	47.135	130.53
5034/2B/9H/3	LV10-276	42-44	57.888	47.325	131.05
5034/2B/9H/3	LV10-277	62-64	58.088	47.438	131.25
5034/2B/9H/3	LV10-278	82-84	58.288	47.618	131.57
5034/2B/9H/3	LV10-279	103-105	58.498	n.e.	n.e.
5034/2B/9H/3	LV10-280	122-124	58.688	47.868	132.01
5034/2D/20H/1	LV10-281	87-89	58.875	47.995	132.23
5034/2D/20H/1	LV10-282	106-108	59.065	n.e.	n.e.
5034/2D/20H/2	LV10-283	8-10	59.297	48.252	132.68

(continue on next page)

Table 7: continued from previous page

Core Section	Sample ID	Section Depth [cm]	Composite Depth [mcblf]	no-Event Depth [mblf-nE]	Age [ka BP]
5034/2D/20H/2	LV10-284	28-30	59.497	48.392	132.93
5034/2D/20H/2	LV10-285	48-50	59.697	48.592	133.28
5034/2B/10H/2	LV10-286	20-22	59.873	48.743	133.55
5034/2B/10H/2	LV10-287	42-44	60.093	48.965	133.94

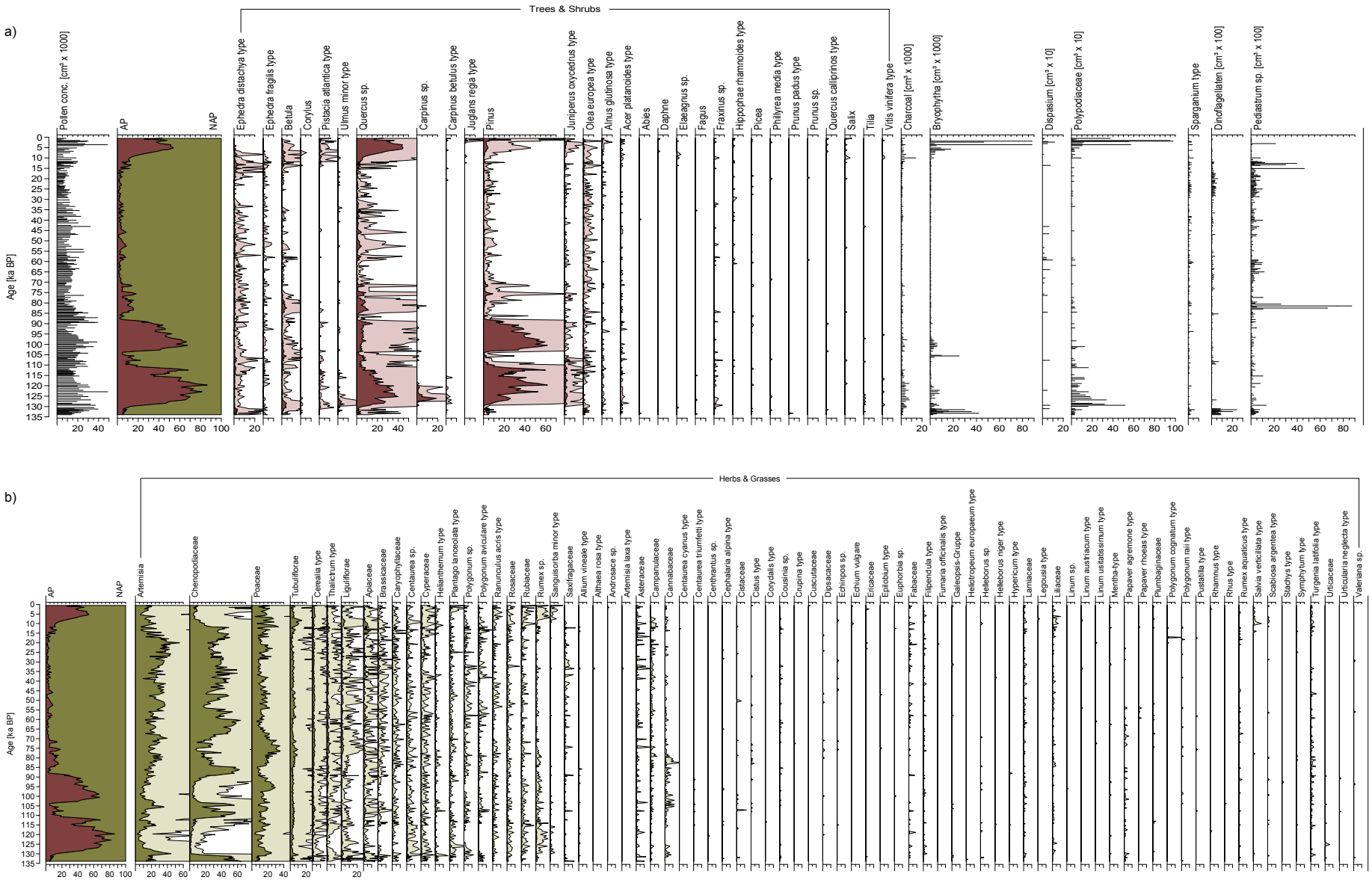

Figure 7.1: Lake Van, complete pollen diagram (%). a) arboreal pollen (AP) including algae, aquatics, bryophytes and pteridophytes in concentrations (grains/cm³); b) non-arboreal pollen (NAP). A x10 exaggeration line (lightly coloured) of the horizontal scale is used to show changes in low taxon percentages.